The form, flow and dynamic character of meanders in a lowland river

Inaugural-Dissertation to obtain the academic degree
Doctor of Philosophy (Ph.D.) in River Science

Submitted to the Department of Biology, Chemistry and Pharmacy of
Freie Universität Berlin

by

Tarun BISHT

Berlin, February 2020

The work on this doctoral thesis was conducted from 1st October 2014 to 30th January 2018 under the supervision of **PD Dr. Martin T. Pusch** (Leibniz Institute of Freshwater Ecology and Inland Fisheries, IGB), **Associate Prof. Dr. Guido Zolezzi** (University of Trento, Italy). The work was carried out at the Leibniz Institute of Freshwater Ecology and Inland Fisheries (Berlin, Germany), Frei eUniversität Berlin (Germany) and University of Trento (Italy).

1st Reviewer: PD Dr. Martin T. Pusch

2nd Reviewer: Prof. Dr. Klement Tockner

Date of defense: 23rd June 2020

The SMART Joint Doctorate Programme

Research for this thesis was conducted with the support of the Erasmus Mundus Programme, within the framework of the Erasmus Mundus Joint Doctorate (EMJD) SMART (Science for MAnagement of Rivers and their Tidal systems). EMJDs aim to foster cooperation between higher education institutions and academic staff in Europe and third countries with a view to creating centres of excellence and providing a highly skilled 21st century workforce enabled to lead social, cultural and economic developments. All EMJDs involve mandatory mobility between the universities in the consortia and lead to the award of recognised joint, double or multiple degrees.

The SMART programme represents a collaboration among the University of Trento, Queen Mary University of London and Freie Universität Berlin. Each doctoral candidate within the SMART programme has conformed to the following during their 3 years of study:

(i) Supervision by a minimum of two supervisors in two institutions (their primary and secondary institutions).

(ii) Study for a minimum period of 6 months at their secondary institution

(iii) Successful completion of a minimum of 30 ECTS of taught courses

(iv) Collaboration with an associate partner to develop a particular component / ap-plication of their research that is of mutual interest.

(v) Submission of a thesis within 3 years of commencing the programme.

This project has been funded with support from the European Commission. This publication reflects the views only of the author and the Commission cannot be held responsible for any use which may be made of the information contained therein.

“There are things known and there are things unknown,

and in between are the doors of perception.”

Aldous Huxley

Table of contents:

List of figures

Supplementary figures

List of tables

Supplementary tables

Abbreviations

R = radius of curvature;

B = channel width;

S= bend sinuosity;

C = curvature, where C= 1/R;

C^{-} = dimensionless curvature;

$C_{max}B$ = width normalized maximum bend curvature;

$C_{mean}B$ = width normlaized mean bend curvature;

Cr = curvature ratio, ratio of maximum by mean curvature;

λ = dimensionless intrinsic meander wavenumber;

Z = migration rates in widths/year;

U= downstream velovity magnitude in m s^{-1};

V= transverse velocity magnitude in m s^{-1};

Summary

Meandering rivers across the globe present a striking similarity in their alignment, and this pattern has intrigued scientific curiosity for almost a century. However, still very little is known about 'unconventional' river meanders with a "zigzagging" planform appearance, but which occur in rivers from the temperate to the tropic regions. In order to compare the characteristics of flow, morphology and morphodynamics of conventional ('round' and 'fat') and unconventional ('sharp' and 'angular') river bends, I studied the Prut (Romania/Moldova), one of the last remaining freely meandering lowland rivers of Europe. The Prut is a clay-bed river that meanders for about 585 km of channel length in its lower section, with an average discharge of c. 90 $m^3 s^{-1}$ and channel width ranging from 39-84 m.

For the analysis of long-term channel dynamics (chapter 2), bend morphometry, morphodynamics and temporal trajectories were determined for a section of Prut that included multiple replicates of each bend type. Data were extracted from historical maps and imagery for a c. 250 km long section of the Prut River spread over a 90-year period (1915-2005). For that, I used a geographical information system (GIS) and state-of-the-art software PyRIS to derive measures of bend-scale morphometry and migration features for a total of 118 simple and back-traceable river bends, after exclusion of compound bends and bends that cut-off during those 90 years. Normalized bend curvatures ($C_{max}B$) ranged from 0.01 to 1.44 (as for 2005). Sharp bends were distinguished from round bends and angular bends from fat bend geometries by width normalized bend curvature, $C_{max}B$ threshold (round < 0.5 and sharp > 0.5) and the maximum to mean bend curvature ratio, Cr threshold (fat < 3 and angular > 3), respectively.

Over the 90 year period, studied bends (N=118) displayed a gradual narrowing and homogenization of channel width (median= 72 m and interquartile range (IQR)= 63-86 m in 1915; median = 52 m and IQR = 50-57 m in 2005), a reduction of migration rates (mean= 0.038 widths/yr, SD=0.028 in 1915-1960 to mean= 0.015 widths/yr, SD = 0.011 in 1980-2005) and a slightly increase of sinuosity (from 1.41 to 1.63). Sharp and angular bends tended to stabilize over longer periods (20-90 years), and concomitantly displayed more unchanged shape transitions (for sharp bends: 1915-1960= 49%; 1960-1980= 61%; 1980-2005= 57%, N=49) compared to their conventional counterparts (for round bends: 1915-1960= 37%; 1960-1980= 22%; 1980-2005= 22%, N=49). These results provide new insights into the

formation and maintenance of unconventional bends (sharp and angular), which on the Prut are mainly due to autogenic processes. In unconventional bends, special patterns of erosion and deposition create features like deeper pools or zones of flow separation, with fallen trees possibly acting as additional allogenic factor.

These interrelationships among bend form, flow and river bed features in unconventional meanders were then investigated in detail fora set of 14 bends (chapter 3). Boat operated ADCP (Acoustic Doppler Current Profiler) field surveys enabled detailed records of 3-D velocity and depth distribution along these bends.This dataset enabled for the first time to systematically compare flow characteristics of unconventional with that in conventional meanders under field conditions. The studied set of bends comprised at least 2 bends of each simple bend shape types (see chapter 2) i.e. angular, sharp, round and fat bend shapes. A significant linear increase in the lateral extent of the Inner-Bank Flow Separation zone (IBFS) at the bend apex with increasing bend curvature was recorded (IBFS = 6.1+ 45.8 $C_{max}B$ + 8.2; R^2= 0.55; $p < 0.001$; N=14). In angular bends, hydraulics was influenced by a locally eroded point bar and a steep sloping upstream riffle to pool transition. This was reflected by the significant increase in depth ratio (ratio of apex pool depth to upstream riffle depth) with stronger bend angularity, as defined by curvature ratio (ratio of maximum to mean of bend curvature) (H_{ratio} = 0.83 + 0.41 Cr; R^2 = 0.44; $p < 0.005$; N=14). These morphological features influenced the extent of the horizontal recirculation occurring within the IBFS zones at the bend apex, and were further associated with the formation of two separate IBFS zones in fat bends compared to a singular zone in angular bends.

Pool depth (H_p) displayed an increasing trend with higher curvature but then to stabilize at bend curvatures greater than c. 0.5, suggesting the existence of a negative autogenic feedback at high bend curvature, as pool depth is also weakly related to the IBFS size (IBFS = -14+ 10.3 H_p + 10.2; R^2= 0.30; $p<0.02$; N=14). The observed interdependence between flow patterns and planform shape inangular and fat bends partially explains their different morphodynamics, too. While fat bends are prone to develop multilobing or a delayed cut-offs, angular bends may display increased temporal stability and even inward migration.

Hence, this thesis demonstrates for the first time the different characteristics of conventional and unconventional meanders in terms of their morphometry and hydraulic geometry based on the study of bends from a real meandering river, and complemented by

documentation of the long-term morphological trajectories of these meander types during a nearly centennial period. Thus, this thesis provides new insights into the so far poorly explored linkages between forms and processes of river bends, and indicates field-based explanations on the formation and relative stability of unconventional bend forms over extended timeperiods.

Zusammenfassung

Mäandrierende Flüsse weisen auf der ganzen Welt eine auffällige Ähnlichkeit ihrer Linienführung auf, und dieses Muster beschäftigtdie wissenschaftliche Neugierde seit fast einem Jahrhundert. Dabeiist jedoch immer noch sehr wenig über "unkonventionelle" Flussmäander mit "zickzackförmiger" Grundrissform bekannt, die jedoch in Flüssen vonden gemäßigten bis in die tropischen Regionen vorkommen. Um die Eigenschaften der Strömung, Morphologie und Morphodynamik von konventionellen („runden“ und „fetten“) und unkonventionellen („scharfen“ und „eckigen“) Flussbiegungen zu vergleichen, untersuchteich den Pruth (Rumänien/Moldawien), einen der letzten noch frei mäandrierenden Tieflandflüsse Europas. Der Pruth ist ein Lehmbett-Fluss, der in seinem unteren Abschnitt über etwa 585 km Flusslänge mäandriert, mit einem durchschnittlichen Durchfluss von ca. 90 m^3 s^{-1} und einer Gerinnebreitevon 39-84 m.Zur Analyse der langfristigen Gerinnedynamik(Kapitel 2) wurden die Morphometrie, Morphodynamik und die zeitlichen Trajektorien der Flussbiegungen für einen Abschnitt des Pruth bestimmt, der mehrere Ausprägungenjedes Biegungstyps umfasste. Die Daten wurden aus historischen Karten und Bildern für einen ca. 250 km langen Abschnitt des Pruth-Flusses extrahiert, die aus einemZeitraum von 90 Jahren (1915-2005) stammen. Dazu verwendete ich ein geographisches Informationssystem (GIS) und die kürzlich entwickelteSoftware PyRIS, um Messwerteder Morphometrie und der Mäandermigration für insgesamt 118 einfache und rückverfolgbare Flussbiegungen abzuleiten, nach Ausschluss zusammengesetzterFlussbiegungen und solcher Biegungen, die während dieser 90 Jahre abgeschnürtwurden. Die normierten Biegungskrümmungen (CmaxB) hatten eine Spannweitevon 0,01 bis 1,44 (im Jahr2005). Scharfe Biegungen wurden von runden Biegungen und eckigen Biegungen von fetten Biegungsgeometrienunterschieden durch die Breite der normalisierten Biegekrümmung, den CmaxB-Schwellenwert (rund < 0,5 und scharf > 0,5) und durch das Verhältnis von maximaler zu mittlerer Biegekrümmung, den Cr-Schwellenwert (fett < 3 und eckig > 3).

Über den Zeitraum von 90 Jahren zeigten die untersuchten Flussbiegungen (N=118) eine allmähliche Verengung und Homogenisierung der Gerinnebreite(Median = 72 m und Interquartilsabstand (IQR)= 63-86 m im Jahr 1915;Median = 52 m und IQR = 50-57 m im Jahr 2005), eine Verringerung der Migrationsraten (Mittelwert = 0.038 Flussbreiten/Jahr, SD=0,028 in 1915-1960 zum Mittelwert= 0,015 Breiten/Jahr, SD = 0,011 in 1980-2005) und eine leichteErhöhung derSinuosität (von 1,41 auf 1,63). Scharfe und eckige Flussbiegungen

tendierten dazu, sich über längere Zeiträume (20-90 Jahre) zu stabilisieren, und zeigten gleichzeitig mehr unveränderteFormübergänge (für scharfe Biegungen: 1915-1960= 49%; 1960-1980= 61%; 1980-2005= 57%, N=49) im Vergleich zu ihren konventionellen Gegenstücken (für runde Biegungen: 1915-1960= 37%; 1960-1980= 22%; 1980-2005= 22%, N=49). Diese Ergebnisse erlaubenneue Einblickeindie Bildung und Erhaltung unkonventioneller Flussbiegungen (scharf und eckig), die amPruth hauptsächlich auf autogene Prozesse zurückzuführen sind. In unkonventionellen Biegungen entstehen durch besondereErosions- und Ablagerungsmuster Merkmale wie tiefere Kolkeoder Strömungsablösungszonen, wobei umgestürzte Bäume möglicherweiseals zusätzlicher allogener Faktor wirken.

Diese Wechselbeziehungen zwischen Biegungsform, Strömung und Flussbettmerkmalen in unkonventionellen Mäandern wurden dann für einen Satz von 14 Flussbiegungen(Kapitel 3) im Detail untersucht. Mit Hilfe von ADCP (Acoustic Doppler CurrentProfiler)-Feldvermessungen, die vomBoot aus durchgeführt wurden, konnten die 3D-Geschwindigkeits- und Tiefenverteilungen entlang dieser Flussbiegungendetailliert aufgezeichnet werden. Dieser Datensatz ermöglichte erstmals einen systematischen Vergleich der Fließeigenschaften von unkonventionellen Mäandern mit denen in konventionellen Mäandern unter Feldbedingungen. Der untersuchte Flussbiegungs-Satz enthieltdabei mindestens zweiBiegungen jedeseinfachen Biegungstyps(siehe Kapitel 2), d.h. eckige, scharfe, runde und fette Biegungsformen. Es wurde dabei eine signifikante lineare Zunahme der lateralen Ausdehnung der Innenufer-Strömungstrennungszone (IBFS) am Scheitelpunkt der Biegung mit zunehmender Biegekrümmung festgestellt (IBFS = 6,1+ 45,8 CmaxB + 8,2; R^2= 0,55; $p < 0,001$; N=14). In eckigen Biegungen wurde die Hydrodynamik durch eine lokal erodierten Geschiebebankund einen steil abfallenden Übergang von der Furtzum Kolkbeeinflusst. Dies spiegelte sich in einersignifikanten Zunahme des Tiefenverhältnisses (Verhältnis von Scheitelpunkt-Kolktiefe zu stromaufwärtigerFurttiefe) mit stärkerem Biegungswinkel wider, derdurch das Krümmungsverhältnis (Verhältnis von Maximum zu Mittelwert der Biegekrümmung) definiert wurde (H_{ratio} = 0,83 + 0,41 Cr; R^2 = 0,44; $p < 0,005$; N=14). Diese morphologischen Merkmale beeinflussten dieAusdehnungder horizontalen Rezirkulation, die innerhalb der IBFS-Zonen am Scheitelpunkt der Biegung auftrat, und waren ferner mit der Bildung von zwei getrennten IBFS-Zonen in fetten Flussbiegungenverbunden,im Vergleich zu einer einzigen Zone in Winkelkrümmungen.

Die Kolktiefe (Hp) nahm tendenziell mit höherer Krümmung zu, stabilisierte sich dann aber bei Biegungskrümmungen von mehr als ca. 0,5, was auf das Vorhandensein einer negativen autogenen Rückkopplung bei hoher Biegungskrümmung hindeutet, zumaldie Kolktiefe ebenfalls schwach mit der IBFS-Ausdehnungzusammenhängt (IBFS = -14+ 10,3 Hp + 10,2; R^2= 0,30; p<0,02; N=14).

Derbeobachtete wechselseitige ZusammenhangzwischenStrömungsmusternund der Form von in eckigen und fetten Flussbiegungen erklärt teilweise auch deren unterschiedliche Morphodynamik. Während fette Flussbiegungenzumehrfachen Ausbuchtungen oder einerverzögerten Mäander-Abschnürungneigen, können eckige Flussbiegungeneine erhöhte zeitliche Stabilität und sogar eine Einwärtswanderung aufweisen.

Somitzeigt diese Arbeit erstmalig die unterschiedlichen Charakteristika konventioneller und unkonventioneller Mäander hinsichtlich ihrer Morphometrie und hydraulischen Geometrie auf, basierend auf der Untersuchung von Biegungen eines realenmäandrierenden Flusses, und ergänzt durch die Dokumentationder langfristigen morphologischen Trajektorien dieser Mäandertypen während einer fast hundertjährigen Periode. Damit liefert diese Arbeit neue Einsichten in die bisher wenig erforschten Zusammenhänge zwischen Formen und Prozessen von Flussbiegungen, und zeigtfeldbasierte Erklärungen zur Bildung und relativen Stabilität unkonventioneller Biegungsformen über längere Zeiträume auf.

1. General introduction

1.1 Motivation

Water flow in rivers represents one of nature's most prominent forces shaping our planet, and river floodplains have served as the cradles of human civilizations in several parts of the world. Unaltered rivers rarely follow a straight path, even that they carve through harder terrains and forms such as bedrock canyons over time. This phenomenon of winding of rivers across a landmass is known as "meandering", originating from the Menderes River on the Asiatic Turkey which in ancient times had the Greek name Μαίανδρος = Maiandros. Meandering as a physical phenomenon is also observable in systems other than just the fluvial systems on Earth, namely, sub-marine flows (Imran et al., 1999), atmospheric jet streams and even as paleo-channels on the Martian surface (Malin & Edgett, 2003).

In rivers, meandering not only adds to the awe-inspiring aesthetics but also shapes the floodplain as it moves through it at a time scale of decades and centuries (Hooke, 1984; Lauer & Parker, 2008). Meandering causes an increased channel length, a decreased channel slope and sediment transport from eroded banks to downstream sedimentation sites, making the lowland sub-system of a river morphodynamically distinct in itself. The increased channel size in the lowland section of the river makes it suitable for harboring megafauna such as river Dolphins, Sturgeons and Gahrials (He et al., 2018). Hence, meandering phenomenon has stirred scientific minds for more than a century now (see, Thomson, 1876; Jefferson, 1902; Davis, 1908), including a contribution of the theoretical physicist Albert Einstein, with his famous "tea-leaves experiment" that explained the cause of meander initiation to be an effect of the Earth's Coriolis force (Einstein, 1926). Thereby, the phenomenon of meandering has raised curiosity in several disciplines of science and engineering such as fluvial geomorphology (Leopold & Wolman, 1960; Hickin, 1974), hydrodynamics (Sukhodolov, 2012; Ottevanger, 2013) and or fluid mechanics (Engelund, 1974; Seminara, 2006), ecology (Greco & Plant, 2003; Garcia et al., 2011; Schnauder & Sukhodolov, 2012), paleohydrology (Williams, 1984), and engineering works (Lagasse et al., 2004).

Due to the fertility of floodplain soils and the many other ecosystem services offered by rivers, river banks have always been preferred sites for human settlement, resulting in profound morphological modifications. As a result, remaining freely flowing rivers around the globe face immense anthropogenic pressures (Dynesius & Nilsson, 1994). In many

places, rivers have been transformed through channelization or straightening (Talbot & Lapointe, 2002; Surian & Rinaldi, 2003), bank stabilization (Bravard et al., 1999; Kiss et al., 2008), damming (Surian & Rinaldi, 2003; Phillips et al., 2005; Chen et al., 2010), Land use change, (Graf, 2008; Salit et al., 2015) or sediment dredging and mining (Petts & Gurnell, 2005). These pressures have resulted in impaired form and processes in affected rivers such as loss of hydrologic connectivity in longitudinal and transversal dimensions (Welcomme, 1985; Ward & Stanford, 1995a); altered flow and sediment regimes (Ward & Stanford, 1995b; Dai et al., 2016); reduction of meander migration dynamics (Magdaleno & Fernández-Yuste, 2011); channel narrowing and incision (Surian & Rinaldi, 2003) and habitat loss. As stronger climate extremes are expected, the increases or decreases in river flow will have implications on their geomorphologic responses, particularly in terms of channel form (sinuosity) and processes (erosion, migration) (Ashmore & Church, 2001; Goudie, 2006). Whereby, alluvial rivers are more sensitive to such modifications than bedrock rivers (Goudie, 2006).

Unaltered meander morphology display high physical heterogeneity at diverse spatio-temporal scales, which are an important prerequisite for high biodiversity and an indicator for an overall good ecological status of river ecosystems. Therefore, restoring meander morphology has been the backbone most of river restoration approaches (Nakano & Nakamura, 2008; Lorenz et al., 2009), wherein, re-meandering of the straightened channel has been a frequently used approach (Kondolf, 2006). Not only for such restoration purposes, is acquiring an in-depth understanding of linkages among forms and processes in alluvial meandering rivers crucial for several reasons. It allows for better predictions and identification of the direction and magnitude of responses of the meandering river-floodplain systems, particularly towards the modifications caused by anthropogenic and environmental variables (Güneralp & Marston, 2012). Moreover, a bulk of information on baseline conditions of forms and processes could also help in deciding the mitigation actions and trade-offs under scenarios varying in space and time. However, several lacunae in the understanding of forms and processes typical to meandering rivers still persist (Hooke, 2013).

The general aim of the present thesis is therefore to improve the understanding of the shape and dynamics of meander bend forms using the example of a lowland river that retains most of its original meandering dynamics by applying field-based recordings with state-of-the-art measurement technology to replicate river bend observations.

1.2 Background

1.2.1 Why rivers meander?

Several theories have been put forward to answer- "why do rivers meander"? However, to date, a precise rationale of meandering across different fluvial systems remains elusive. The prominent historical contributions of hydrodynamic theories can be summarized as follows.

Einstein, (1926) argued that meandering might be induced by the Coriolis force generated due to Earth's rotation that acts on all moving fluids on Earth. In straighter channels, this might produce secondary currents which could lead to erosion in such channels in a manner similar to the centrifugal forces acting in meandering channels. However, the strength of the Coriolis force might be too weak in generating any significant effect on channel boundaries (Rhoads & Welford, 1991).

Tanner, (1960) proposed that periodic reversal of helical flow could generate stream curvature; however, there was no direct evidence on such helical cells provided in his glass-plate experiments. Gorycki, (1973a) confirmed the periodic reversal of helical flow to gradually develop from curved flow filaments as flow discharge is increased and also argued that such reversal might occur in naturally occurring straight channels as well. Davies & Tinker, (1984) on the other hand argued that an intrinsic phenomenon such as the periodic reversal of helical flow either does not exist or is inadequate in generating meander bends. Einstein & Shen, (1964) proposed the development of two converging helical flows in straight channel creating pools and bars to develop in an alternating manner and so formed bar-pool topography to be highly dynamic. So, the surface water moves in a meandering pattern from one scour hole to next.

A fundamentally different paradigm was proposed to explain the initiation of meandering based on the assumption that an inherent instability in the form of perturbations occurring in the flow, bed topography and or the channel planform would trigger meandering from an initially straight channel. This paradigm entailed three theories, namely, the bar theory (Callander, 1978), bend theory (Ikeda et al., 1981) and a unified bar-bend theory (Blondeaux & Seminara, 1985; Seminara & Tubino, 1989). According to bar theory, there are alternatively migrating perturbations (bars) at the bed that give rise to migrating bars in straight channels which deflect flow towards the banks causing them to erode and in the process initiate meandering. This theory although could predict formation of large-scale

forms of rivers (Federici & Seminara, 2003) and could determine the meander wavelength and its effect on migration (Rhoads & Welford, 1991), but assumed that banks are non-erodible so that erosion is not allowed and therefore lacks a mechanistic explanation of development of curvature in channels (Hooke, 2013).

The bend instability theory stated that in straight rivers a randomly occurring perturbation can initiate meandering; these perturbations can be in flow, bed topography and or channel planform. This theory also established a connection with the bar theory in that the wavelength at which bend instability would occur is in correspondence with the threshold wavelength of instable alternating bars predicted by bar theory, indicating a combination of both migrating bars and erodible banks would lead to meandering.

The unified bar-bend theory advocates that small perturbations create disturbances that grow in amplitude. Moreover, it accounted for the formation of alternate bars from a straight channel that causes curvature development therein and interactions between alternate bars, point bars and curvature. It could also demonstrate a previously unknown phenomenon of 'resonance' which is related to the selection of meander wavelength to be close to the fastest rate of amplification, this range falls in a similar range to that of the alternate bars in the channel. Furthermore, it was found that the resonance phenomenon could also explain the relationship between channel width and meander wavelength.

Several shortcomings have been highlighted in the theories explaining the development of meandering patterns (for detailed review on this see, Rhoads & Welford, 1991; Seminara, 2006), and a need of deeper insights on meander form-process linkages through field-based studies and validation of existing components of models was thus recognized (Seminara, 2006; Hooke, 2013). Nonetheless, most of these theories consistently rationalize some form of inherent instability occurring within flow and bed features of channels i.e. intrinsic in nature (autogenic) to be the underlying cause of meandering (Rhoads & Welford, 1991; Hooke, 2003). Several relevant parameters of a meandering channel such as meander wavelength, width, and curvature are found to be intricately related with some threshold values of flow and or bed features based on experimental and field observations (Zolezzi & Seminara, 2001a; Seminara, 2006). Hence, the instability perturbations occurring within the linked variable set 'flow-bed topography- channel planform' cause-effect loops lays the foundation for the generation of meandering.

1.3. Meander planform, flow and associated processes

1.3.1 Planform

The majority of the groundwork on research on meandering phenomenon in rivers has been laid after the 1950s only. Including quantification of several key empirical relationships, such as that between meander wavelength and discharge; channel width and meander wavelength; radius of curvature and wavelength; radius of curvature and channel width (Leopold & Wolman, 1957, 1960), along with correlations between important form parameters like shape of meanders and cross-section geometry (Schumm, 1963).

These pioneering works were mostly driven by the striking similarity among river planforms, which indicated a generality in the underlying formative mechanisms (Leopold & Wolman, 1960; Davy & Davies, 1979). In a morphometric sense, meanders are best described when viewed from above i.e. in planform view, and there has been ample amount of research efforts directed at defining and analyzing meandering planform shapes. Initially, meandering planforms were characterized as regular paths composed of symmetrical bends. In this regards, studies attempted to characterize the shape of an individual bend or pair of bends planform using a simpler methods such as circle fitting to individual bends (Brice, 1973) or the more sophisticated mathematical curves (Langbein & Leopold, 1966; Ferguson, 1975) and converged onto the sine-generated curve to closely resemble the ideal shape of meanders (Kinoshita, 1961; Langbein & Leopold, 1966).

Analysis of meandering planforms has been facilitated by the use of maps and other cartographic sources (Hooke, 1977a). Whereby, river planform (as bank lines) is first extracted in GIS (Hooke, 1984), followed by digitization of the channel centerline and a piecewise linear interpolation to the set of digitized points to produce the centerline (Ferguson, 1975; Hickin, 1977; Hooke, 1977a; Howard & Hemberger, 1991). Morphometric parameters such as the planform curvature (C = 1/radius of curvature, radius of curvature is denoted by R) is calculated by the directional change between successive piece-wise segments fitted to the digitized points and subsequent determination of the rate of change in direction over distance (Ferguson, 1975; Howard & Knutson, 1984; Parker & Andrews, 1986; Furbish, 1991).

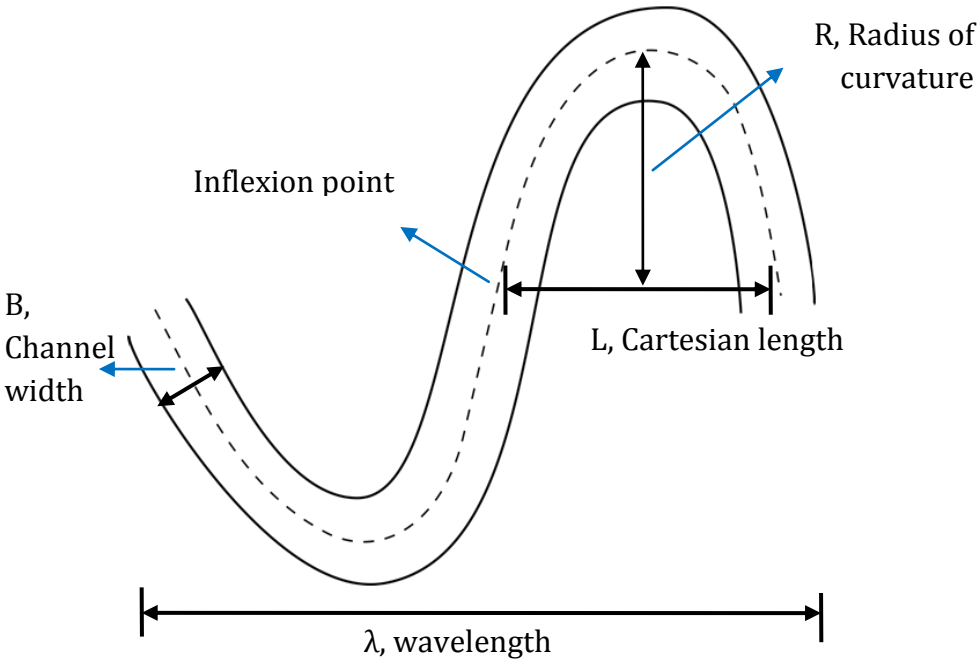

Fig 1 Meandering planform shape characteristics (modified from Leopold and Wolman, 1960).

Other parameters to quantify meander planform was also derived, such as wavelength (λ) i.e. the curvilinear length between the apexes, sinuosity (S) i.e. the ratio of curvilinear length to the cartesian or valley length (L) and channel width (B) (Fig 1).

However, it was soon realized that naturally occurring meandering planforms are scarcely regular (Schumm, 1963; Ferguson, 1975; Carson & Lapointe, 1983). So that observed irregularities from real rivers planform constitute of features like bend asymmetry (Carson & Lapointe, 1983), compound bends (Brice, 1974), skewing in bends (Parker et al., 1983; Parker & Andrews, 1986); fattening (Ikeda et al., 1981). In these regards, a need for defining additional parameters to describe these individual irregularities in terms of individual bends emerged (Howard & Hemberger 1991; Parker et al., 1983). A rather recently discussed irregularity in planform is the 'zigzagging' appearance of some rivers constituted of presence of longer straight sections with quickly turning apex (discussed later in detail), which has only been recently discussed in terms of their formative conditions and mechanisms of bend development (Andrle, 1994; Vermeulen et al., 2014), even though such planforms have been observed from several river types, as alluvial (Vermeulen et al., 2016), tidal (Kleinhans et al., 2009) of different sizes and geographic location, smaller temperate streams (Mansfield creek- Andrle 1994, Houston River- Alford et al. 1982) and in larger tropical rivers (Fly river- Dietrich et al., 1999; Purus and Jurua Rivers- Latrubesse et al.,

2005; Mahakam river- Vermeulen et al., 2014) around the globe. Most irregularities in the planform have been suggested to arise from floodplain properties, as local geological and sediment constraints (Ferguson, 1973, 1976, 1979). However, others suggest more autogenic influences in the maintenance of such planforms (Vermeulen et al., 2014). Therefore, an apparent gap remains in fully understanding the generation of such planforms.

1.3.2 Flow Structure and its interaction with hydraulic geometry

Flow in meander bends is governed by upstream flow properties modified by the continuous, and related, variations in channel curvature and bed topography (Camporeale et al., 2005). Therefore, the geometry of the bedforms and the flow field around the meanders are highly interlinked (Dietrich et al., 1979). The curving part of meander bends also known as the bend apex features steeper outer banks where erosion occurs, together with a pool located and sloping bed from the point bar on the opposite inner bank where deposition occurs, so that, the cross-sections produced are asymmetrical. Riffles are present in regions of inflexions (points of zero curvature) usually at the bend arms upstream and downstream of the apex and are relatively symmetrical at the cross-sections (Hooke, 2013). This presents the classical picture of the hydraulic geometry in meander bends (Markham & Thorne, 1992). Thus, an asymmetrical distribution of velocity occurs in meanders that often mimic the asymmetrical cross-section shapes of river meanders (Leopold & Wolman, 1960).

Flow in meander bends has been categorized into three regions, the inner, middle and outer channel regions (Markham & Thorne, 1992). At the inner channel region flow is controlled by the shoaling effect of the point bars which directs the flow outward towards the channel center (Hickin, 1978; Dietrich & Smith, 1983). Flow separation often develops within the inner region (Leeder & Bridges, 1975; Nanson, 2010) and is discussed in a detailed manner in the following section. The mid-channel region is occupied by helical flow also known as secondary flow cell that turns clockwise around the primary flow direction (Leopold & Wolman, 1960), thus representing a three-dimensional in structure (Dietrich, 1987). This flow helix turns in a manner that flow is outwardly directed (towards outer banks) at the surface and inwardly (towards inner banks) near the bed. And it is driven by local imbalance between outwardly directed centrifugal forces and an inwardly directed pressure gradient and is known to be affected by higher meander curvature (Bathurst et al., 1977), lower bank roughness higher width to depth ratios (Thorne & Furbish, 1995) and presence of a point bar (Dietrich & Smith, 1983).

At the outer-channel region, the bulk flow is shifted towards the outer half of the channel due to a combined effect of the bend geometry and centrifugal forces, thereby causing superelevation of water surface (Leopold & Wolman, 1960; Dietrich et al., 1979). An outer-bank cell rotating in a direction opposite to that of the mid-channel helix might also form in this region (Bathurst et al., 1977; Blanckaert & De Vriend, 2004). Furthermore, flow separation is also observed near the outer bank and is associated with the presence of an adverse pressure gradient (Blanckaert, 2010).

1.3.3 Flow separation at inner-banks and its significance

At the inner bank, a zone of separation can develop downstream of the bend apex on a horizontal plane i.e. around a vertical axis and this phenomenon is hereafter referred to as Inner-Bank Flow Separation zone, IBFS. Factors such as higher curvature and or high flow inertia (Froude number) have been known to favour the production of IBFS (Leeder & Bridges, 1975), a sudden break in bank-line of inner banks that can cause a sudden expansion of flow which in general favours IBFS (Parsons, 2002), as the main flow is unable to follow the channel boundary, producing a separation zone, with a zone of weakly recirculating flow located at the inner bank (Leeder & Bridges, 1975; Van Alphen et al., 1984).

On a horizontal plane (two-dimensional) IBFS is demarcated by a shear layer that separates the slower moving filament at the inner half of the channel and faster moving flow filament on the outside (Blanckaert et al., 2013; Blanckaert, 2015). This shear layer has been mathematically determined by calculating the inflexion in the S-shape curve formed in the cross-sectional 2-D plane of meanders (Blanckaert, 2015) (Fig 2).In bends of higher curvatures, even recirculation or stagnation of flow might develop near the inner banks (Fig 2).

Furthermore, IBFS can occur in two stages, as closed and opened (Blanckaert, 2015), whereby, in the former, the reattachment of separated flow occurs some point downstream of the point of separation while in the latter stage no reattachment occurs. Hence, IBFS has several implications for flow and processes within meander bends, such as in altering cross-stream currents (Bagnold, 1960), channel migration (Blanckaert, 2011), reducing effective channel width (Leeder and Bridges 1975) and point-bar growth (Burge and Smith, 1999). Moreover, stagnation zones formed at the inner banks of high curvature bends often also have organic-rich depositions (dead material) (Jackson, 1981) and IBFS by its action is also known to accumulate heavy metals deposits (Best & Brayshaw, 1985).

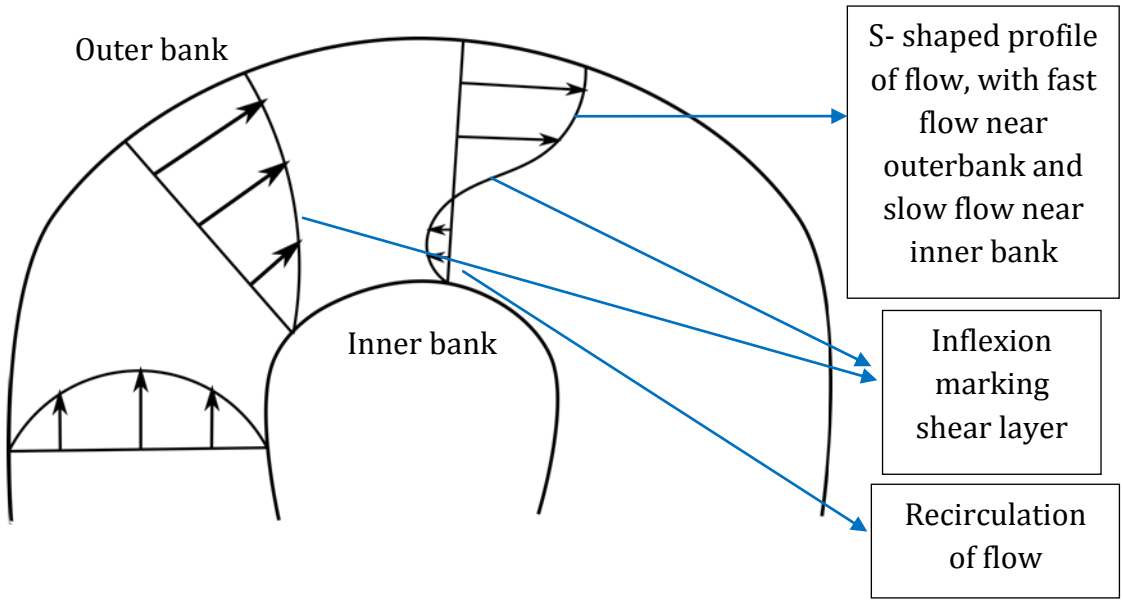

Fig 2 S-shaped, two-dimensional flow profile at meander apex (modified from Blanckaert, 2015).

1.3.4 Erosion and deposition processes

It has well been established that curvature induced velocity redistribution in bends and some degree of erodibility of bed and bank materials constitute the two key components for meandering dynamics (Camporeale et al., 2007). Bank erosion is a necessary condition for meandering to occur from an initially straight channel (Rhoads and Welford 1991). Also, a balance between erosion at the outer bank and deposition at the inner bank is necessary to maintain an equilibrium condition in a migrating meander bend (Thorne & Welford, 1994).

Erosion occurs at the outer bank region downstream of the meander bend apex and is associated with increased shear stress in that region (Hooke, 1975; Dietrich, 1987; Furbish, 1988). As an effect of curvature in meander bends, the maximum velocity of flow is shifted towards the outer bank region and the phase lag induced by the cross-over between bends displaces this high velocity past the bend's apex. Moreover, a stronger downwelling of flow occurs where the center region helix combines with counter-rotating outer bank helix directing the maximum velocity filament towards the lower part of the outer bank (Bathurst 1977; Markham and Thorne 1992; Furbish 1991). Overall, this leads to higher shear stress that is responsible for erosion that leads to undercutting of banks and subsequent bank failure (Hooke, 1995).

On the other hand, deposition occurs at the inner bank at the point bar region where the velocities are lower resulting in relatively lower shear stress. Structurally, point bars have a flat upper surface, a steep lower surface or point bar face and a depositional edge of the point bar crest. Moreover, IBFS zone is also known to enhance point bar growth as it deflects higher velocity flow away from the inner banks, and its recirculation core acts as an effective sediment trap (Dietrich & Smith, 1983; Nelson & Smith, 1989). In very sharp bends, deposition can also be caused upstream of outer bank and are termed as concave bank benches (Woodyer, 1975; Andrle, 1994), while in compound bends more than one point bars have been observed to occur (Hooke & Harvey, 1983).

1.4 Meander morphodynamics and scales of development

Spatial and temporal scales at which processes that govern meandering occur display a wide range, from the smaller spatial scale processes such as the interactions among flow structure, sediment transport, and bed morphology in individual bends (Dietrich & Smith, 1984; Frothingham & Rhoads, 2003) to larger-scale processes such as the planform evolution of a series of meander bends (Güneralp, 2007; Hooke, 2007; Gautier et al., 2010). Temporal scales range from shorter processes like channel-bar dynamics occurring over a few decades (Hooke & Yorke, 2010) to longer temporal scale processes such as floodplain development over hundreds to thousands of years (Howard, 1996; Sun et al., 2001; Camporeale et al., 2005; Frascati & Lanzoni, 2009). Several factors affect the rates of meander change over the medium and long term scales that modify interactions between flow and bed morphology (Lagasse et al., 2004), such as, discharge (Schumm, 1968; Nanson & Hickin, 1986), mobility of bed sediment (Nagabhushanaiah, 1967), erosion of basal material from the outer bank toe (Hickin and Nanson 1984), sediment supply (Ackers & Charlton, 1975), erodibility of bank material (Hasegawa, 1989), riparian vegetation (Hickin and Nanson 1984), land-use change-deforestation (Burckhardt & Todd, 1998) or afforestation (Murgatroyd & Ternan, 1983).

Meanders often not only laterally extend or grow in amplitude but, also translate in the downstream direction and display other modes of change such as rotation and compounding (Hooke, 1977). A temporal sequence of meander development was discerned by Hickin (1977) as initiation, growth and termination, which was described to be successively occurring for a typical bend. Additionally, a trend of transition between these developmental phases was characterized by a non-linear trend in migration rates with relation to decreasing width normalized radius of curvature (R/B), i.e. bends tending towards

becoming sharply curving (Hickin, 1977; Hickin and Nanson 1984). This non-linear trend is marked by different phases of development: In the initiation phase, slower migration rates are observed in bends displaying a radius of curvature to channel width (R/B) c. 4.5 and higher, while in growth phase migration reaches the maximum migration rates with the values of R/B ratios falling in the range 3- 4.5, finally in the termination phase an abrupt decline in migration rate along with a drop in the R/B ratio to about 2. Therefore, meanders in initial stages of development grows at higher rates, before reaching a mature phase where migration slows down, following which they might compound and or proceed to cut-off (Hooke, 2013).

1.5 Bend-scale approach to study meanders

Meander trains are composed of individual bends represented by periodic reversals of curvature series (Hooke, 1984; O'Neill & Abrahams, 1986) where each bend is demarcated as the path between two consecutive inflexion points (Howard & Hemberger, 1991). Since forms are intricately linked with their morphodynamics(Furbish, 1988; Güneralp & Rhoads, 2009), a bend-scale framework is helpful in linking static planform shapes to their historical dynamic signatures (Schwenk et al., 2015).

Bend scale morphodynamics represents a naturally occurring intermediate scale between global (river-valley) and local (cross-sections) scales that are therefore helpful in linking local-scale physical processes to reach scale. As cut-off meanders are frequently preserved at this scale (Schwenk et al., 2015) also engineering works often deal with morphodynamics of single bends (Shields et al., 2005; Rossell & Ting, 2013). Meandering models predict the hydrodynamic effect from nearby bends to become negligible beyond a length of one meander wavelength (Ikeda et al., 1981; Zolezzi & Seminara, 2001). While comparing three contemporary models of meander morphodynamics, Camporeale et al., (2005) noted that the outputs of these models are statistically indistinguishable, particularly for predicted meander wavelengths and curvature, as the models are smoothened by reach wide averaging. Indeed the problem of statistical averaging has been discussed previously (Hooke, 1984), particularly, when averages of already averaged parameters are commonly used when considering scales higher than individual bends. In addition to this, inhomogeneity in the characterization and nomenclature of bend shape types has been observed throughout literature studies on meander bends (Carey, 1969; Andrle, 1994) and presents an initial challenge towards the understanding of the bend form-process linkages (Vermeulen et al., 2016).

1.5.1 Ambiguity in the nomenclature of bend forms

Meander bends are difficult to classify with single measures (Ferguson, 1975), and that averaging over already averaged quantities results in loss of information. Therefore, individual bend-shapes features have been elaborated making the use of a suite of morphometric parameters (for example in Howard & Hemberger, 1991). However, such works have focused mostly focused on spatial analyses of morphometry rather than on bend dynamics.

Brice, (1973) delineated meander bends into 4 basic forms namely- simple symmetric, simple asymmetric, compound symmetrical and compound asymmetrical. This typology provided quantitative means of demarcation between simple and multilobed bends, employing simple morphological variables such as bend wavelength, curvature and amplitude. Early research such as those of Brice (1973, 1974) and used circle fitting method to calculate the R/B ratio as the radius of a best-fit circle divided by bend averaged channel width (Leopold and Wolman 1960). This method, however, is often subjective because of the average radius that could fit into a bend (Hooke 1984), therefore, giving a singular value that does not take into account the curvature in the arms to that at the shape of bends.

Recently, with advancements in mapping and computational power more objective techniques such as digitization of centerline spatial series of bends have been used (Zolezzi & Seminara, 2001a, 2001b; Legleiter & Kyriakidis, 2007; Monegaglia et al., 2018). And classification and analysis of meandering behavior using curvature distribution have been recommended (Hooke & Harvey, 1983). Regardless of this, ambiguity in the nomenclature and morphometric characterization of simple bend shapes, typically between low curvature and high curvature bend classes has appeared constantly throughout literature which therefore presents an initial challenge towards the understanding of the form-process linkages.

Moreover, it was realized that several variations in simple bend shapes can exist in freely meandering rivers. Several types of simple bend shapes have therefore been described such as bends with curvature slowly varying between consecutive inflexion points, the whereby radius of curvature to width ratio (R/B) does not fall below 2 (Hickin and Nanson, 1984), termed as ‘round’ or ‘mildly curving’ bends. These are opposed to bend forms with curvature to width ratio (R/B) lower than c. 2 that have been termed in literature as tight or sharp (Hickin 1977). Additionally, elongated mature forms exist with a hairpin-like appearance termed as ‘fat’ forms (Parker et al., 1982b). Fat bends also display an initial bi-

peaked curvature distribution that closely resembles that of a compound bend (Langbein and Leopold 1966; Güneralp and Marston, 2012). On the other hand, bends with straighter arms and high curvature apex (Dietrich 1999) were termed as abrupt angle bends (Carey 1969), a series of these bends would give a zigzagging planform view (Vermeulen et al., 2014). Other variations in meanders like bend asymmetry (Carson & Lapointe, 1983) displaying an upstream or downstream skew have also been recognized (Parker et al., 1983; Zolezzi & Seminara, 2001a; Marani et al., 2002; Güneralp & Rhoads, 2011).

The most accepted morphometric difference in shapes like round versus sharp bends have been defined through early works of Hickin, (1977) and Hickin and Nanson, (1984), whereby they suggested a ratio of radius to width (R/B) below 2 (or 0.5 for B/R) to delineate sharp bends from round ones based on differences in their migration behaviour. Moreover, studies have also used functional thresholds to delineate round from sharps bends, such as by quantifying relative differences in strengths of centrifugal force induced secondary flows between these bend shapes (Pittaluga & Seminara, 2011).

Additionally, differences between low and higher curvature bend shapes have been extended to their flow characteristics, hydraulic forms and morphodynamics as well. For instance, low curvature bends are known to display features such as weaker secondary flow and associated weaker flow redistribution and lower shear stress across the apex (Hickin, 1978; de Vriend, 1981; Blanckaert & De Vriend, 2003), slowly varying bed-topography (Pittaluga et al., 2009), overall shallower depths and erosion at the outer banks and deposition at the inner banks (Leopold & Wolman, 1960). In contrast, high curvature bends display stronger flow redistribution (Ottevanger et al., 2012); flow separation at inner and or outer banks (Hickin, 1977, 1978; Andrle, 1994); deep scour holes (Vermeulen, 2015); concave bank benches (Woodyer, 1975) develop; circular-shaped meander pools (Andrle, 1994) and an inverted erosion-deposition pattern erosion-deposition around the bend apex (Hickin, 1978; Vermeulen, 2015). Given these features, high curvature bends also display great variation in their migration dynamics (Hickin & Nanson, 1975, 1984; Hooke, 1987; Hudson & Kesel, 2000), which has been generally attributed to their unconventional form, flow and associated flow processes (Blanckaert, 2011).

Altogether, an apparent knowledge gap in the parameterization of these distinct shapes challenges our current understanding of meandering form and processes. Particularly, as some of the aforementioned planforms are not reproduced even by state-of-the-art meander evolution models that are based on the approximate solution of the momentum and mass conservation equations for the water and sediment phases (Ikeda et al., 1981; Parker & Andrews, 1986; Zolezzi & Seminara, 2001a; Frascati & Lanzoni, 2009). Furthermore, modeling aimed at predictions of meander behavior would allow dealing with bends that take into account the existing knowledge on form and processes in these bends, but will be unsuitable for bends with shapes such as those of abruptly curving or angular bends, and where form-process linkages have so far rarely been studied in the field.

1.6 Summary of research gaps and aims of this thesis

Several lacunae in the theoretical understanding of the cause of meandering in rivers still remain (Rhoads & Welford, 1991). Various degree of irregularity has been commonly observed in many naturally occurring river planforms whereby, typical zigzagging river planforms are observed to develop in river systems across the globe (Andrle 1994; Latrubesse et al., 2005; Ettmer & Alvarado-Ancieta, 2010; Vermeulen et al., 2014), even though these rivers show both contrasting and common characteristics in terms of their channel gradient, size, sediment supply, floodplain material and environmental conditioning. Moreover, in zigzagging planforms the meander trains are constituted of bends that showcase long straight reaches connected with abrupt turns and that are different from river planform that display more sinuous appearance and are constituted of gradually curving bends. Therefore, deeper insights on underlying formative conditions and characteristics of bends composing such planforms is crucial in understanding how these planforms develop, behave and are maintained at various time-scales.

Simulations from morphodynamic models whereby elongated mature fat forms, bend asymmetry, and compound bends are reproduced, mostly do not represent bends with high curvature forms like abruptly curving or angular forms. Understanding meander bend forms-process linkages at the bend-scale have been perceived to be critical in understanding the historical dynamics of meanders (Schwenk et al., 2015). Whereby, a detailed description of bend morphometry using several parameters has been prescribed to be crucial (Howard and Hemberger, 1991), particularly for lesser-known bend types like those in high curvature categories. High curvature bends show unconventional behavior in terms of their occurrence

in planforms, planform and hydraulic form which is reflected in their anomalous dynamics, and therefore detailed knowledge on such bends is necessary to discern the governing morphodynamic feedback processes. Detailed field-based investigations of flow, macro-scale bedforms and their interactions in such bends are still lacking.

Such knowledge gaps have been only partially filled in the last decade mostly due to increased capacity in field data collection and higher computational power to process field data. In order to contribute to further improved understanding especially of the morphology, hydraulics and morphodynamics of unconventional river meanders, I selected a 400-km long reach of Prut River (Romania/Republic of Moldova) that still retains its original dynamics while displaying bends with diverse planimetric forms, including some highly zigzagging and fat bends. The dynamic nature of Prut is observable through several recognizable geomorphological features. See for example *Plate I* for steep vertical banks; that are prone to undercutting as was observed by exposed roots on such banks; lateral connectivity with adjacent land during high flow and *Plate II* for chute cut-off; complete trees slumped into channel due to bank failures; deposition patches due to deadwood; erosion of point bars in high curvature bends.

Plate I


Eroding steep banks in Prut bends
Photo:MT Pusch


Photo:MT Pusch
Exposed roots due to undercutting of banks


Photo:MT Pusch
Inundated riparian area

Plate II

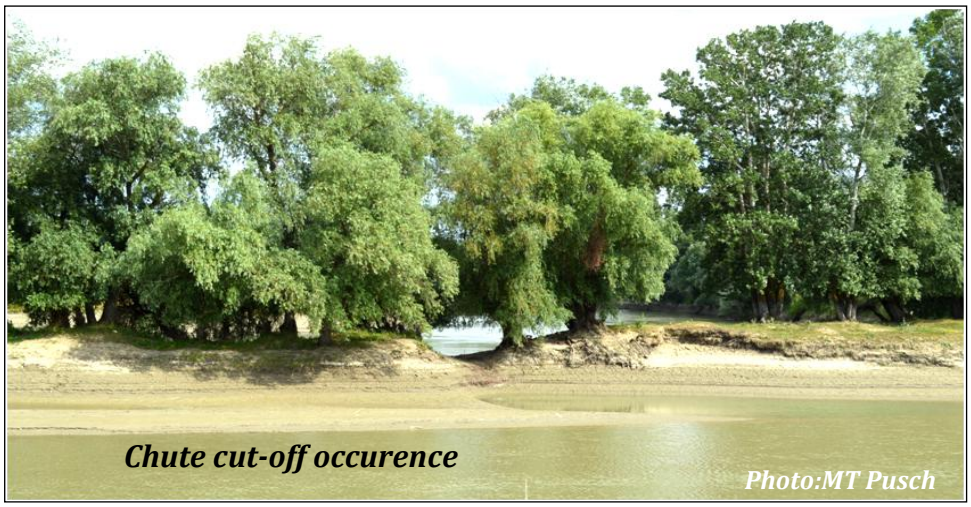

Chute cut-off occurence ***Photo:MT Pusch***

Slumped trees in the channel ***Photo:MT Pusch***

An eroded point bar in a sharp bend ***Photo:MT Pusch***

In detail, this thesis aims to achieve these research objectives:

1. Characterization of the shape and distribution of simple **bend types** occurring on the Prut.
2. Comparison of bend-scale **morphometric characteristics** among simple bend shapes, with a focus on comparing unconventional (sharp and angular bends) and conventional (round and fat) bend types.
3. Comparison of **morphodynamic characteristics** and temporal trends among simple bend types.
4. Analysis of **extrinsic versus intrinsic controls** over observed bend planforms.
5. Demonstration the **long term channel dynamics** of the Prut River.
6. Quantification of **inter-relationships** between planform and hydraulic geometry variables in selected meander bends.
7. Investigation planform and hydraulic geometric **controls on flow processes** such as flow separation at inner-banks of bends.
8. Analysis characteristic differences among flow and hydraulic geometry occurring between **conventional and unconventional** bends.

1.7 Thesis outline (chapter wise aims and objectives)

This thesis is comprised of two main research pieces. Chapter 2 discusses morphometric properties of different simple bend shape types and links this to their morphodynamic character on Prut River. Chapter 3, elaborates a novel dataset on bend form, flow and bathymetry collected from a set of meander bends. Next, it analyzes flow separation occurring at the inner banks in bends of varying planform shapes. Major implications of the form-process linkages are presented as a simple model for bend developmental trajectories.

Chapter 1:

General introduction

Chapter 2:

Tarun Bisht, Stefan Gramada, Federico Monegaglia, Martin T. Pusch and Guido Zolezzi. Long-term trajectories and morphodynamics of meander bends in a European lowland river.

Ready for submission to peer reviewed journal

Author's contributions: TB designed the study and lead the writing. SG acquired and prepared cartographic material. FM extracted data through PyRIS. GZ and MP interpreted and conceptualized and contributed to the text.

Chapter 3:

Tarun Bisht, Federico Monegaglia Guido Zolezzi and Martin T. Pusch. Planform and hydraulic geometry controls of the inner-bank flow separation in meanders of a lowland river.

Ready for submission to peer reviewed journal

Author's contributions: TB designed the study, carried out the field work, analyzed the data and lead the writing. FM extracted data through PyRIS. GZ and MP interpreted analysis and conceptualized and contributed to the text.

Chapter 4:

General discussion

2. Long-term trajectories and morphodynamics of meander bends in a European lowland river

2.1 Abstract

Most European rivers have been heavily modified so that natural channel patterns and dynamics have mostly vanished. This especially concerns meandering rivers, typically found in lowland areas, which have been subject to most intense hydro-morphological regulation, as their floodplains are now fertile cropland. Here, I investigate the morphodynamics of one of the longest remaining dynamic lowland river in Europe, the Prut River (Romania/Moldova). I analyze and compare the morphodynamic properties of the different river bend geometries found there (sharp, round, angular and fat shapes), with an emphasis on the angular and sharp bends that are less common in other meandering rivers. I demonstrate the historical dynamics of the river planform for c. 250 river km, based on three historical maps and a recent aerial image spread across a 90-year period. The investigated river segment showed a temporal morphological trajectory characterized by a gradual narrowing, reduction of migration rates and increasing sinuosity. Approximately 28% (N=118) of simple (i.e. not compound) bends exhibited an angular and or sharp planform geometry that differs from round and fat shapes, respectively. Sharp bends were distinguished from round and angular from fat bend geometries by width normalized bend curvature and the maximum to mean curvature ratio, respectively. Dimensionless wavenumber further adds characteristics lengths of the different bend shapes. Round and fat bends were discerned as conventionally occurring, long bends, whereas sharp bends were mostly short bends, while angular bends were not invariably short. Sharp and angular bends tend to stabilize for longer periods (20-90 years) under the observed trajectory of the Prut. Hence, this study describes for the first time the centennial evolution of a meandering river in Europe, also contributes to the analysis of the poorly explored linkages between forms and processes of river bends, including explanations for the formation and relative longevity of unconventional bend forms.

2.2. Introduction

A fundamental characteristic of many natural lowland rivers is a meandering planform(Rosgen& Silvey, 1996). Meanders result from the interplay between a continuous elongation of the river channel, which increases its sinuosity at characteristic, physically unstable length scales (Blondeaux & Seminara, 1985) until the meander is cut-off (Camporeale et al., 2005), which intermittently limits channel sinuosity, and locally accelerates downstream sediment transfer through enhanced channel-floodplain interaction (Zinger et al., 2011). Such morphological changes in natural meandering rivers occur at a variety of temporal scales (Güneralp et al., 2012), from short-term dramatic events related with neck cutoffs (days to months) (Hooke, 2004), to slower scales of bend development before cutoff (tens to hundreds of years) (Howard, 1992; Frascati & Lanzoni, 2009) and channel adjustments associated to the effects of human intervention (Surian & Rinaldi, 2003). Meandering rivers of apparently very similar planform may show huge differences in terms of the time-scale of bend development, possibly associated with differences in the rate of sediment supply (Constantine et al., 2014). This makes it difficult to associate specific time scales to each process because these scales can vary enormously across different streams.

Despite such marked difference in time scale, meandering rivers show surprisingly high similarity in planforms, with meander bends developing quite similar shapes across different spatial scales. Many meandering rivers worldwide tend to develop bends with a radius of curvature much higher compared to the channel width (Leopold & Wolman, 1960; Lagasse et al., 2004) and with a typically rounded appearance so that their curvature varies slowly relative to the stream distance. Thereby, the detailed shape of such meander bends is described in terms of their fattening and skewing (Parker et al., 1982b). And in these cases, either the ratio of width to local radius of curvature in a bend does not reach high values in any cross-section of the bend (hereafter, “round bends”), or the peak value of bend curvature does not show large discrepancies relative to average bend curvature value (hereafter, “fat bends”)

(Ikeda et al., 1981). In addition, meandering rivers studies, namely on the Mahakam River, Indonesia (Vermeulen 2014), Ucayali River, Peru s(Ettmer & Alvarado-Ancieta 2010), Devon streams and Dane River, England (Hooke 1977 and 2007) and Mississippi River (Carey, 1969; Hudson & Kesel, 2000)have reported less conventional and regular bend shapes.These shapes I will refer to as “sharp” and or “angular” (or collectively as

unconventional bends) (Fig 3A), as opposed to round and or fat (conventional bends) (Fig 3B), respectively.

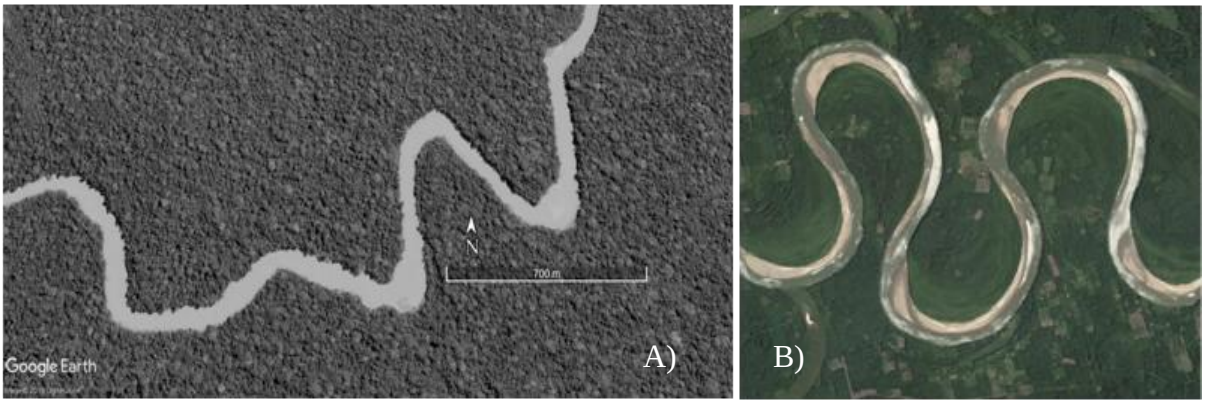

Fig 3 Examples of planform view from two rivers in the Bolivian Amazon. (A) typical "unconventional" meander bends (location: 64° 12'52.21" W, 16° 06'1.70'' S) and (B) typical "conventional" meander bends (location: 64° 47'28.67" W, 16° 54'53.50'' S) (source: Google Earth).

The nomenclature and morphometric characterization of simple bends have not been homogenous throughout literature. For example, angular bends have also been referred to as abruptly turning, unconventional or unusual bends (Carey, 1963; Alford et al., 1982; Richards, 1987; Andrle, 1994); fat bends being descriptively referred to as round or full (Güneralp & Marston, 2012); round bends as mildly curving bends (Ikeda et al., 1990) and sharp bends as tight bends (Nanson, 1980; Parker et al., 1983).

Physically, sharp bends are characterized by unusually high local values of centerline curvature, while, angular bends can be viewed as a subtype of sharp bends comprised of typical long, almost straight river stretches joined by an abruptly turning apex. Interestingly, models of meander morphodynamics based on the approximate solution of the momentum and mass conservation equations for the water and sediment phases, typically reproduce only conventional meander bend shapes (eg. round and fat forms in Ikeda et al., 1981; Parker & Andrews, 1986; Zolezzi & Seminara, 2001; Frascati & Lanzoni, 2009). This reflects the paucity in the understanding of underlying principles of generation, maintenance, morphometric characteristics and simply even the relative proportion of occurrence of such bend forms in nature. On the other hand, complex bend forms (compound bends and multilobed bends) may emerge as modeling outcomes only when spatial heterogeneity of floodplain erodibility is externally imposed (Güneralp & Rhoads, 2011). In order to observe

the evolution of bends at natural rivers, morphological changes are usually detectable through analysis of maps and imagery for a minimum of several years (Nanson & Hickin, 1986). Therefore, long-term (> 20 years) data is crucial to discern detectable changes in meander form.

Theoretically, bends undergo a typical evolution cycle that entails stages of bend initiation from a rather straight channel, lateral growth and downstream translation of the bend and a subsequent termination stage by cut-off (Hickin, 1977, 1978). While many studies focused on the first two types of changes i.e. meander bend evolution (Hickin & Nanson, 1975; Nanson & Hickin, 1983; Hooke, 1997; Hooke, 2003) and cutoff description (Howard & Knutson, 1984; Camporeale et al., 2005; Schwenk et al., 2015; Schwenk & Foufoula-Georgiou, 2017) fewer studies are available in relation to channel adjustment caused by anthropic effects on the morphodynamics of meandering rivers (Hudson & Kesel, 2000; Shields Jr et al., 2000; Urban & Rhoads, 2003) In comparison, long-term channel adjustments, resulting from intensive hydro-morphological alterations across Europe particularly in the past decades, have been mainly analyzed for braided or wandering streams (Surian & Rinaldi, 2003; Comiti et al., 2011; Kiss & Blanka, 2012; Provansal et al., 2014).

This study attempts at reducing the above-mentioned knowledge gaps by focusing on a long (circa 250 km) section of the Prut River, one of the few remaining freely meandering (single thread) lowland rivers in Europe, which has been subjected to much lower hydro-morphological pressures compared to most other rivers of similar size and morphology. Specifically, the aims of the paper are to

1. investigate the channel morphodynamics and adjustments that had occurred on Prut river during 1915-2005, at various spatio-temporal scales,
2. characterize and compare the bend-scale morphometry of simple bend shapes occurring in the 250-km long section, with a focus on sharp and angular types, and
3. quantify and compare the bend-scale morphodynamics of different bend-types, particularly, sharp vs. round and angular vs. fat bends.

The aim was to shed light on the form-process linkages that describe the planform morphology and morphodynamics of the unconventional bends of the Prut River. Further, to these aims, I collated a database on meander morphometry and dynamics extracted from a larger *c.* 400-km section of the Prut River (Romania/Moldova) as one of the last relatively

freely-meandering river segments in Europe. This analysis uses available historical maps since 1915, allowing us to analyze > 200 meanders for a 90-year period. For this, I adopted a bend scale, where conceptually, the developmental trajectories of individual bends were traced through time (Schwenk et al., 2015).

2.3 Material and methods

2.3.1 Study area

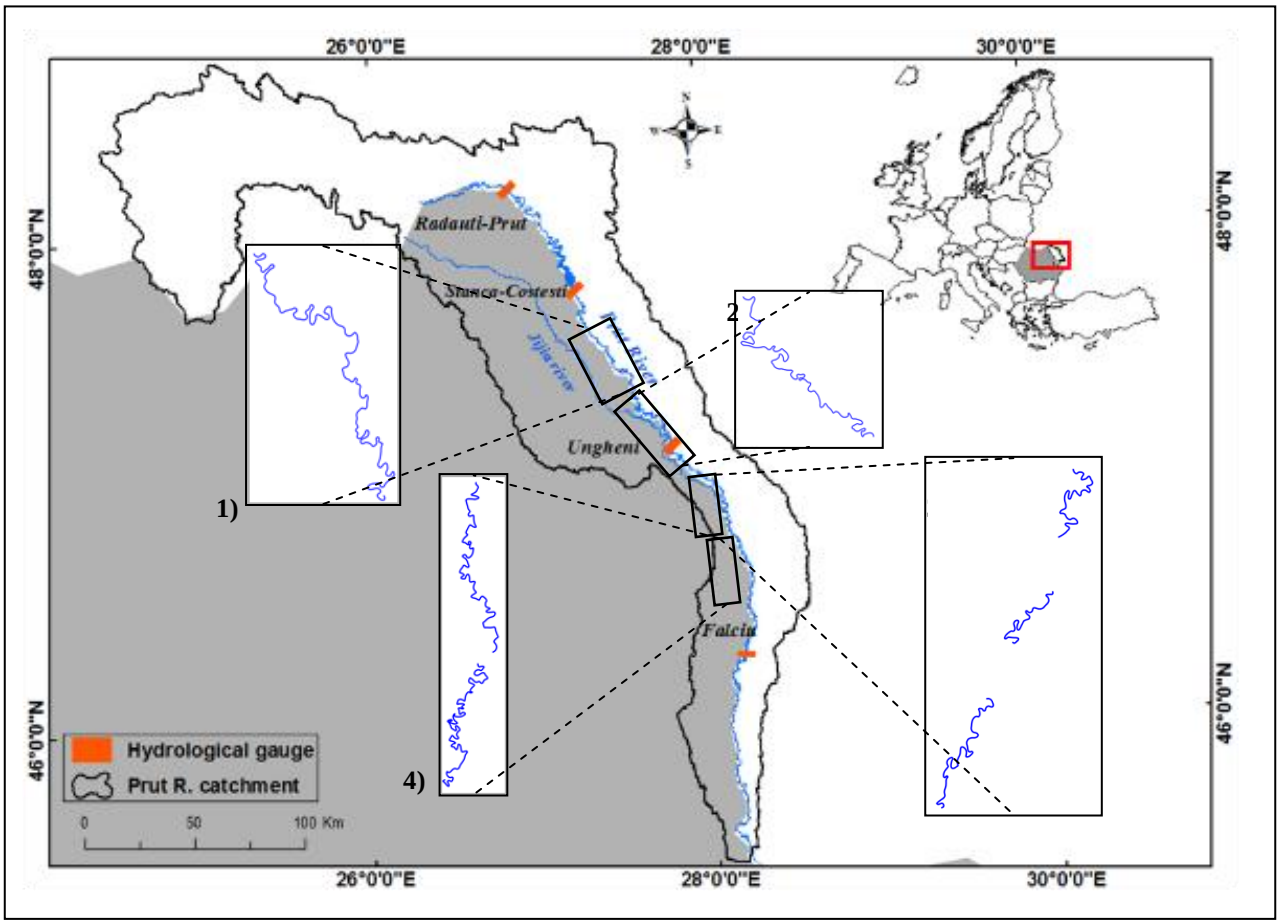

Fig 4 Location of study sections of the Prut River, with numbered boxes highlighting the 4 river sections included in the study (territory of Romania shaded).

The 400-km long segment of the Prut River in southeast Europe (Fig 4) that forms the border between Romania and Republic of Moldova consists of a large set of dynamic and mostly unconstrained meanders, an almost unique example in Europe among alluvial rivers of comparable size and length. The meandering of the Prut has been laterally unconstrained for most of its length nearly until the present, with only a few local bank reinforcements and widely-spaced levees over a linear distance of nearly 300 km.

The Prut River originates from the east Carpathian Mountains near the highest peak (Howerla, 2061 m) of Ukraine. It has a total length of 953 km and drains a catchment area of 27540 km^2, covering parts of Ukraine, Romania and the Republic of Moldova. The course of the river is interrupted only by one dam forming the Stanca-Costesti reservoir that was constructed during the period 1973-1978, which has a maximum capacity of 1400 million m^3 (Romanescu et al., 2011). Downstream the reservoir, the Prut River flows another 570 km, also acting as an international border between Romania and the Republic of Moldova, before eventually joining the Danube as its last left-side tributary. The average channel slope in the Romanian/Moldavian territory upstream to the Stanca-Costesti reservoir is about 0.61 m/km, while in the downstream section (up to Falciu) it is reduced to an average of 0.17 m/km, while sinuosity is around 1.1 in the upstream section and 2.0 in the downstream section. Once arrived in the Romanian/Moldavian plains, the river flows ina roughly southward direction until it joins the Danube east of the city of Galati. A peculiar feature of the Prut River, related to the highly tapered shape of its catchment, is the relative absence of major lateral tributaries in the plains, which results in spatially constant average flow conditions for hundreds of kilometres of river length. The multi-annual average discharge of Prut River (for 1950-2008) increases from 78.1 m^3s^{-1}near Radauti (upstream of the reservoir) to 86.7 m^3s^{-1} near Ungheni and after that still slightly increases to about 93.8 m^3s^{-1} at Oancea, just before joining the Danube (Romanescu et al., 2011). The only lateral tributary joining the middle-lower Prut is the Jijia River. It joins the Prut at Gorban, at the beginning of midsection and it adds a discharge of about 10 m^3s^{-1} (Doltu & Dumitran, 2011).

2.3.2 Cartographic databases

Meander analyses were based on three cartographic maps from 1915, 1960, 1980 and one orthophoto from 2005, hence covering a 90-year period between 1915 and 2005 and referring to the territories of Romania and Moldova (Table 1). These documents were georeferenced using the georeferencing function in Arc GIS (version 10.2). This function further allowed rectification of coordinates in a map based on reference points that were existent in all cartographic documents. For instance, the topographic maps from 1915 and 1960 period were rectified by establishing a minimum of four common points from both maps (churches or road intersections). Four river sections could be found in all the four considered data sources (named 1 to 4 in Fig4) and they were then selected for analyses. The total length of the river channel in these four sections is 250 km.

Table 1 Details of cartographic documents employed for the planform analysis of Prut River.

Map type	**Date of survey**	**Year published**	**Scale**	**Projection**	**Institution**	**Resolution**
Topographic plans	1915	1959	1:20000	Lambert Gauss - Kruger	Romanian Military Topographic Service	1.68m /pixel
Topographic maps	1958	1961	1:25000	Gauss – Krüger Pulkovo, Cylindrical Projection 1942	Romanian Military Topographic Service	2 m/pixel
Topographic Maps	1977	1980	1:25000	Gauss – Krüger Pulkovo, Cylindrical Projection 1942	Military Topographic Department	2 m/pixel
Orthophotos	2005		1:5000	Stereographic projection Stereo 70ellipsoid Krasovschi	National Agency for Cadastre and Land registration	0.5 m/pixel

2.3.3 Extracting meander bend morphometry and morphodynamic data

Properties of meander bends were extracted using the recently developed PyRIS software (Monegaglia et al., 2018). PyRIS (Python- RIvers from Satellite) is fully automated, process-based software for extracting extensive information on meandering river morphodynamics from multi-temporal, multi-spectral remotely sensed imagery. The PyRIS algorithm allows the following main automated computations relevant to the present work: (i) detection of the centerline of the main river channel (Fig 5A); (ii) computation of local migration vectors between subsequent centerlines (Fig 5A); and (iii) computation of bend-scale morphometric parameters and migration rates (Fig 5B and 5C). In the present work, PyRIS has been applied to extract local and bend scale curvature and meander migration rates to the river channels extracted from the three cartographic maps and from the 2005 orthophoto.

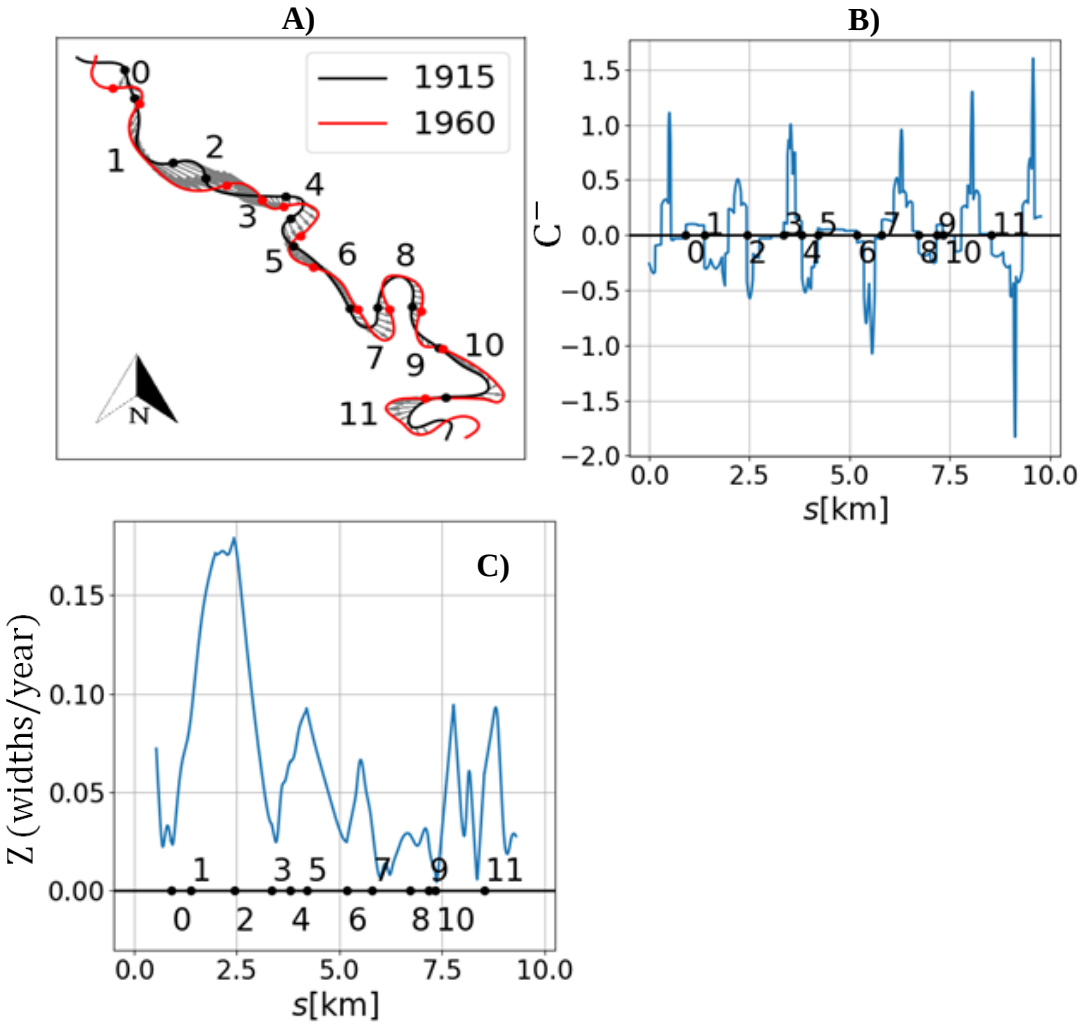

Fig 5 Exemplified illustration of the main meander parameters computed through the PyRIS software. A) Two centrelines taken at consecutive times (1915- black, 1960- red) of a sample reach of the Prut River with the result of individual bend separation (marked by dots denoting inflexion points) and local migration vectors; B) local curvature (C^-) along a 10-km river reach of the 1915 centreline, where S is the distance along the reach in km; C) computed local migration rates between 1915 and 1960 for the same reach, with dots denoting meander inflexion points. Note: the numbers in panels signify detected bends numbered from upstream to downstream.

Centerlines were extracted in the form of the (x_i, y_i) coordinates of centerline points P_i, digitized at a regular spacing of $\Delta s = W/2$ (W, being the section-averaged channel width) and smoothed using a Polynomial Cubic Spline interpolation (Güneralp & Rhoads, 2008). From the (x_i, y_i) coordinate points in the Cartesian space three spatial series were computed: the meander arclength between two successive points i.e. *i-1* and *i* (intrinsic coordinate s_i),

the local meander inflexion angle, θ_I and the local channel curvature C_i, through the following standard relations:

$$s_i = \sqrt{(x_i - x_{i-1})^2 + (y_i - y_{i-1})^2}$$

$$\theta_i = \arctan\left(\frac{y_i - y_{i-1}}{x_i - x_{i-1}}\right)$$

$$C_i = \frac{\theta_{i+1} - \theta_{i-1}}{2delta\ S}$$

To allow comparability with other rivers and among bends in different reaches, curvature values are scaled with the bend-averaged channel width (B), so that:

$$C_i^- = C_i * B$$

Meander inflexions are defined as the centerline points corresponding to a change in sign of the centerline curvature. The part of a meander centerline occurring between two successive inflexion points (Howard & Hemberger, 1991), is hereafter referred to as a 'bend'. I adopted a bend-scale perspective for our analysis, meaning that many of the extracted bend properties are either local values or bend-averaged values (Schwenk et al., 2015). For each section, the bends were numbered starting from upstream to downstream along the channel arclength. Following this, more than 200 bends in each of the four analyzed cartographic/image sources (1915, 1960, 1980 and 2005) were recognized in the study sections. For each centerline point (x_i , y_i), local migration vectors were computed through PyRIS (Moengaglia et al., 2018)in terms of magnitude and orientation.

Bends were classified into "simple" and "compound". Simple bends had only one single curvature maxima between two consecutive inflexion points (eg. Güneralp & Rhoads, 2008). Afterwards, simple bends that did not undergo cut-off through a 90-year period were selected for the morphometric and morphodynamics analysis. This resulted in 118 bends. Furthermore, through visual inspection of the cartographic documents, bend confinement was assessed using the following criteria. Firstly, from the apparent closeness to the dike and secondly, from the mode of migration of the bend before and after the dikes were constructed. In brief, bends that were too close to a dike and displayed a restrained-migration style were classified as confined.

The following bend shape metrics were computed for all 118 bends analyzed for each of the time points:

Bend sinuosity:

$$S = \frac{L}{Lx} \dots \dots \dots \dots \dots \dots \dots \dots \dots \dots \dots \dots \dots \dots \dots \dots \dots \dots \dots \dots \dots \dots \dots \dots \dots . (1)$$

Curvature ratio:

$$Cr = \frac{C_{max}}{C_{mean}} \dots \dots \dots \dots \dots \dots \dots \dots \dots \dots \dots \dots \dots \dots \dots \dots \dots \dots \dots \dots \dots \dots . (2)$$

Dimensionless maximum bend curvature:

$$C^{-} = C_{max} * B \dots \dots \dots \dots \dots \dots \dots \dots \dots \dots \dots \dots \dots \dots \dots \dots \dots \dots \dots \dots \dots \dots . (3)$$

Dimensionless cartesian wavenumber:

$$\lambda_x = \frac{\pi}{\left(\frac{2L_x}{B}\right)} \dots \dots \dots \dots \dots \dots \dots \dots \dots \dots \dots \dots \dots \dots \dots \dots \dots \dots \dots \dots \dots \dots (4)$$

Dimensionless meander wavenumber:

$$\lambda = \lambda_x * S \dots \dots \dots \dots \dots \dots \dots \dots \dots \dots \dots \dots \dots \dots \dots \dots \dots \dots \dots \dots \dots \dots \dots (5)$$

Meander migration rate (M) was scaled with the mean channel width (B) to express it as follows (expressed in widths/year, see Eq. 6)

$$Z = \frac{M}{B_{mean}} \dots \dots \dots \dots \dots \dots \dots \dots \dots \dots \dots \dots \dots \dots \dots \dots \dots \dots \dots \dots \dots \dots (6)$$

With:

L = bend length measured along the centerline

Lx = cartesian length, between two consecutive inflexion points,

C_{max} = maximum value of curvature in a bend,

C_{mean} = mean value of curvature in a bend.

2.3.4 Classification of different bend types

To objectively distinguish rounds from sharps I used the criterion provided by Hickin and Nanson, (1984), according to which sharp bends are those for which dimensionless maximum bend curvature exceeds 0.5 (Eq. 3), see Fig 6.

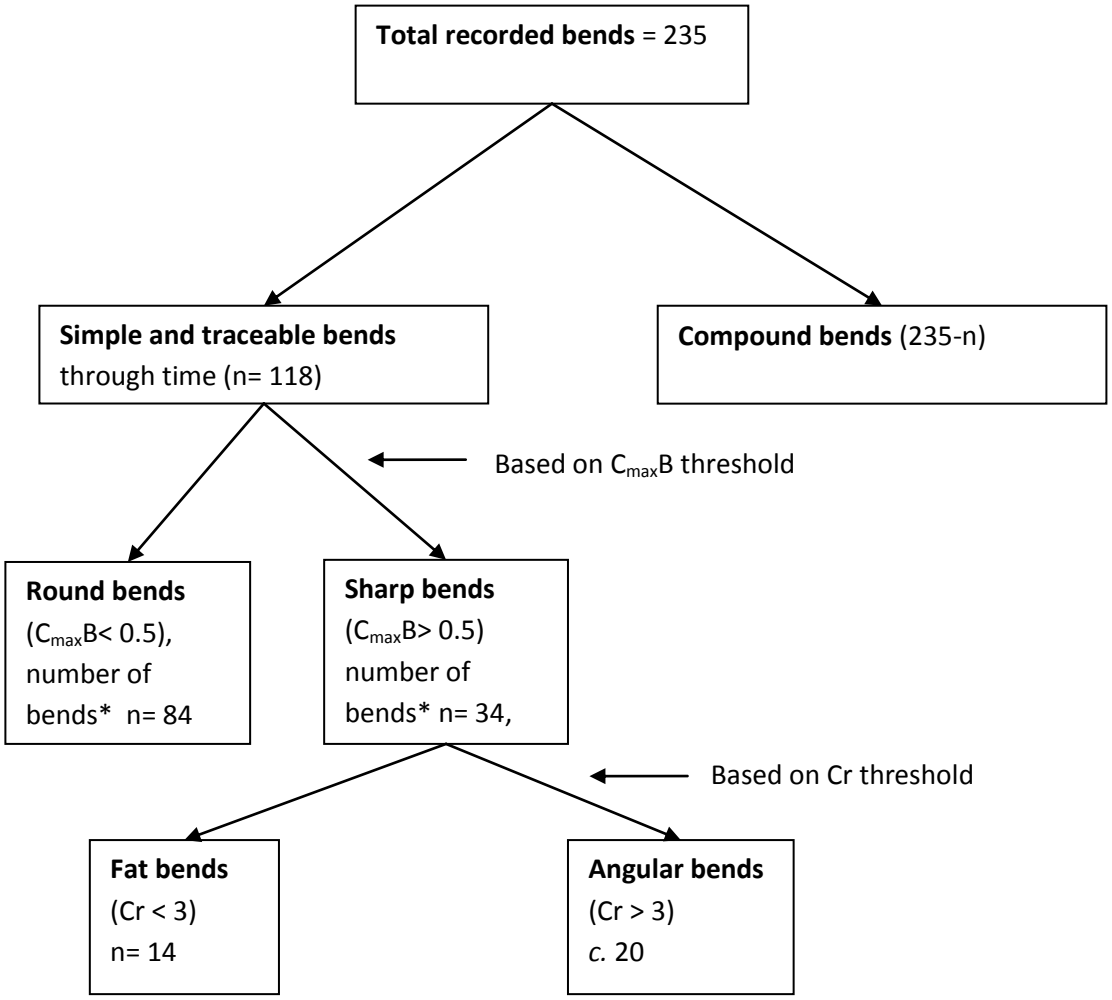

Fig 6 Schematic diagram showing the step-by-step break down of bend categories and numbers of studied bends within each category. NOTE: The number of bends refers to as the average number of bends across the four-time points (1915, 1960, 1980 and 2005).

Within the classified sharp bends, angular bends were detected using a new criterion that I propose, namely based on the curvature ratio Cr (Eq. 2) exceeding a certain threshold (Fig 6). High values of this metric hence describe bends for which the bend-scale curvature maximum is much higher compared to the bend-averaged curvature (see for examples, Fig 7). The curvature ratio Cr has been previously used for characterizing bend asymmetry (Howard & Hemberger, 1991) and recently for defining the roundness of bend-cutoffs (Schwenk et al., 2015). As opposite to angular bends (Vermeulen et al., 2016), fat bends were classified as all sharp bends not fulfill the criterion for angular bends (Cr < 3), see Fig 7.

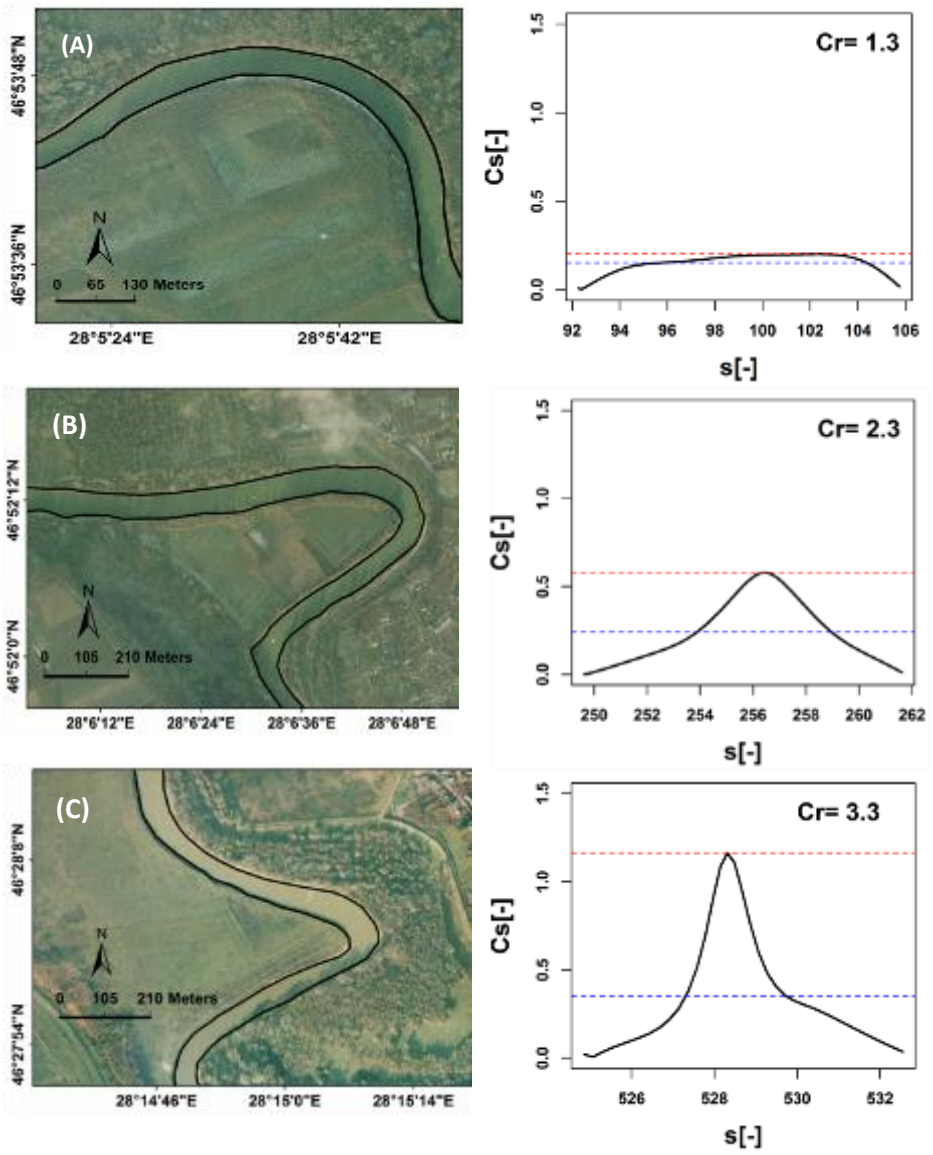

Fig 7 Examples of different simple bend types and related normalized local curvature spatial series. (A) round bend; (B) fat bend; (C) angular bend. Data refer to the year 2005. Dashed lines on the right panels indicate the dimensionless maximum bend curvature (red) and bend average curvature (blue) of the bend. Flow is always north to south. Note: panels B and C represent typical sharp bend geometry.

Further analysis was dedicated to capture the temporal evolution of the unconventional bends and to detect the possible transition of the bends into and from the unconventional types. This necessitated a preliminary detection of bends whose evolution could be tracked across all the four-time points (1915, 1960, 1980 and 2005), which resulted

in 118 bends. Next, a total of 49 instances[1] were recorded, where a bend was sharp in at least at one of the four-time points. While 32 instances were recorded where a bend was angular in at least one of the four-time points. Subsequently, for the selected instances an analysis was made to detect which and how many transitions between complementary bend classes (round to sharp or vice versa and fat to angular or vice versa) were experienced by the same river bend during its time evolution (1915-1960, 1960-1980 and 1980-2005).

The overall data processing and statistical testing were performed using R software (R Core Team, 2017). A Kruskal-Wallis (presented as z scores) test followed by a posthoc Dunn's test (Dunn.test package in R, Dinno 2017) with Bonferroni correction was performed to compare the significance of change among the groups i.e. four-time points or three time periods. In the case of normal data, Student's independent T-test was employed for testing differences between two groups. Measures of central tendencies (median) and dispersion (interquartile range, IQR) of the data was also computed for the 118 simple bends.

2.4 Results

Prut River is still mostly an unconfined and irregularly meandering river with almost 50% of the total bends (i.e. > 200) categorized as compound meanders (i.e. not simple). Overall, bank stabilization was found to only occur in minor sections of the river, and only about 34% (out of 118 simple bends) of the studied bends were found to be confined, particularly, at locations where the river channel has migrated close to the dike.

[1] An "instance" was recorded when a bend was sharp in any one of the time points. Likewise, for angular bends, an instance was selected if the bend is angular at any one time point. Further, that bend's shape information in the other corresponding time points together constituted of a single "instance".

Table 2 Summary of morphometric parameters of studied bends, with N=118, bends for each time point. IQR= Interquartile range; Q1= 25% percentile; Q3= 75% percentile; M= Median

	1915				1960				1980				2005			
Bend metric	**M**	**IQR (Q1-Q3)**	**min**	**max**	**M**	**IQR (Q1-Q3)**	**min**	**max**	**M**	**IQR (Q1-Q3)**	**min**	**max**	**M**	**IQR (Q1-Q3)**	**min**	**Max**
Cr	1.8	1.6-2.3	1.2	5.8	2.0	1.7-2.6	1.3	8.7	2.0	1.7-2.6	1.2	11.0	2.0	1.7-2.7	1.3	8.1
B	72	63-86	48.9	166	58	54-65	43.3	105	66	58-74	43	94.7	52	50-57	38.8	83.9
S	1.4	1.2-1.7	1.0	3.0	1.6	1.2-2.0	1.0	4.9	1.6	1.2-2.0	1.0	5.7	1.6	1.3-2.2	1.0	4.8
λ	0.15	0.13-0.2	0.06	0.3	0.12	0.1-0.14	0.04	0.4	0.12	0.1-0.16	0.05	0.4	0.1	0.1-0.13	0.04	0.3
$C_{mean}B$	0.19	0.1-0.2	0.01	0.5	0.14	0.1-0.2	0.01	0.4	0.16	0.1-0.2	0.02	0.61	0.14	0.1-0.2	0.01	0.33
$C_{max}B$	0.32	0.3-0.5	0.02	2.16	0.30	0.2-0.5	0.01	1.3	0.32	0.2-0.5	0.03	2.01	0.30	0.2-0.5	0.01	1.44

2.4.1 Reach-scale channel adjustment and meandering characteristics

The analysis of channel adjustment was focused on typical indicators used in the literature for this purpose (Rinaldi et al., 2015): multi-decadal variations in channel width and meander centerline sinuosity. Due to unavailability of multi-temporal cross-sectional surveys, it was not possible to develop evolutionary trajectories in terms of the mean bed elevation. However, the availability of PyRIS software enabled the reconstruction of bend-averaged migration rate that leads to a clearer view of the overall morphodynamic characteristic of studied sections.

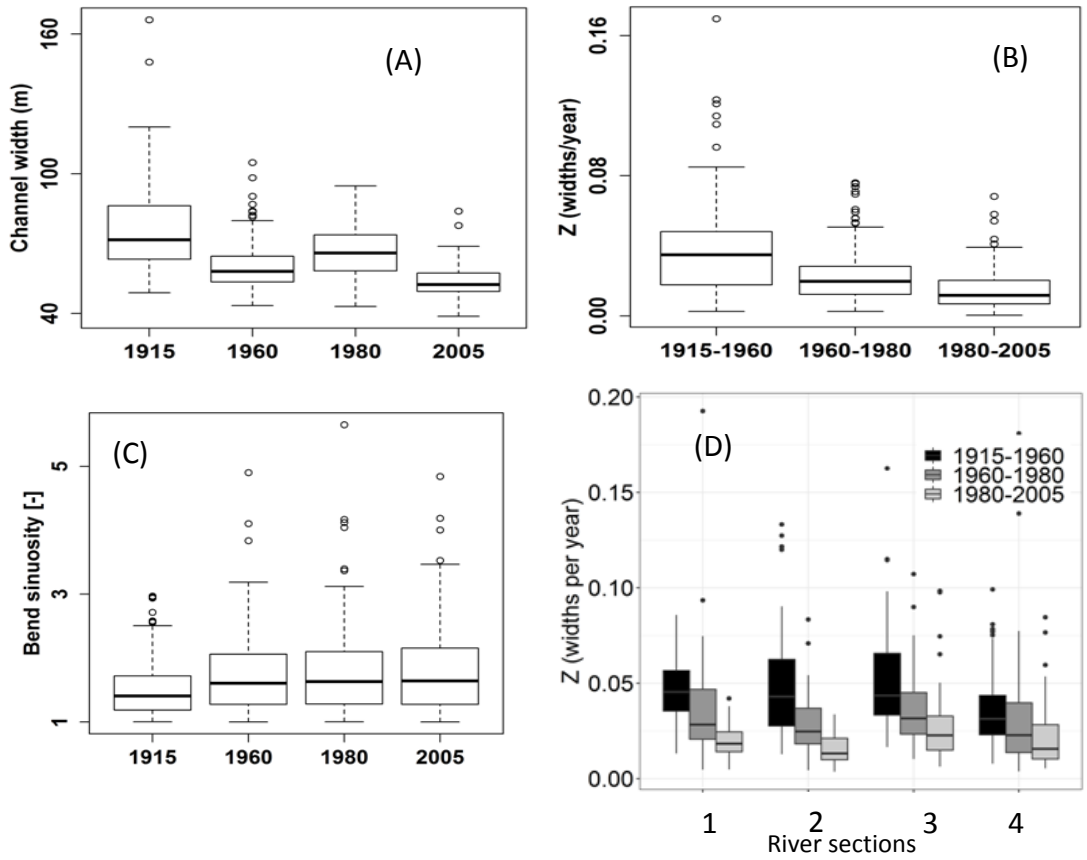

Fig 8. Indicators of observed channel adjustment and section-wise migration rate between 1915 and 2005. The box center line represents (the median), the outer lines of the of the box are the 25th and 75th percentile (A) bend averaged channel width; (B) width normalised migration rate, Z (C) dimensionless bend sinuosity, (D) reach-wise bend migration rates (all bends included to display the general character of migration, i.e. N > 200 for each time point).

Variables indicating channel adjustments differed among the observed time-points and between time-periods (Fig 8). Median channel width initially decreased from 72 m in 1915 to 58 m in 1960 (z score= 7.2, $p < 0.005$), while an increase was observed from 58 m in 1960 to 66 m in 1980 (z score= -4, $p < 0.05$) and finally a decrease from 66 m in 1980 to 52 m in 2005 (z score= 9.1, $p < 0.05$). Concomitantly, a steady decrease in the spatial variability of local channel width were observed through the 90 period, whereby the variability was highest in 1915 (Median = 72 m, IQR = 22.9) and lowest in 2005 (Median= 52 m, IQR=7.9). Similarly, meander migration rates (Z, widths/year) declined significantly between each successive period, i.e. 1915-1960 (Mean Z= 0.038 widths/year) compared to 1960-1980 (Mean Z= 0.023 widths/year) ($t=4.9$, $df =191$, $p<0.05$), 1960-1980 compared to 1980-2005 (Mean Z= 0.015 widths/year) ($t= 4.5$, $df=207$, $p<0.05$). Furthermore, the period of 1980-2005 displayed the lowest variability in the rates among the three time periods (Fig 8B). Bend sinuosity was found to be significantly higher ($z = -3.5$, $p<0.05$) in 2005 (sinuosity =1.6) compared to 1915 (sinuosity =1.4) (Fig 8C).

Furthermore, comparable median migration rates were displayed by section 1, 2 and 3 during 1915-1960 (pre-Stanca-Costesti reservoir) period, however, for the same period section, 4 had lower rates in comparison to rest of the sections (Fig 8D). Notably, section 1 and 4 showed lower migration rate variability in 1915-1960 (IQR=0.02) compared to that of section 2 and 3 (IQR=0.03) for the same period of time, conversely for 1960-1980, higher variability was observed in section 1 and 4 (IQR=0.03) compared to section 2 and 3 (IQR=0.02). The overall median migration rate for section 4 was found to be lower than the rest of the sections and section 3 relatively higher migration rates than the rest during all three observed periods.

2.4.2 Morphometric characterization of sharp and angular bends on the Prut

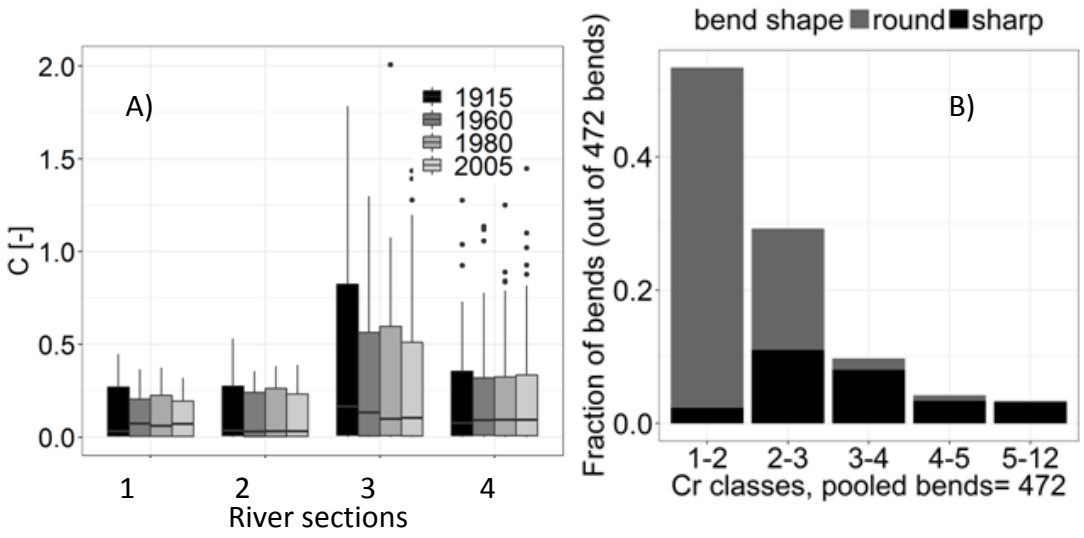

Fig 9. Curvature distribution characteristics of the Prut. (A) Maximum curvature for the four studied sections of the Prut (all bends included, i.e. N>200 for each time point). (B) The proportion of bend shapes as sharps and rounds for several Cr classes (data pooled for all time points, N= 472 bends).

Based on the bend curvature threshold provided by Hickin & Nanson, (1984) ($C_{max}B$> 0.5), c. 28% (N=118, per time point) of the bends on the Prut planform were quantitatively classified as sharp, while the remaining ones as round bend (see, Fig 6 in the methods section). Median values of $C_{max}B$ ranged from 0.30-0.32 and the IQR was always nearly similar among all time points (Table 2). In a spatial context, section 1 and 2 included in general rounder bends, while sections 3 and 4 displayed a considerable proportion of sharper bends interspersed with round bends (Fig 9A). Notably, in section 3 the sharp bends made up c. 34% of total bends observed in 1915 (N=55), whereas, for section 4 this was c. 14% of the total bends in 1915 (N=88). Moreover, over the 90-year period, the proportions of sharp bends did not change considerably between different time points (shown by the color gradient in Fig 9A).

To define a curvature ratio (Cr) threshold, I analyzed the distribution of sharp and round bends overlain onto Cr frequency classes (Fig 9B). I detected an abrupt increase in the proportion of sharp bends (80%) in comparison to round bends as Cr exceeded a value of '3' (Fig 9B). Following this, angular bends were characterized as a subset of sharp bend forms. Conceptually, the Cr metric integrates mean and maximum curvature of a bend. Hence, sharp

bends with Cr > 3 were discerned as angular bends (abruptly curving or unconventional bends) and the remaining as fat bends (smoothly curving or conventional bends).

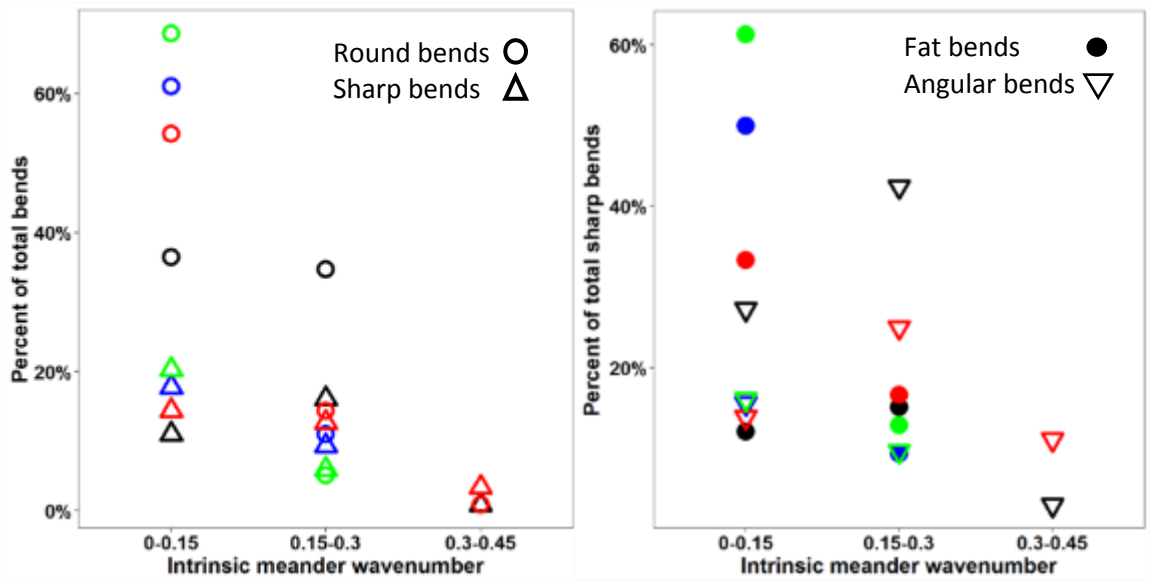

A) B)

Fig 10. Characteristic intrinsic wavenumber (λ) classes displaying relative proportions of different bend shape types. (A) sharp vs. round bends,(B) angular vs. fat bends. Symbols represent the bend shape types (see legend) and colors represent time points:black= 1915, blue= 1960, red= 1980, green= 2005. Total bends are 118 for any time point for sharp vs. round (panel A) and total bends were 26 for angular vs. fat (panel B).

Median values of intrinsic wavenumber (λ) ranged from 0.1- 0.15 (table 2) with, the median intrinsic wavenumber decreasing over the 90-year period from M = 0.15 in 1915 to M = 0.1 in 2005. Similarly, a decrease in the 3rd quartile of the interquartile range (table 2) was also be noted, with 75 % of the data points falling below λ= 0.2 in 1915 whereas below λ= 0.13 for 2005. For 1960, 1980 and 2005 majority of the bends (3rd quartile i.e. 75%) fell in the class of longer bends c. λ< 0.16 with similar median values (see IQR and M in table 2). Whereas, for 1915 greater dispersion in wavenumber occurred with the majority of the bends (75%) occurring below 0.2 and median value falling at 0.15.

Furthermore, among the longer bend class (0< λ< 0.15) round bends contributed a relatively higher proportion compared to the sharper ones (Fig 10A). The latter represents only about 10-20% of the total bends in the longer bend class at any given time-point (represented by colors in Fig 10A). Out of the longer bends (λ < 0.15) about *c.* 39% (N=118)

were round bends in 1915 which increased to *c.* 75% in 2005. A similar trend was observed for fat bends in the longer bend class, whereby fat bends were c. 10 % of the total sharp bends(N= 32) in 1915 this proportion increased up to c. 60% in 2005(N=30) (Fig 10A and B).

Furthermore, for the class $0.15 < \lambda < 0.30$, no distinct trend was observed in terms of proportions of particular bend-shape types. However, in 1915 round bends were found in higher proportions compared to sharp bends for the $0.15 < \lambda < 0.30$ wavenumber classes. For both the contrasting morphology types, only a low fraction of bends fell in the wavenumber class for very short bends ($\lambda > 0.3$). Not only did the angular bends occurred in all wavenumber classes, for the $0.15 < \lambda < 0.30$ wavenumber class the angular bends were distinctly higher in proportion compared to fat bends during 1915 followed by angular bends occurring in 1980, therefore, displaying a high variance in wavenumbers (Fig 10).

2.4.3 Morphodynamics of sharp and angular bends and their conventional counterparts

Migration rate as a function of increasing bend curvature displayed a non-linear trend, which was apparent in all the investigated periods (Fig 11). A higher scatter in migration rates was displayed by rounder bends ($C_{max}B < 0.5$), (marked by vertical black line in Fig 11), while, for sharper bends ($C_{max}B > 0.5$) the migration rates were generally lower than the 3rd quartile of the overall migration rates of all periods (marked by the horizontal black line in fig 11). Migration rates by conventional and unconventional bends (i.e. sharp vs. round and angular vs. fats) (Fig S1 in appendix A) during the three studied time periods do not show significant differences among median migration rates of these bend types. Though, the unequal numbers in bends falling into different shape types made it difficult to interpret the dispersion of data points.

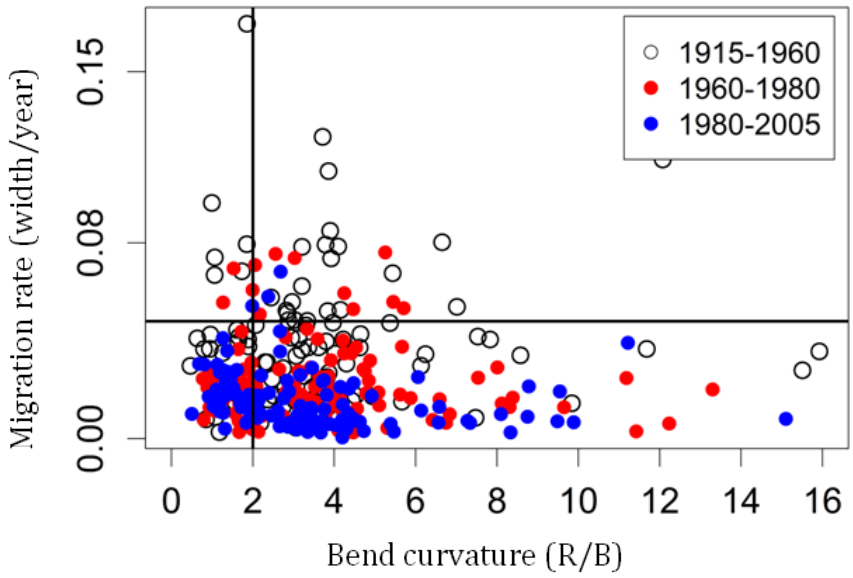

Fig 11. Bend migration rate as a function of bend curvature. The horizontal black line represents the 3rd quartile of migration rate pooled over the 3 periods. The vertical black line represents the threshold for bend sharpness R/B < 2 or $C_{max}B > 0.5$. The number of bends for each period was 118.

I also examined the temporal changes in the types and proportion of bend-shape transitions (fig 12), that occurred among 1915-1960, 1960-1980 and 1980-2005. A total of 49 instances were recorded (see methods), whereby a bend was found to be sharp at any one of the 4-time points (fig 12A). Within these instances, the fraction of round to round shape transitions gradually increased over the 90 year period with the highest occurring in 1980-2005. Contrastingly, the round to sharp transitions decreased steadily in the complete period and was lowest in 1980-2005. No specific trend was observable for the sharp to round transitions. While for sharp to sharp, the fraction of the total transitions increased after 1960 and seemed to stabilize.

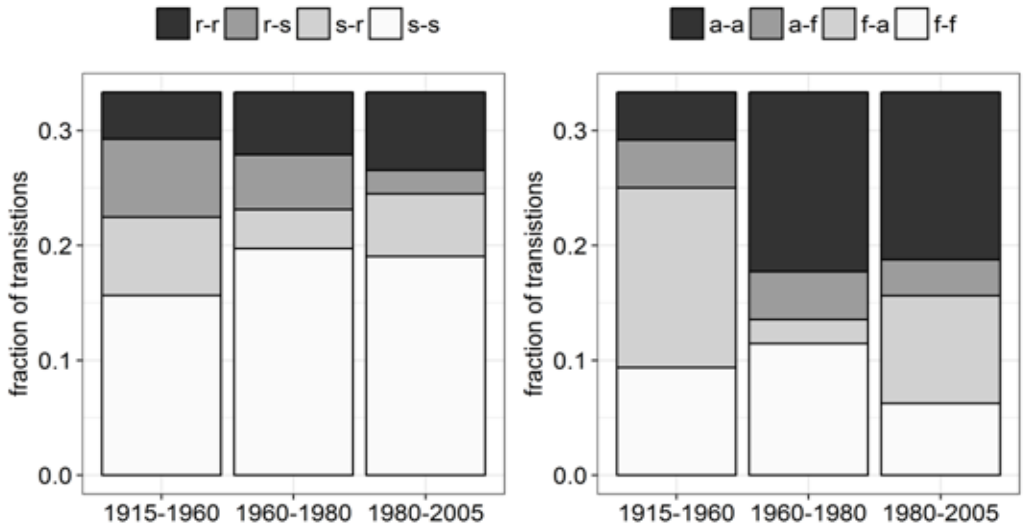

A) B)

Fig 12. Bend transition instances occurring within selected bends during each time period. A) round (r) and sharp (s) transitions, N= 49, where each instance is marked by the presence of a sharp bend in at least one time point. B) angular (a) and fat (f) transitions, N= 32, where each instance is marked by the presence of an angular bend in at least one time point. Legend- a-a= angular to angular; f-f= fat to fat; r-r= round to round; s-s= sharp to sharp; a-f= angular to fat; f-a= fat to angular; s-r= sharp to round; r-s= round to sharp

In total 32 instances were recorded where a bend was found to be angular at any one of the 4-time points. Within these instances, the fraction of angular to angular shape transitions was lowest in 1915-1960 period and increased in 1960-1980 and in the 1980-2005 period (fig 12B). In contrast, angular to fat transitions showed a gentle decrease among the time periods with the lowest being in the 1980-2005 period. Similarly, a decrease was also noticeable for fat to fat transitions whereby the lowest fraction of transitions occurred in 1980-2005. On the other hand, the fraction of fat to angular transitions showed a marked decrease in occurring especially from 1915-1960 towards 1960-1980, and again an increase in the 1980-2005 period.

2.5 Discussion

The temporal evaluation of channel adjustments ascertained a significant reduction in the morphodynamics of the Prut River. With, a decrease in channel width and an increase in bend sinuosity, from 1915 to 2005. In addition, for the same period, the migration rate had declined steadily. Furthermore, morphometric properties of the sharp and angular bends

(collectively referred to as unconventional bends) were also established using spatially averaged curvature metrics and dimensionless intrinsic meander wavelength.

In addition to this, an analysis of the proportion of bend shape transitions was undertaken whereby, between different time points the changes in the proportion of bend shape transitions (as a surrogate of bend scale morphodynamics) were noted and these changes seemed to be greater for unconventional bends. For instance, an increase in the proportion of round-round and sharp-sharp shape transitions, indicating, that some bends are able to retain their initial geometries and stabilize for seemingly long periods (20-90 years). Conversely, the shape transitions between different bend shapes types were reduced in proportions, i.e. round to sharp and vice versa, which is also consistent with the reduced dynamics of the Prut River as the bends tend to get easily stabilized. Overall, this might be an indicator of an overriding effect of non-autogenic factors in the maintenance of unconventional bend forms. However, effects on fat and angular bend shapes were reversed, so that, fat to angular transitions were found to have increased in numbers from 1915-2005.

2.5.1 Temporal morphological trajectory of the Prut over the 90 years

The observed narrowing and incision adjustments on the river Prut's channel might be in response to the lowered sediment input of the river which is probably due to human-induced alterations over the years. Longitudinally, a drastic reduction of sediment discharge has occurred immediately downstream of the Stanca-Costesti reservoir after its construction 1974–1978 (see fig 6 in appendix). Similar effects have been recorded for alluvial rivers occurring in a wider range of climatic and geomorphologic settings, whereby, dams have been a major contributor to types of adjustments discussed henceforth. For instance, the discernible influence of dams on the downstream sediment balance and subsequent narrowing and or incision has been presented for big alluvial rivers of Europe (Surian & Rinaldi, 2003) and smaller streams of California (Kondolf & Swanson, 1993). Notwithstanding, the channel adjustments have also been attributed to an over-arching and collective effect of socio-economic, climatic and land-use factors compared to the alterations by hydropower and gravel mining in the lower section of the Rhone River, France (Provansal et al., 2014). In fact, alterations are known to slowly dampen out as the downstream distance increases from the dam, mainly, due to the increased supply of water and sediment, vis a vis, the enlarged catchment (Batalla, 2003; Batalla & Go, 2004). Concomitantly, major lateral tributaries also bring in more water and sediment. However, this cannot be assumed for the Prut, whereby,

not only the catchment tapers in the downstream direction from Stanca-Costesti reservoir, but there is also no major lateral tributaries joining the Prut channel, except Jijia that carries a meager, *c.* 0.1% of Prut's discharge (see study area, Fig 4). Further, the difference in the mean sediment discharge is drastic between Stanca-Costesti (2 kgs^{-1}) and Ungheni (20 kgs^{-1}), located 161 km apart, while, after Ungheni it seems to have remained constant till the Falciu gauge, located 235 km apart at *c.* 20 kgs^{-1}(see, Fig S2 in appendix A for spatio-temporal variation in water and sediment discharge on the Prut). Besides, the Prut basin also lies in inherently low sediment generating zone of Romania (<0.5 tons/ha/yr). Notably, the Stanca-Costesti to Ungheni section of the river also falls into the wider region of the Prut catchment area, whereas, Ungheni onwards there appears to occur a reduction in the catchment area, as the catchment tapers (Fig 4).

For the Prut River, other historical anthropogenic alterations such as rampant gravel mining, extensive land-use change and in-channel factors like the cohesive nature of the river banks might also have contributed to the low sediment load. The following factors may have contributed to the observed adjustments in the Prut. Historically, Romanian rivers have been subjected to intensive gravel mining during the communist regime (1970-1989, on Romanian territory) (Radoane et al., 2017), whereas in case of Prut this might have started already during the post-WWII era (post-1950) in the upper catchment (Ukranian Carpathians) with a common motive of rapid infrastructure development. Similar cases of historical sediment mining (mostly post WWII) have been reported from other European rivers, for instance, Tuscan rivers, Italy mostly became single thread sinuous from being braided (Surian & Rinaldi, 2003). Moreover, in-channel mining is directly responsible for reduced sediment load in affected rivers, leading to a higher erosion capacity of the river water (Kondolf, 1997). Concomitantly, for Prut river an overall dominance of erosion processes, particularly, in the downstream of dam river segment was documented by Radoane et al., (2007), which seems to be the manifestation of the sediment-shortage in the river. Another valid reason for reduced sediments might also be the afforestation policy adopted by the Romanian government that was launched post-1970 (Zaharia et al., 2011) which might have lead to the decreased flow and sediment input from the riparian zones of Prut. In a similar channel narrowing of the Siret River (neighboring the Prut to the west), during the 1970-1983 was attributed collectively to the engineering works and afforestation (Salit et al., 2015). Moreover, the segment of the Prut included in our study also exhibits cohesive-banks (made up of clay and sand) along with fine-coarse sand as dominant bed sediment (Radoane et al.,

2007). Therefore, the discussed factors consistently suggest that the Prut behaves typically, as a sediment starved river, whereby, the river has severely reduced suspended sediment load and the only way to compensate is by eroding the bed sediments. Simply meaning that the Prut river is on a trajectory towards an incising river so that, the dominant erosion regime is an effect of reduced sediment supply that in turn might also affect other autogenic processes of the river (Hooke, 2013).

2.5.2 Morphometric characteristics of planform and bends on Prut river

Spatial curvature series based on river centerline has been widely used as means of describing river channel morphometry (Howard & Hemberger, 1991; Güneralp & Rhoads, 2009) and, building upon earlier methods circle fitting (Hooke, 1984), it provides ability timely method of capturing detailed changes in meander bends (Monegaglia et al., 2018).

Fat and angular bends were not differentiable based on the simple knowledge of maximum bend curvature, $C_{max}B$ (see Fig 7B and C in the methods section). As the spatial curvature series among fatter and angular bend forms can differ significantly, particularly sometimes exhibiting several curvature peaks. For example, in fat bends curvature series along the streamwise distance can be double-peaked (a single major and a minor peak) (Langbein & Leopold, 1966) while, angular bends can be single-peaked (Vermeulen et al., 2016). Apart, from the number peaks differentiating between these two bend shapes, the curvature ratio Cr) metric (used here also takes into account the higher mean curvature values ($C_{mean}B$) due to the relatively more curving arms of fat bends compared to angular bends (Fig 7B and C). This metric has been previously used by (Howard & Hemberger, 1991) along with other bend scale statistical variables in order to describe the bend shape and size, while, recently (Schwenk et al., 2015) used it to describe the shapes of individual cut-off bends, namely, longer and rounder cut-off shapes. Although this study, takes advantage of a large number of simple bends (N=118) deployed for testing the bend shape metrics, caution should be laid when transferring these shape metrics to other river systems. For example, the curvature ratio threshold (Cr=3) calculated from the studied set of bends on the Prut should be applied to other rivers, after confirming the curvature ratio distribution for that river (see Fig 9B)

A considerable proportion of sharp bend types were found to occur interspersed among rounder bends (Fig 9A, also). This gives the Prut a typical zig-zagging planform appearance in some sections (for example see section 3 and 4 in Fig 4) compared to a more

regular appearance in others, where regular means comprising of more conventionally occurring round and or fat bends (for example see section 1 and 2 in Fig 4). In fact, differing degree of regularity within the sub reaches of the same river has also been noted for other rivers (see Red River as an example in Zolezzi & Güneralp, 2016). Although such zigzagging can be commonly encountered in natural rivers (see examples below), it has been only recently discussed from the Mahakam, a large tropical river (Indonesia) based on the spatial distribution of the centerline curvature series plotted against the streamwise distance (*see fig 4 C in* Vermeulen et al., 2014). Also, river planforms included in the previous scientific literature display visually obvious zigzagging, some examples are, River Rio Beni(*see fig 1 in* Schwendel et al., 2015), Kinabatangan River, Malaysia (*see fig 1B in* Horton et al., 2017). Notably, these are tropical rivers that display the low amount of human modification and a seemingly intact sediment regime, with higher suspended sediment load, contrary to that observed in Prut's case. However, the zigzagging of planform has also been observed to occur from smaller temperate streams (Andrle, 1994).

The proportion of sharp bends displayed by the Prut planform (c. 28 % of 118 simple bends at any time point) appears to be coherent with the frequency analysis outcome from data compiled on 79 streams that found about $1/3^{rd}$ of the bends to fall below $R/B < 2$ (or $C_{max}B > 0.5$) i.e. as sharp bends (Williams, 1986). Overall, this provides some initial evidence that Prut river's planform exhibits typical characteristics. Thus, the results observed at the Prut also contribute to the so-far scarce knowledge on the proportion of such bends in freely meandering rivers.

Intrinsic wavenumber values (λ) reported here concur well with the values reported from other real river examples (Red River, Zolezzi & Güneralp, 2016) and meander models (Zolezzi & Seminara, 2001a; Frascati & Lanzoni, 2009; Xu et al., 2011), and these values are generally of the order 10^{-1} (Zolezzi & Seminara, 2001a). Longer bend often corresponds to smaller wavenumbers, usually c. $\lambda < 0.15$, and are proposed to be more dynamic (Pittaluga et al., 2009). Indeed, the conventional bends (round and fat) falling clearly into distinct wavenumber classes compared to unconventional (sharp and angular), confirms yet another bend shape characteristic for such bends (apart from just $C_{max}B$ and Cr). Irrespective of the observed time point, the majority of the conventional bends (round and or fat) always belonged to longer types (Q3 in IQR of $\lambda < 0.16$ for 1960 to 2005 and median wavenumber $\lambda = 0.15$ in 1915) which complements the general observation of higher proportions of longer bends (and mildly curving) in real rivers (Pittaluga & Seminara, 2011).The wide range of

intrinsic wavenumbers observed on the Prut also suggests planform irregularity (Zolezzi & Güneralp, 2016), which is concomitant with the zigzagging shape of the Prut river planform due to presence of unconventional bends i.e. sharper and angular forms (Vermeulen et al., 2014).

This study also provides novel insight into differences among the wavenumber characteristics of fat compared to angular bends from a real river example. These differences are indicative of hydrodynamic conditions in these bends (Pittaluga et al., 2009). Firstly, the fat bends, in general, were longer than the angular bends (fig 10B, $\lambda < 0.15$), thus, further adding to the distinctive geometric characteristic between the two bends types. Secondly, the angular bends occurred throughout all the wavenumber classes, implying, higher variance in lengths of such bend shapes. The length differences among conventional and unconventional are broadly known, in that, sharper (high curvature i.e. unconventional) bends develop shorter bend lengths (Furbish, 1988) and vice versa (Ikeda et al., 1981; Crosato, 2009). The characterization of bend-scale angularity through comparison with fatness has only recently shown for a real river example from the tropics (Vermeulen et al., 2016). Whereby, Vermeulen et al., (2016) established differences among some river planforms in terms of their overall fattening or angular appearance, employing the Ikeda's fattening coefficient (Ikeda et al., 1981), so that a positive coefficient value was attributed to fat and a negative coefficient to angular bends.

Despite, being a sub-category of higher curvature bend types (Fig 6), the angular bends were not found to be invariably shorter as expected for higher curvature bends (Pittaluga & Seminara, 2011). Such deviation might then manifest as variability in the hydrodynamic in angular bends, for example, affecting adaptive phase lag that occurs in bends (see, Pittaluga et al., 2009) and that can, in turn, affect the morphodynamic behavior of angular bends. Indeed, for shorter (sharp) bends the maximum migration rate tends to occur at the downstream end of the bend (near the exit), corresponding with the velocity attaining a maximum value (Furbish, 1988; Crosato, 2009). Incidentally, inner-bank flow separation which is seemingly stronger in shorter bends (Blanckaert et al., 2013), which can aggravate erosion at the outer banks (Leeder & Bridges, 1975).

2.5.3 Morphodynamic character of bends and its form and trajectory of the Prut

For all studied three time periods, namely 1915-1960, 1960-1980 and 1980-2005 the shape of the migration-curvature scatter (Fig 9) was similar to the classical envelope curve

displaying the typical non-linear relationship between migration-curvature data reported by others (Hickin & Nanson, 1975, 1984; Hooke, 1987; Hudson & Kesel, 2000). For instance, compared to data on 18 reaches from different rivers in Canada (Nanson & Hickin, 1986) and 100 bends from River Dane (Hooke, 1987). This essentially implies that the majority of bends on the Prut display a range curvature with migration dynamics similar to those reported in rivers differing in size and hydro-geological settings. Furthermore, I establish that under the observed channel adjustment trajectory of the Prut River (section 4.1), the basic shape migration of curvature scatter adheres to a non-linear one, albeit with dampened migration rates.

Markedly, the tail of the (i.e. values below R/B < 2 in Fig 11) also indicates the presence of very high curvature bends occurring during each period on the Prut, with such bends developing in some rivers reaches while missing in others. For instance, Nanson and Hickin(1986) in their data of about 118 meander bends extracted from 18 rivers with channel width ranging from 37-278 m and D_{50} size ranging from 0.18-90 (Wentworth scale) show no meander bends falling below R/W< 1 i.e. very sharp bends ($C_{max}B$> 1, in Prut's case). On the other hand, for Dane River, a small gravel-bed river, Hooke (1987) reported several bends below R/W<1. Most discussed explanation to the generation of unconventional bends from real rivers remains with the presence of non-erodible material (clay plugs, paleomeanders, recent cut-offs) occurring in the river floodplain (Carey, 1963; Hooke, 1987; Thorne, 1992; Hudson & Kesel, 2000; Schwendel et al., 2015). Whereby, often the downstream migrating arm is arrested as it migrates towards an erosion-resistant material and in time allowing the upstream arm to migrate closer to it, causing overall tightening of the bend. Unconventional bends are even produced in river systems that often also feature conventional bends in their planforms *(planform view of Mamore River, Amazon Basin,* Constantine et al., 2014; *Kinabatangan River, Malaysia,* Horton et al., 2017). Overall, this might be the case for rivers carrying very large amounts of sediment load, consequently, migrating at higher rates and producing higher cut-offs that in turn get filled up relatively faster with finer sediments by the action of river itself (Constantine et al 2014). However, such a presence of non-erodible material near the downstream arm of the bend as a cause for the formation of unconventional bends is not probably for the Prut, as unconventional bends show high periods of stabilization (20-90 years) (Fig S3 in appendix A, for exemplary shape transitions during long periods) on the Prut, which would not be possible of the still dynamic upstream arm of the bend would approach the arrested downstream arm causing cut-off.

Contrastingly, Vermeulen et al., (2014) observed most unconventional bends to occur in the section where the studied river section was morphodynamically dormant. To add to this, they found no relationship between the presence of unconventional bends and the variables of land cover in the floodplain. They suggested that the overall lowered morphodynamics of that river reach might be due to anomalously large scour holes present at the apices those unconventional bends, thus implying some in-channel (autogenic) feedback rather than an external (allogenic) imposing in such bends. Also, the actively migrating nature of Prut causes large trees to slump down into the channel through bank failures mainly as a result of undercutting. Following a bank failure trees either stand vertically (attached to river bed) or after a time slant across the channel, this can interact with flow and cause accentuated deposition, erosion and shear stress (Gurnell & Petts, 2006; Constantine et al., 2009) and could, therefore, contribute to the formation of unconventional bend geometries. The studied sections of Prut displayed a certain extent of homogeneity in its hydrological and sediment conditions mostly due to the typically tapered catchment and no major tributaries joining in (study area). Moreover, comparable median migration rates i.e. no extreme differences were observed particularly in the period 1915-1960 (c. 0.03-0.04 widths/year) (before construction of Stanca-Costesti reservoir), among all four studied sections spread across c. 400 km (Fig 8D), which might indicate the low level of longitudinal heterogeneity of the floodplain material in the Prut. Rivers meandering in clay-rich deposits generally exhibit lower migration rates, as according to the Hjulström curve those cohesive deposits are more resistant to erosion (also see Schwendel et al., 2015). Despite this, the number of unconventional bends was higher in sections 3 and 4 compared to sections 1 and 2 throughout all time points (Fig 9A). Altogether, this suggests some autogenic process that might aid in the maintenance of unconventional bend types in the Prut, especially as the sharp bends have been actively migrating with median values of c. 0.03-0.04 widths/year and are not simply stalled as often observed for such unconventional bends elsewhere (Thorne, 1992; Andrle, 1994). Obviously, the occurrence of such bends then has a much lower dependence on floodplain erodibility than previously discussed (for example in Sun et al., 1996). Particularly, when, modeling attempts that included floodplain heterogeneity were able to reproduce planforms displaying compound bends and a range of curvature but not angular examples (Güneralp & Rhoads, 2011; Motta et al., 2012).

The differences in proportions of bend shape transitions, particularly, before and after the modification periods (construction of Stanca-Costesti reservoir) on the Prut also confirm

the effect of reduced dynamics and channel adjustments that had occurred only post the modifications. In particular, the stabilization of bends is indicated by the increased proportions of ‘round to round’(r-r) and ‘sharp to sharp’(s-s) (i.e. similar-shape) transitions between the studied historical periods that can be attributed to the decline in migration rate among these bends. This conclusion is further supported by the decrease in the r-s (transitions between shape types) during the studied 90-year period. One might also argue that the reduced numbers of transitions between shape types might be due to the insufficient number of years for detectable migration to occur on the Prut, particularly, between 1960-1980 and 1980-2005, i.e. 20 and 25-year period, respectively, as have also been argued by Nanson & Hickin, (1986).To confirm this migration rates were calculated (in m/year) for such transitions (see Table 1, appendix A) and found to be never ‘zero’ for the shape transitions occurring from 1960 onwards. This essentially means that the bends after 1960 displayed movement, albeit, of lower magnitude, that concomitantly leads to less frequent changes in their geometries. The fact that the proportion of sharp bends did not change much in the 90-year period (Fig 12A marked by color gradient) and that the same bend could transit into different shapes (conventional to unconventional and vice versa) again supports our assumption that the mechanism at the basis of the formation and maintenance of the unconventional bends could of autogenic nature. Thus, a bend geometry causal loop could be assumed starting from an autogenic characteristic in the flow that shapes bed topography and sediment transport and eventually influences bank erosion.

2.6. Conclusion

Based on an extensive set of bends from a real-world river, with additionally their trajectories over a time period of 90 years available, I present a comprehensive characterization of "unconventional" meander bends in one of the few remaining lowland meandering rivers in Europe. A typical planform feature of Prut river is its irregular, zig-zagging appearance and of the studied bends c. 28% (N=118) were as attributed to the category of sharp bends.

Studies on the morphology and dynamics of unconventional bends are rare, and existing meander morphodynamic models cannot explain their generation and or maintenance. Unconventional bends herein have been classified as "sharp" (opposed to round) and angular (opposed to fat) through local and bend-scale channel centerline curvature metrics. This study complements the so far established separation criteria between among

conventional and unconventional bends with other geometric features, such as intrinsic wavenumbers that physically represent bend length. The characteristic differences between fat (longer with lower curvature ratio < 3) and angular bends (variable lengths with higher curvature ratio > 3) will have substantial implications for hydraulic geometry, adaptive phase lag, flow separation and eventually the morphodynamics of such bends.

In the last century, the studied reaches of the Prut River show consistent channel narrowing, accompanied by a reduction of meander migration rates and increasing sinuosity. In terms of morphodynamics, Prut concurs with migration-curvature features that are common in such rivers. Generation (formative conditions) and maintenance of unconventional bends on Prut River, however, seems to occur by an autogenic process, with fallen trees being an additional possible allogenic effect. Shape-transitions provide suggestive insight into form-process linkages of unconventional bends, suggesting again the role of in-channel variables in the maintenance of unconventional bends through causal feedback along with the causal chain flow–riverbed– sediment transport–bank erosion. The present results hence add substantial knowledge to the understanding of physical processes responsible for the generation of meander bends with unconventional planform morphology in meandering rivers.

3. Planform and hydraulic geometry controls of the inner-bank flow separation in meanders of a lowland river

3.1 Abstract

Flow processes such as the lateral extent and frequency of occurrence of separating flow at the inner-banks and its interactions with macro-scale bed topography in meander bends have been rarely explored from real river bend examples. Particularly, as these flow-bed interactions are known to vary significantly among bend planform shapes. Hence, planform shape and hydraulic geometry parameters in a set of 14 bends in a dynamic lowland river (the Prut, Romania/Moldova) were examined. A significant increase (IBFS = 6.1+ 45.8 $C_{max}B$ + 8.2; R^2= 0.55; $p < 0.001$; N=14) in the lateral extent of inner bank flow separation (IBFS) at the bend apex with increasing bend curvature was noted. And, bends exemplary of angular opposed to fat bends also display contrasting hydraulic geometry features, namely, a locally eroded /non-eroded point bar and steep/ gradually sloping upstream riffle to pool transition in angular/fat bends. With this, depth ratio (ratio of apex pool depth to upstream riffle depth) increases significantly (H_{ratio} = 0.83 + 0.41Cr; R^2 = 0.44; $p < 0.005$; N=14) with increasing bend angularity, curvature ratio (ratio of maximum to mean of bend curvature series). These features seemed to affect the extent of the horizontal recirculation occurring within the IBFS zone at the apex and were further associated with the presence of two IBFS zones in fat bends compared to a singular zone in angular bend. While the pool depth increased with curvature it tends to stabilize in bend curvatures greater than c. 0.5, suggesting the existence of a negative autogenic feedback, as pool depth is also weakly related to the IBFS size (IBFS = -14+ 10.3 H_p + 10.2; R^2= 0.30; $p<0.02$; N=14). These results angular and fat bends could lead to different bend developmental trajectories which can affect IBFS features occurring therein and vice versa. Based on the presented field evidence, shown effects of controlling factors on IBFS size may facilitate predictive morphodynamic modeling of river bend migration.

3.2 Introduction

Meandering lowland rivers often feature a diversity of bend planform shapes (Thorne & Furbish, 1995) which is known to influence the autogenic (i.e. in-channel) flow structure and bed topography (Ikeda et al., 1981; Odgaard, 1986; Whiting & Dietrich, 1993a, 1993b) therefore, affecting the prevalent hydro-morphodynamics occurring at the meander bends. One such flow process occurring at meander bends is the separation of flow (Bagnold, 1960) occurring on a horizontal plane near the inner banks of meander bend apices (Leeder & Bridges, 1975), hereafter referred to as inner-bank flow separation zone (IBFS).

IBFS is generated as a response to the curvature induced imbalance in the centrifugal forces that are created as the flow passes the point of highest curvature ($C_{max,}$ highest point of curvature) of the bend (Leeder & Bridges, 1975; Van Alphen et al., 1984). This imbalance created downstream of the highest point of curvature results in the split of river flow into a slow-flowing zone at the inner-half of the bend apex, and a fast-flowing zone at the outer half. The lateral extent of the IBFS i.e. from inner towards the outer banks is delimited by a shear layer created between the slow and fast flowing filaments (Bagnold, 1960; Blanckaert, 2015).

IBFS is known to influence the effective channel width (Dietrich & Smith, 1983; Van Alphen et al., 1984) and hence the hydraulic conveying capacity of the river channel at the respective bend (Ferguson et al., 2003). Moreover, the recirculation core forming within the IBFS acts as a sediment trap (Leeder & Bridges, 1975), which may initiate and support the growth of point bars in such bends, therefore narrowing the channel at this point and thus enhancing meander migration rates (Blanckaert, 2011). In short, this means that the lateral extent of IBFS significantly influences the bend-scale flow and sediment dynamics in a meandering river. Thereby, the extent and flow characteristic of IBFS directly or indirectly affect biota, too, as their reduced flow velocities provide flow refuge e.g. for juvenile fish (Rodriguez et al., 2004). This is especially important as apex pools of meanders often may not provide such kind of refuge, as they experience submergence of the stronger surface flow filament that may lead to increased near-bed velocities in the pool (Ferguson et al., 2003).

The varying planform geometries of river bends have been broadly classified into the categories of low curvature (width normalized curvature < 0.5, hereafter referred to as ‘round’) and high curvature (width normalized curvature > 0.5, hereafter referred to as ‘sharp’) bends (Bagnold, 1960; Leeder & Bridges, 1975; Hickin, 1977). Round bend shapes

are characterized by curvature that is slowly varying in streamwise direction and herein parameterized by $C_{max}B < 0.5$ (see chapter 2).These bends are known to display features such as weaker secondary flow and associated weaker flow redistribution and lower shear stress across the apex (Hickin, 1978; de Vriend, 1981; Blanckaert & de Vriend, 2003), slowly varying bed-topography (Pittaluga et al., 2009), overall shallower depths and erosion at the outer banks and deposition at the inner banks (Leopold & Wolman, 1960). In contrast, sharp bends are known to display stronger flow redistribution (Ottevanger et al., 2012); flow separation at inner and or outer banks (Hickin, 1977, 1978; Andrle, 1994); deep scour holes (Vermeulen, 2015); concave bank benches (Woodyer, 1975) develop; circular-shaped meander pools (Andrle, 1994) and an inverted erosion-deposition pattern erosion-deposition around the bend apex
(Hickin, 1978; Vermeulen, 2015). Given these features, high curvature bends also display great variation in their migration dynamics (Hickin & Nanson, 1975, 1984; Hooke, 1987; Hudson & Kesel, 2000), which has been generally attributed to their unconventional morphology and associated flow processes (Blanckaert, 2011).

As the sharp bends opposed to round bends, exhibit a gradually curving apex and arms; within the sharper bends ($C_{max}B > 0.5$) there have also been discerned a gradually turning 'fat' type as opposed to abruptly curving 'angular' ones on the Prut River planform (chapter 2). Altogether, the rounder and fatter forms provide a sinusoidal appearance to the river planform (Fig 13 B), contrary to a zigzagging appearance which is constituted of more sharp and angular forms (Vermeulen et al., 2014) (Fig 13A). Physically, angular bends display an abruptly curving apex with straight upstream and downstream arms and have been often observed on several river planforms of differing sizes and physio-geographical settings (see, Carey, 1963; Alford, 1982; Andrle, 1994; Jurmu & Andrle, 1997; Vermeulen et al., 2016). A typical morphometric difference between fat and angular bends is that fat bends display an initial double peakedness in their spatial curvature series (Langbein & Leopold, 1966; Parker et al., 1982), whereas, angular bends display a single peak (Vermeulen et al., 2016). Shape differences between angular and fats were quantified by differences in their curvature ratio (Cr), i.e. ratio between maximum to mean of centerline curvature series (see chapter 2, fig 7B and C), whereby, angular bends display higher ($Cr > 3$) maximum to mean curvature ratio values compared to fat bends ($Cr < 3$). From findings on Prut River, fat bends were also

characterized by longer bend lengths while angular bends by varying bend lengths (chapter 2, results, Fig 10B).

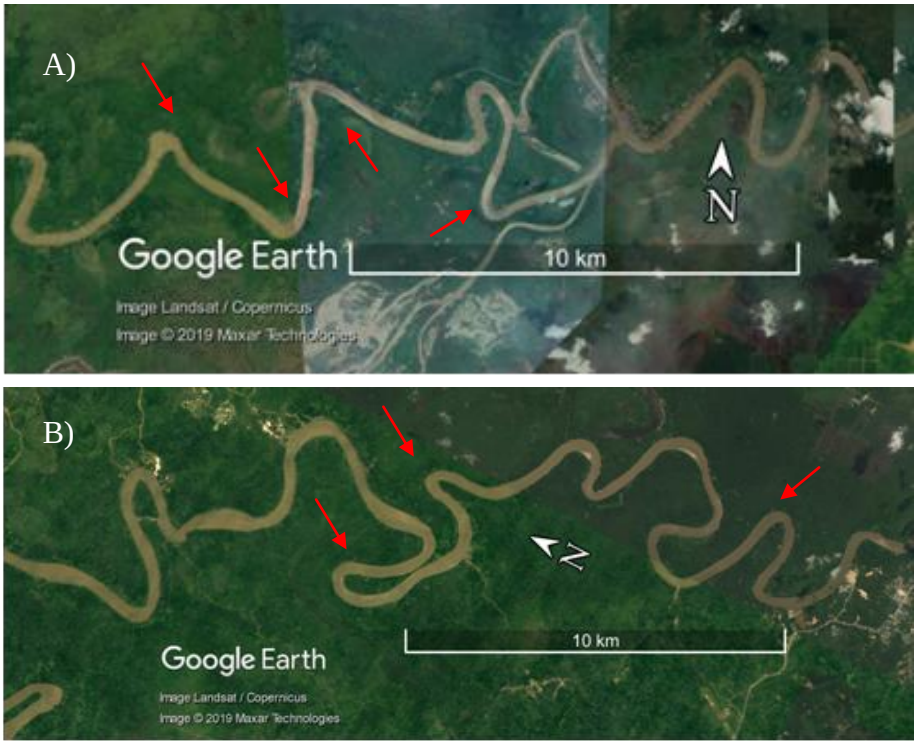

Fig 13. Examples of typical angular and fat forms occurring in nature. A) Angular bends that create an overall zig-zagged planform and B) fat forms on the Mahakam river, Indonesia (river section between 0 04’ 34.91” S,115 44’ 27.19” E and 0 20’ 08.05” S, 116 27’ 36.85” E).

Notwithstanding, little is known about the governing factors of varying flow and bathymetry among such bend shapes, even that the role of planform shape has been long recognized in altering key autogenic processes occurring within meandering rivers (Leopold & Wolman, 1960). Especially, there has been only a limited number of field-based studies on meandering rivers in the last 30 years (Rozovskiĭ, 1957; Leeder & Bridges, 1975; Jackson, 1975; Bathurst et al., 1977; Parsons, 2002; Ferguson et al., 2003; Frothingham & Rhoads, 2003; Nanson, 2010; Rhoads & Massey, 2010; Engel & Rhoads, 2012; Schnauder & Sukhodolov, 2012; Vermeulen, 2015). And even fewer studies have attempted to analyze the effect of bend shapes on flow separation features using field-based data recorded from varying bend planforms (Leeder & Bridges, 1975; de Vriend & Geldof, 1983; Parsons, 2002; Ferguson et al., 2003). On the other hand, mechanisms leading to the induction and promotion of IBFS in sharp bends have been studied in detail in flumes (Blanckaert, 2015).

Parsons, (2002) performed flow and bed topography survey on 22 bends on Dean River (bankfull width c. 3-5 m). Whereby, banklines were surveyed using a total station, with points placed 1 m apart along each bank. Geometric properties of the bends were calculated using the data from bankline surveys that resulted in the following parameters; non-dimensional radius of curvature (averaged from curvature at both banks and normalized by average width), the maximum change in inner and outer bankline. The surface area of IBFS was calculated in two steps. First, by the delineation of the extent of IBFS, this involved using surface floats at apex areas that were visually interpreted locations of flow separation and the boundary points were delineated using a total station. Second, the bankline and the delineated extent of IBFS were then used to calculate an area polygon of the zone of flow separation. Overall this implies that the data collected at the 22 bends was of a coarser resolution from a wadeable stream and of overall low reproducibility for the calculation of IBFS area for this study. However, the size of the separation zone was correlated to geometric and hydraulic variables and thus could demonstrate that increasing curvature showed a positive correlation with the area of IBFS.

In another study, (Ferguson et al., 2003) compared flow recirculation and mean flow structure in two sharply curving bends also on the Dean River. The authors collected field data on flow and depth, but those data were of a coarse spatial resolution, whereby flow was measured at only 12 cross-section for the first bend and for 17 cross-sections on the second, therefore, they combined it with time-averaged Computational fluid dynamics (CFD) model in order to obtain a high spatial-temporal resolution for their data. They attributed the major differences in flow features in the studied bends to the differences in the planform of the upstream river reach, which caused an asymmetry of the inflow velocity field into the bend. Nevertheless, the extent of IBFS was not explicitly calculated and correlated with bend shape parameters (curvature or angularity).

Hence, the following knowledge gaps were identified:

1. The **lateral extent of IBFS** has been only subjectively quantified (also including detection and delineation of the zone) from real river examples which prevents comparisons to be made between studies. And its systematic analysis with high-resolution 2-D field data on meander bends of a dynamic river channel collected during a small time-frame at similar discharge conditions has rarely been achieved;

2. In-depth understanding of **factors governing IBFS characteristics** across bend planform shapes are still lacking, particularly for the form-process linkages and
3. Differences in flow and hydraulic geometry such as macro-scale bed features of **meander bend planform**, particularly fat (mature, hairpin-like) v/s angular (abruptly curving) bends have been rarely discussed from a set of natural river bends.

To address the aforementioned gaps, the following research aims were followed:

1. Quantify inter-relationships among planform and hydraulic geometry bend parameters.
2. Quantification of the lateral extent (inner bank towards channel center) of the IBFS at the apex.
3. Quantify the relationships of bend planform and hydraulic geometry parameters with the lateral extent of IBFS.
4. Investigate differences in key flow and macro-scale bed topography between angular and fat planforms, in light of their relevance to the features of IBFS along with implications of their morphodynamic influence.

In this regard, a section of the Prut River (Romania / Moldova) was selected which is one of the few remaining actively meandering lowland rivers in Europe, that still retains the meandering dynamics. 14 meander bends were surveyed differing in bend geometry and elaborated a database on them with the high-resolution flow and bathymetry information, calculated parameters of bend planform, flow and hydraulic geometry, which were then used to delineate the respective extent of the inner-bank flow separation zones for each bend. Such quantitative knowledge on the factors governing IBFS size and characteristics would enable better predictions of meander morphodynamics and channel flow conveyance capacity and hence improve developing river restoration strategies, particularly those aimed at re-meandering river channels.

3.3. Material and methods

3.3.1 Study area

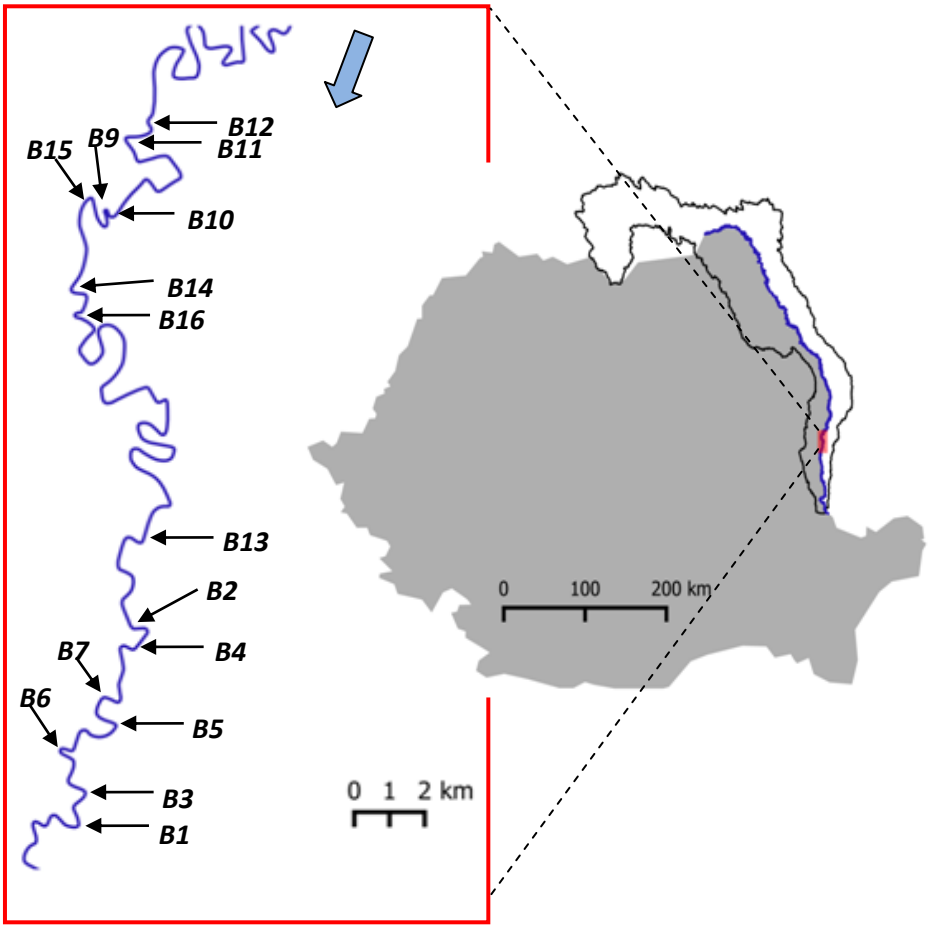

Fig 14. The geographical location of the Prut River catchment and of the river section that includes bends studied herein. The border of Romania is shaded grey, with the inset showing the study section. Note: B stands for bend.

The studied bends were located within a 50-river km section of the Prut River (between Falciu and Vadeni) and this section of the river falls in the tapered region of the catchment (Fig 14). This ensured hydrological homogeneity throughout the study period, specifically, as there are no incoming major tributaries and the negligible effect of precipitation run-off. The slope in this section of the river was around 0.06 m km $^{-1}$ and the mean daily discharge ranged between 39-40 m^3s^{-1} during the field-work period. Moreover, no significant change in water stage was observed in this period at the banks indicating stable flow conditions.

The selection of studied meander bends rested on numerous factors so that bends were selected with, low level or no bank stabilizations, presence of least amount of woody debris or fallen trees, particularly around the bend apex region as this can significantly alter flow and sediment processes in bends (Gurnell and Petts 2006), and on presence of similar land-use types on both banks i.e. mostly forested and low anthropogenic impact reaches.

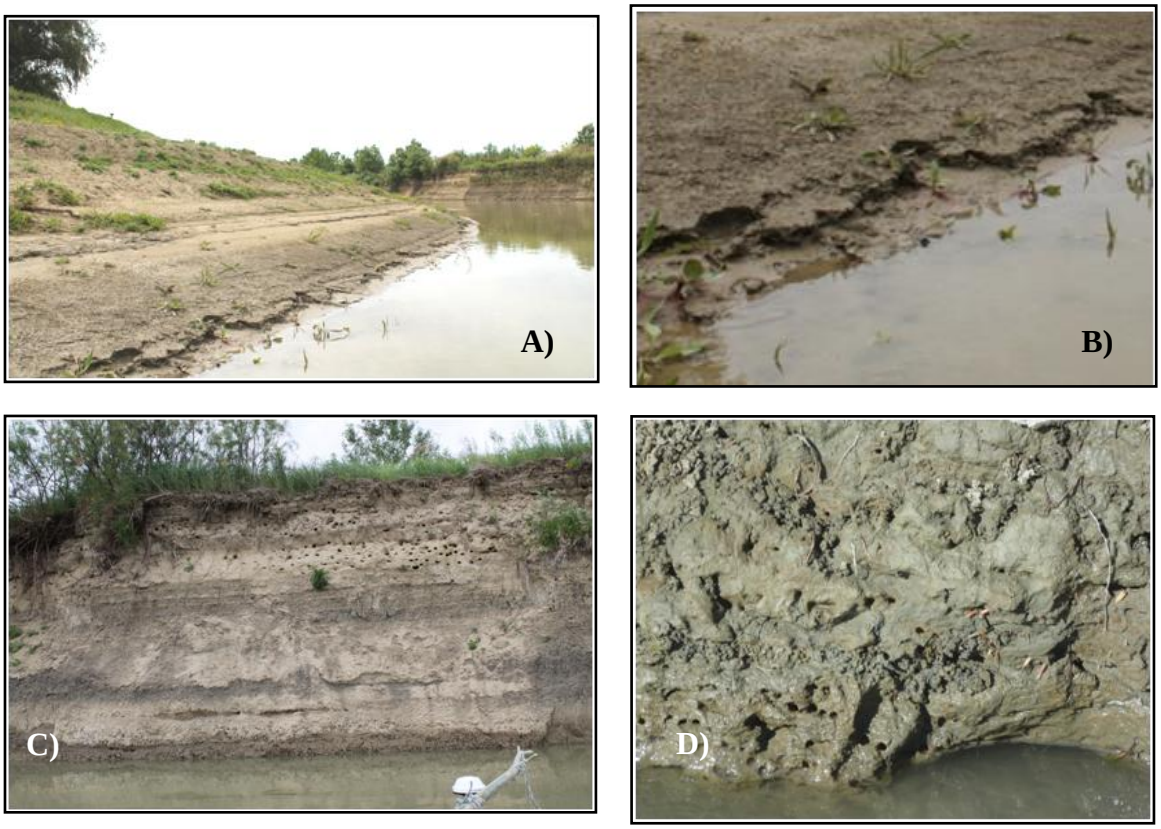

Fig 15. Geomorphological features of meander bend on Prut. A) Point bar, B) fine sand deposits at point bars, C) vertical outer bank and D) clay-fine silt composition of lower parts of
outerbank (bend B9), also burrow holes produced by the larvae of the mayfly *Palingenia longicauda*. Photos A-C were provided by Tarun Bisht, D was provided by Dr. Gabriela Costea, IGB, Berlin.

The meander bends displayed typical vertical banks at the outer banks with signs of undercutting and subsequent bank failures (Fig 15C), whereas the inner banks displayed point bars (Fig 15A). Visual inspection of outer banks showed clayey-fine silt material to dominate the lower parts of the banks (Fig 15D) while upper parts were mostly composed of finer sand (Fig 15 C). Point bar deposits were mainly composed of coarser sand and gently sloping

towards the channel center (Fig 15A). The upper parts of outerbanks of meander bends on Prut provided nesting habitats for sand martin (*Riparia riparia*). Whereas, the lower parts of these banks were found to harbor burrows of the Tisza mayfly larvae (*Palingenia longicauda*), which is indicative of the clayey texture of the banks, as clay dominated banks provide much more structurally stable environment for the typical U-shaped burrows of these mayfly larvae.

3.3.2 Data acquisition on field

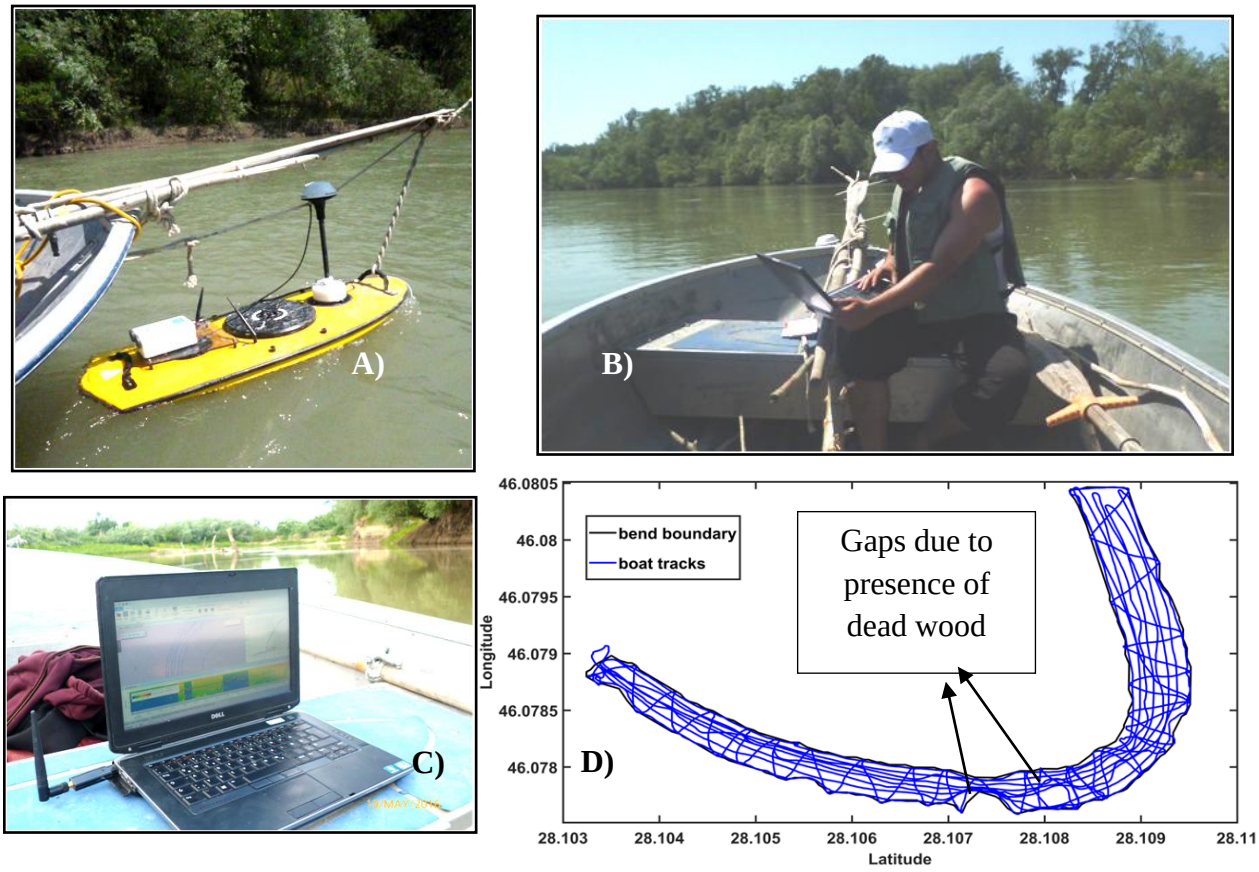

Fig 16. Flow and bathymetry data acquisition at the field sites. A) Vessel mounted Acoustic Doppler Current Profiler (ADCP) used in this study, B) ADCP operation C) Hydrosurveyor software D)An example bend (bend B1) showing ADCP zig-zag and longitudinal runs.

A total of 14 bends were measured for flow and bathymetry variables using an ADCP (Acoustic Doppler Current Profiler) mounted vessel (Fig 16A) coupled with Hydrosurveyor software (Fig 16B and C) during the field campaign. ADCP vessel runs were made with the aim of capturing maximum information by performing zig-zag and longitudinal runs (Fig 16D) that resulted in a mesh of soundings. Owing to the active migrating nature of the Prut

River, finding a meander bend without large woody debris was rare. This often leads to the selection of meanders on the field, nonetheless, efforts were made in order to select the meanders with no visible large woody debris (protruding from the surface) in the apex region of the bend. However, some smaller fallen trees were still present in bends and these lead to the missing gaps in the ADCP data as the vessel could not access those regions (see, Fig S4 in appendix B for examples of fallen trees on meanders of Prut).

3.3.3 Post-processing of data

For each bend, the data collected on the field was interpolated through a two-step process. This included an initial averaging and interpolation of missing gaps in velocity and depth points using Hydrosurveyor's (ADCP software interface provided by Sontek) in-built algorithm. Followed by interpolation and fitting of velocity and depth values onto cross sections in a curvilinear grid (SNZ coordinate system) using the PyRIS algorithm (Monegaglia et al., 2018). Ensemble averaged 3-D velocity and depth data were obtained from Hydrosurveyor. In the Hydrosurveyor's interpolation procedure the soundings were de-spiked first and then spatially averaged based on user-defined grid spacing. After averaging, a Delaunay triangulation of the scattered data is computed and interpolation is performed using a natural neighbor algorithm. Thus, the data gaps occurring in the ADCP zigzag runs were filled with meaningful values. Subsequently, this dataset was exported into PyRIS environment whereby, after defining a curvilinear grid (SNZ), the bend centerline was sampled based on the outer and inner bank boundary points. In order to avoid over or under interpolation, centerline points were sampled at a spacing, which produced an overall number of data points compared to those in corresponding Hydrosurveyor datasets (see. Table S2 in appendix B)

Subsequently, for each point of the centerline, a cross-section was created which was placed normal to its position on the centerline. These cross-sections were equally spaced within the bends along with the points occurring on each cross-section. Finally, using a third-order cubic spline interpolation the data points (velocity and depth) were filled onto the defined cross-sections. Also, for each point on the centerline, the local curvature (C^{-}) or which is the inverse of the radius of curvature (Hickin and Nanson 1975; Furbish 1991) and cross-sectional width (B) were calculated.

3.3.4 Calculation of bend planform shape and hydraulic geometry parameters

The following bend planform shape and hydraulic geometry parameters were calculated based on data on local curvature (C^{-}), local cross sectional width (B) and local depth (H) for each bend. The width and depth variations among the bends is an important factor controlling the flow through the bends (Markham and Thorne 1992), based on this several key hydraulic parameters were then calculated. Such as, the width to depth ratio (B/H) was calculated based on averaged values of channel width and depth. Bend averaged flow depth (H_{mean}) and maximum cross-sectional depth (H_{max}) were also calculated. In addition to this, the pool depth (H_p) was calculated as the averaged depth of five cross-sections located upstream and downstream of the deepest point at the bend apex. While the upstream riffle depth (H_{ru}) was calculated by averaging depth across 5 cross-sections located upstream and downstream of the shallowest depth point (as noted from the longitudinal depth distributions of bends). An important parameter recognized was the depth ratio (H_{ratio}) calculated as the ratio of H_p by H_{ru}, it explains the degree of relative deepening of the pools to that of the upstream riffle (Parsons, 2002).

Bend curvature is perceived to be a key parameter in governing flow structure around the bends (Bagnold 1960; Leeder Bridges 1975; Furbish 1988). Width normalized bend curvature ($C_{max}B$) was calculated or the inverse of width normalized bend curvature (R/B). The '0.5' threshold was used to delineate round ($C_{max}B< 0.5$) from sharp ($C_{max}B> 0.5$) (see Vermeulen et al 2014). In our case, I used the maximum value of local curvature (C_{max}) to define the bend curvature because the channel centerline was sampled (using PyRIS) at small intervals normally ranging from 0.5-1.5 m, therefore even slightest change in the local curvature series was detectable and C_{max} was, therefore, a reliable value. Furthermore, maximum or peak curvature rather than averaged bend curvature is often argued for bearing a direct relevance information flow separation zones (Parsons, 2002). Furthermore, the curvature ratio (Cr) was calculated as C_{max} by C_{mean}. And Cr= '3' is used as a delimiter for angular and non-angular bends on the Prut (chapter 2). This ratio of maximum to mean curvature gives an idea about the straightness of upstream and downstream arms of the bend whereas the maximum curvature value decides how abruptly the bends turn.

3.3.5 Delineation of the extent of the inner-bank flow separation (IBFS) zone

3-D velocity was recorded in ENU system as velocity in easting, northing and up directions and was converted to a stream-wise coordinate system (in PyRIS). Hydrosurveyor

further enabled automatic calculations of 3-D depth-averaged velocity from raw data extracted from different water column zones, namely: over the complete depth, called depth-averaged velocity (U in ms^{-1}), over a certain depth from surface into water column, called near-surface velocity (U_{surf} in ms^{-1}) and over a certain above the bottom, called near-bed velocity
(U_{bed} in ms^{-1})(see, Table S3 in appendix B). Previous flume studies have identified the cross sectional gradient of the streamwise velocity (U) as the indicator of flow separation, as an inflexion point in the model S-shaped curve physically marking the development of shear layer between the faster and slower flowing adjacent flow within a cross-section (see, Blanckaert 2013 and 2015). While for other field studies studying IBFS only visual on-field validation was performed when defining the lateral extent of IBFS (see Parsons 2002, Ferguson et al 2003). However, for the present dataset, calculation of a mathematical inflexion point was not adopted. Instead, I adopt a two-step procedure, which takes advantage of the high number of equally spaced data points on the cross-sections, mean spacing between cross-sections being c. 1 m and of the fact that each data point has a depth-averaged magnitude (ms^{-1}): V (transverse velocity magnitude) and U (downstream velocity magnitude)

For the first step, a ratio of transverse to downstream velocity (V/U) was calculated for each point in each cross-section. This ratio physically depicts points of slower or no flow whereby, values of V/U ~1 mark slower flow compared to V/U<1 or V/U>1 for very higher or lower downstream or transverse flow, respectively. Typically, the cross-sectional velocity profiles form an S-shape in case of streamwise flow (U in fig 17A) with higher values associated with the outer bank while, contrastingly, inverted S-shape forms in case of transverse flow (V in fig 17A), with higher values occur near inner banks. Expectedly, V/U around bend apices should be unity, often spatially distorted near the inner banks and far from unity, spatially uniform/regular towards the outer banks (fig 17B). The spatial distortion of V/U values, from inner to outer bank physically marks the zone of slow downstream flow. In order to systematically capture this distortion in the V/U values (zone of slower flow) rolling standard deviation (SD) was applied on each cross section. For this a window of ‘3’ points was applied to the ‘n’ points occurring on each of the cross sections, so that, for each cross section a total of ‘n-2’ values of SD were returned (fig 17B).

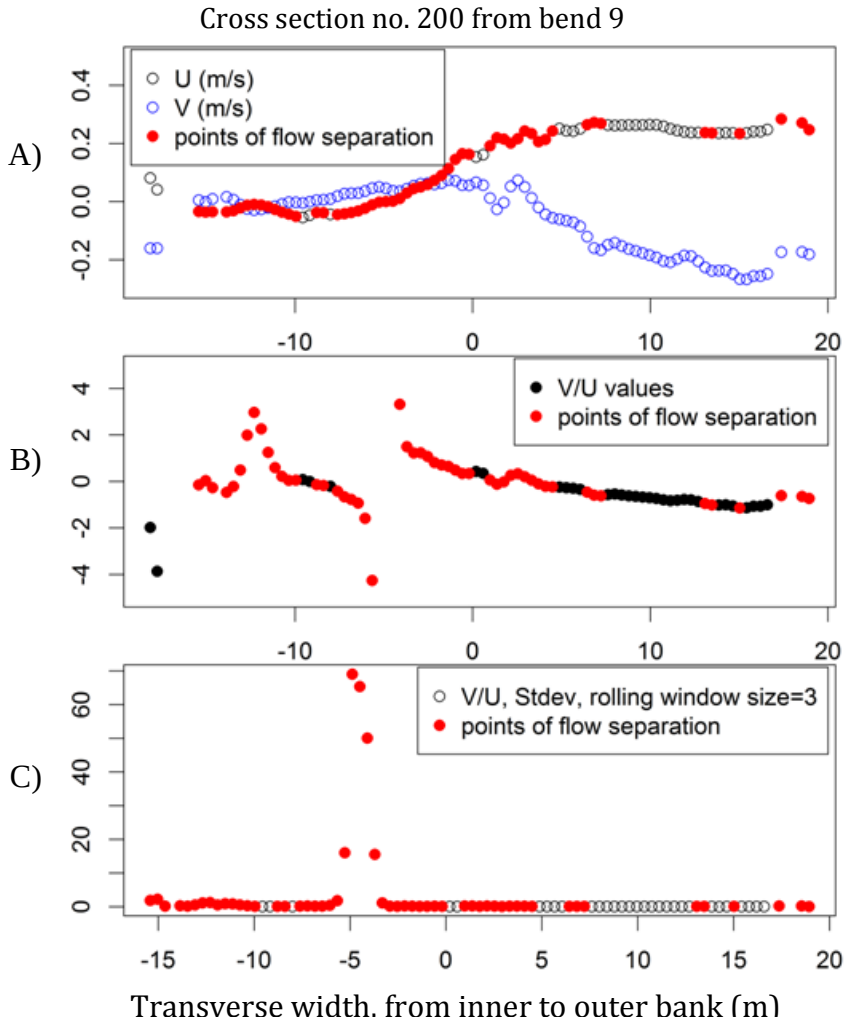

Fig 17. An example of cross section displaying the method of delineating the extent of IBFS adopted in this study.A) cross-sectional velocity profile forming an S-shape in case of streamwise flow(U and V in m/s), B) Ratio of V/U with points where flow is separated, C) Result of sensitivity analysis i.e. after application of rolling standard deviation. Note: red points mark the points included as IBFS points after applying the SD>0.056 thresholds.

In fact, rolled SD (n=3) is sensitive towards change in variance within the cross section that enables detection of a change at a finer resolution i.e. for every consecutive V/U value in the cross section. Subsequently, the calculated SD values for all bends were pooled together in order to check the global distribution of SD among the 14 meander bends. This aided, in a selection of a single threshold of SD exceeding which the points can be included as points falling within the IBFS zone across the 14 bends. This selection was achieved using a sensitivity analysis whereby, the points (spatial coordinates) exceeding different quantiles (Q_{75}, Q_{90}, Q_{95} etc) of the global SD were plotted along with bend boundaries to confirm if

they fell into the expected zone of IBFS, around the apices of the bends. Consequently, points that had SD values higher than Q_{90} (SD>0.056) were selected (Fig 17C), as these represented the most realistic picture of IBFS zone across all meander bends. Next, in order to remove the obvious erroneous values, two additional trims were made on the selected data points. First, the values higher than $Q_{99.9}$ of the SD were removed as outliers. Second, a 10^{th} of channel width points were manually removed from the inner banks of each bend, as this high SD was created due to the effect of the banks itself and these values if not removed could hinder the demarcation of the IBFS edge in the next step.

For the second step, the spatial coordinates of the selected data points were used i.e. points with SD>0.056 to demarcate the boundary of IBFS for the 14 bends. In fact, the spatial distribution of points included IBFS zone displayed some points that were seemingly generated due to local smaller-scale turbulence and eddies that are constantly formed at the bend apex.

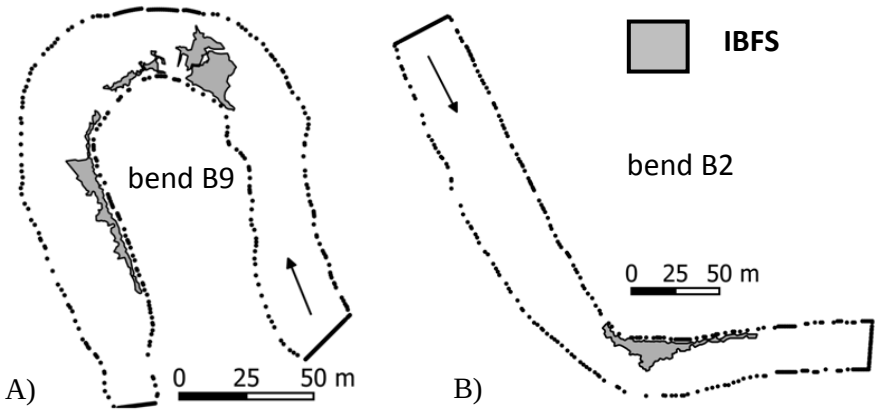

Fig 18. The lateral extent of IBFS as demarcated by the concave hull function in Q GIS (2.12).A) Bend B9, B) Bend B2. Black arrows denote the flow direction.

Hence, to screen out such values, the lateral extent of IBFS was demarcated based on the density of points with high SD (SD>0.056) using a concave hull function (Moreira & Santos, 2007) in QGIS version 2.12. This function allows for density dependent creation of boundary around a cloud of points, whereby the user can define the *k*-nearest neighbors to be considered around a selected boundary point when including a set of points into the boundary. I used comparable k values i.e. 2 to 3 neighbors and N- neighborhood size i.e. 5 to 8 for creating the boundaries of IBFS (Fig 18).

Finally, to calculate the fraction of width covered by the lateral maximum extent of IBFS, I selected n > 6 points of the data points falling on the edge of the demarcated zone where the IBFS laterally extended to the maximum of the channel width. Subsequently, the width from the inner banks to these points was then averaged and the percent of width occupied by the lateral extent of IBFS zone was calculated for each bend as follows:

$$IBFSpercent = (IBFS_B \div B_{mean}) * 100$$

Whereby, $IBFS_B$ is the averaged width of the selected boundary points displaying the maximum extent of IBFS around the bend apex and B_{mean} is the averaged width of the cross sections corresponding to the presence of IBFS.

3.4 Results

3.4.1 General characteristics of studied river bends

Table 3. Summary of geometric and hydraulic parameters of the studied river bends. Bend shape legends: S= sharp; R= round; A=angular; F=fat.

Bend name	Bend shape based on $C_{max}B$	Bend shape based on Cr	Q (ms^{-3})	$C_{max}B$	$C_{mean}B$	B_{mean}	Cr	H_{mean}	H_{ru}	H_p	H_{ratio}	B/H
B1	S	A	40.0	0.58	0.1	35.0	4.1	3.2	2.1	5.4	2.5	11
B2	S	A	39.2	0.78	0.2	47.4	4.6	2.5	1.5	5.2	3.5	20
B3	R	NA	40.0	0.42	0.2	38.1	2.5	3.2	2.7	4.7	1.7	12
B4	S	A	39.2	0.70	0.2	40.1	3.7	3	2.0	5.5	2.7	14
B5	S	F	-	0.76	0.3	34.9	2.6	3.7	3.2	5.2	1.6	9.4
B7	S	A	39.2	0.60	0.2	42.7	3.5	3.3	2.5	5.3	2.1	13
B9	S	F	39.6	0.80	0.4	37.0	2.0	3.8	4.1	5.5	1.3	9.7
B10	S	F	39.6	0.60	0.3	39.7	2.0	2.8	2.1	3.8	1.8	14
B11	S	A	39.6	0.94	0.3	35.6	3.8	4	3.3	5.5	1.7	9.0
B12	R	NA	39.2	0.26	0.2	37.6	1.7	2.4	2.4	3.1	1.3	16
B13	S	F	38.9	0.85	0.4	41.9	2.4	2.8	1.9	5.3	2.8	15
B14	S	NA	-	0.52	0.2	38.1	3.1	3.2	2.2	5.2	2.4	12
B15	S	A	39.6	1.0	0.2	44.0	5.0	2.6	2.1	5.3	2.5	17
B16	S	F	39.6	0.8	0.4	41.1	2.0	4	3	5.1	1.7	10

The study set of 14 meanders had very similar discharge (Q = 38.9 - 40.0 ms^{-3}) and similar mean channel width (35 - 44 m), but spanned a considerable range of bend curvature ($C_{max}B$ = 0.26 to 0.94) and bend angularity (Curvature ratio, Cr = 1.7 to 5.0) (Table 4). Based on curvature ratio (Cr), I distinguished an abruptly curving bend type (including B1, B2 and B15) with a curvature ratio (ratio between maximum curvature and mean bend curvature) surpassing a threshold of three (Cr > 3), which are thus, later on, referred to as 'angular' bends. While bends falling below the threshold of three (Cr < 3) are referred to as 'fat' bends. In morphometric sense, the studied bend set then includes at least two bends of each bend shape type, as, round bends ($C_{max}B$ < 0.5) exemplified by bends B3 and B12; sharp bends ($C_{max}B$ > 0.5) exemplified by bends B9 and B15; angular bends ($C_{max}B$ higher than three times the $C_{mean}B$) exemplified by bends B2 and B15; fat bends ($C_{max}B$ lower than three times the $C_{mean}B$) exemplified by bends B9 and B5.Pool depth (H_p)averaged at 4.96 m (range = 3.8– 5.5 m). The channel aspect ratio (B/H) highly varied within the bends, ranging from 7.3 to 20. Most bends are to be considered as relatively wide and shallow (B/H >10).

3.4.2 Covariance among bend planform shape and hydraulic geometry parameters

In order to identify the parameters controlling IBFS size, covariations among the potential governing geometric and hydraulic parameters were explored by computing Pearson's correlation coefficients among them (Fig 19). A strong positive correlation (r= 0.68, n= 14, p < 0.01) was found between bend curvature ($C_{max}B$) and mean depth at the pool (H_p). The positive relationship between bend curvature and depth variation is also supported by the significant positive correlation (r = 0.54, n = 14, p < 0.05) between mean bend curvature ($C_{mean}B$) and upstream riffle depth (H_{ru}). Accordingly, curvature ratio (Cr) showed a strong positive correlation (r = 0.7, n = 14, p < 0.005) with depth ratio (H_{ratio}), i.e it is high tendency for angular bends to display a higher deeper pools compared to upstream riffles. In accordance with these findings, mean width at the respective upstream riffle (B_{ru}) displayed a strong negative correlation (r = -0.91, n = 14, p < 0.005) with the upstream riffle depth (H_{ru}) and also with mean bend depth (H_{mean}) (r = -0.66, n = 14, p < 0.01).

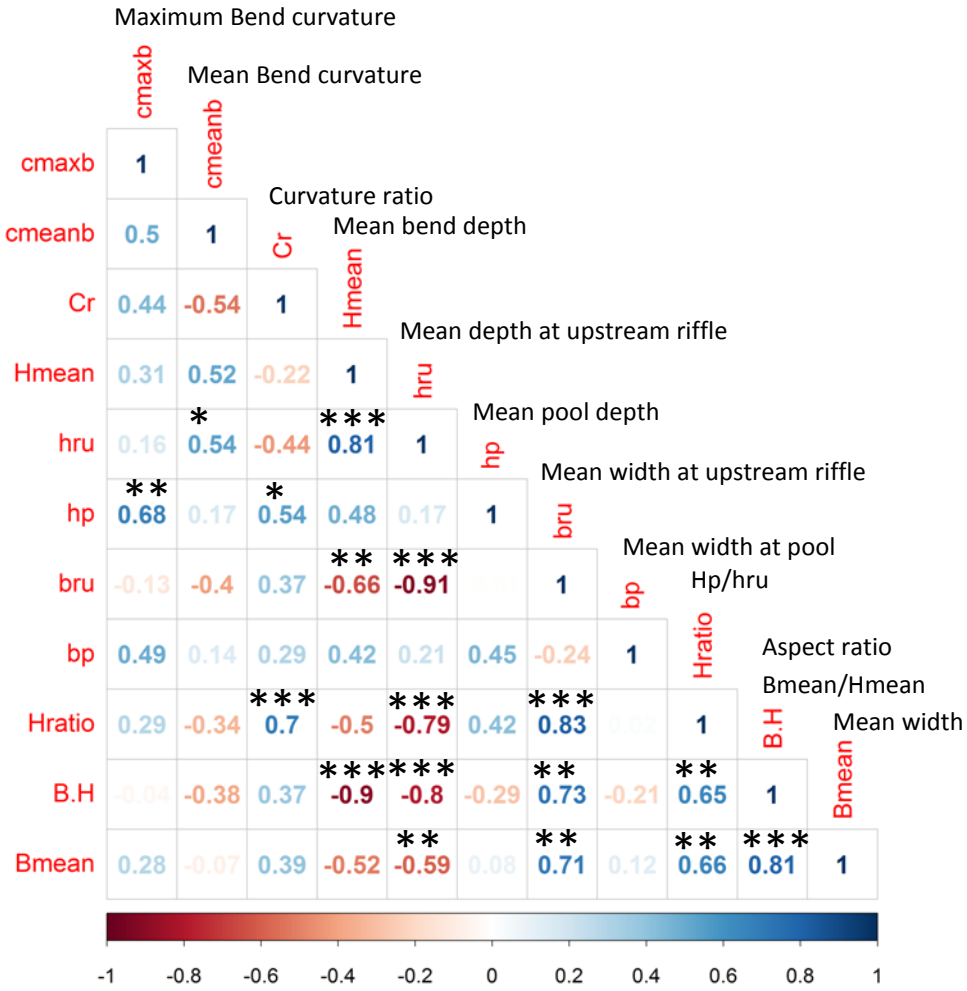

Fig 19. Correlation matrix computed to analyze parameter corvariance among geomteric and hydraulic variables. Note: P-value scale used: * < 0.05, ** <0.01, *** < 0.005.

The analysis of the covariance between geometric and hydraulic parameters shows that bend curvature ($C_{max}B$) and curvature ratio (Cr) represent key parameters for the shape of a bend and thus also for the emergence of an IBFS zone, as well as pool depth (H_p) representing the intensity of scour, and depth ratio (H_{ratio}) that indicates the magnitude of deepening of the pool relative to that at the upstream riffle.

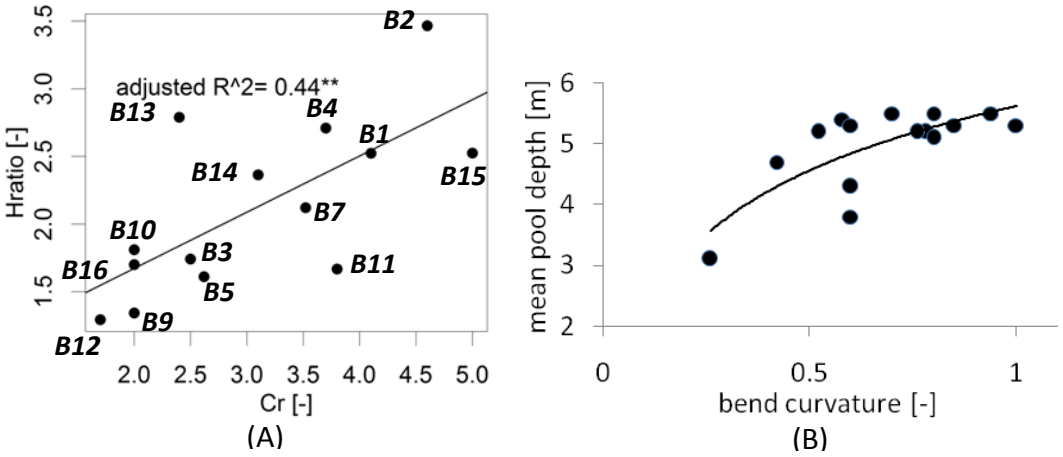

Fig 20.Relationship and trends between bend shape and hydraulic geometry parameters. A) Simple linear regression between depth ratio (H_{ratio}) and curvature ratio (Cr), H_{ratio} = 0.83 + 0.41 (Cr); and B) trend between pool depth (H_p) and bend curvature ($C_{max}B$). Note: [-] indicates the dimensionless nature of parameters.

In order to explore the interrelationships of these variables in a quantitative way, linear regressions were then performed among these variables. Results (Fig 20A and B) revealed that depth ratio (H_{ratio}) increases significantly with an increase in bend angularity (Cr), (H_{ratio} = 0.83 + 0.41Cr, adjusted R^2 = 0.44, n= 14, $p < 0.005$) (Fig 20A). While, H_p increased with higher $C_{max}B$ values, although it appeared to stabilize as $C_{max}B$ exceeded 0.5. Thereby, bend hydraulic geometry parameters could be well predicted by the bend planform shape parameters. However, some bends deviate considerably from the regression line (see Fig 20A: B2, B11, B13) which may be explained for the case of B11 by an exceptionally high cross sectional width at the apex (pool width is 1.5 times of upstream riffle) that accordingly includes a relatively shallow pool. For the case of bend B13 it appears that its mean curvature (C_{mean} B) is extraordinarily high due to the fact that the downstream arm of the bend is curved.

3.4.3 Influence of bend curvature and pool depth on IBFS size

An IBFS was detected in all of the studied bends, and there covered a range of c. 14-60 % of the cross sectional width at the apex of these bends, respectively (Fig 21). Curvature ratio (Cr) and the ratio of upstream riffle to pool depth (H_{ratio}) did not show any relationship with IBFS size. Instead, bend curvature ($C_{max}B$) was found to display a significant positive relationship with IBFS size (fig 21A) (IBFS size = 6.1+ 45.8 $C_{max}B$ + 8.2, $p < 0.001$, adjusted

R^2= 0.55, N=14). Also, IBFS size displayed a weak yet significant increase with increasing pool depth (H_p) (Fig 21C) (IBFS size = -14+ 10.3 H_p + 10.2, p<0.02, adjusted R^2 = 0.30, N=14). Thereby, bends with higher bend curvature were mostly also deeper and narrower (B/H<10) (Fig 21B).

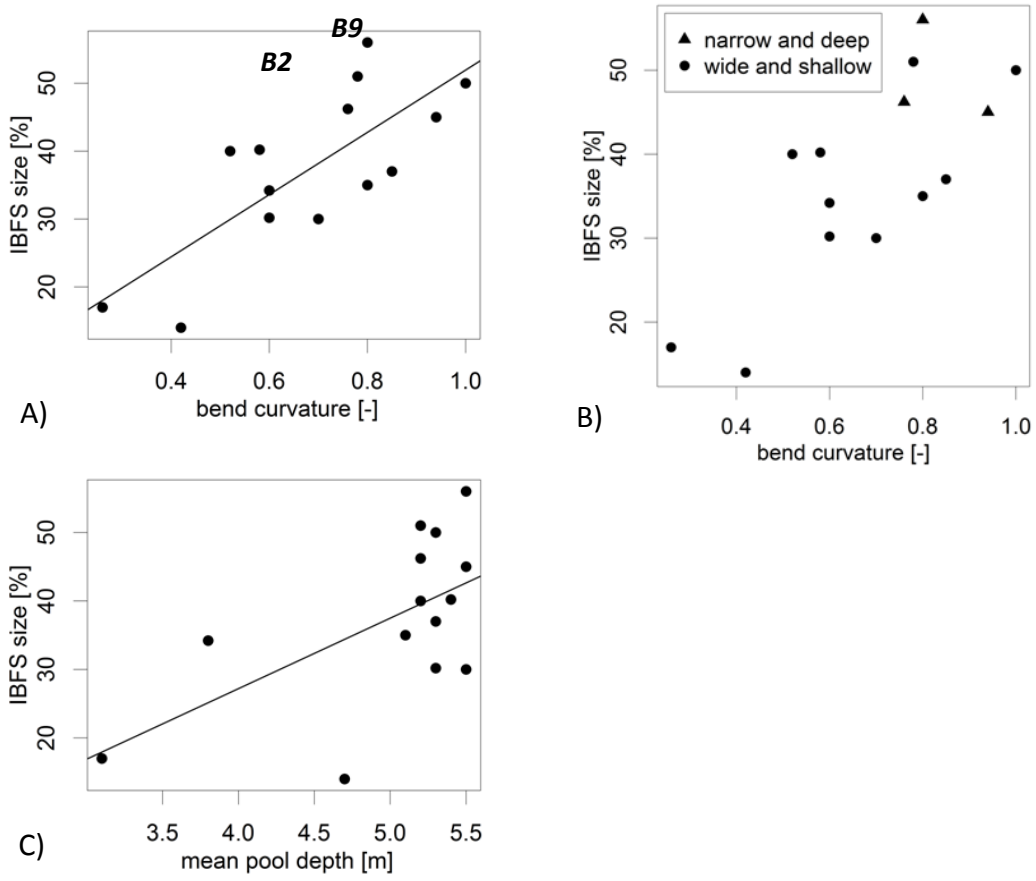

Fig 21. Relationships and trends between IBFS size, as expressed by the percentage covered from total channel width at bend apex, and bend shape and hydraulic parameters. (A) Between bend curvature and IBFS size (IBFS size = 6.1+ 45.8 $C_{max}B$+ 8.2, p < 0.001, adjusted R^2= 0.55, N=14); (B) between bend curvature and IBFS, with data symbols representing narrow and deep and wide and shallow bends separately; (C) between mean pool depth (m) and IBFS size, (IBFS size = -14+ 10.3 H_p + 10.2, p < 0.02, adjusted R^2= 0.30, N=14). Note: [-] indicates the dimensionless nature of parameters.

3.4.4. Descriptive features of flow and bed topography of exemplary fat and angular bends

Even that the size of the IBFS zone is well predicted by bend curvature, its features in the horizontal and vertical dimensions may differ. Moreover, an unusual difference in the hydraulic geometry features (depth ratio) in bends of comparable curvature values featuring similar IBFS extent prompted an analysis to explain such variation.

Table 4. Characteristics of IBFS in the two bends (angular, bend B2 and fat, bend B9). Note: The horizontal recirculation here is defined as the maximum extent of the reversed flow within the IBFS.

Bend ID	**IBFS size (% width)**	**Horizontal recicurlation of flow**			**IBFS type[2] at apex**	**No .of IBFS zones**
		extent at surface (fraction width at apex)	velocity magnitude at surface (ms^{-1})	velocity magnitude at bed (ms^{-1})		
B9	56	1/2	-0.1	-0.05	Closed	2
B2	51	1/5	-0.1	-0.06	Closed	1

Table 5. Common and contrasting features o flow and bed-topography between bend B2 (fat) and bend B9 (fat).

Bend	**$C_{max}B$**	**Cr**	**Bend type**	**H_{ratio}**	**Inflow into apex**	**Point bar and circular pool**	**Concave-bank bench**	**Upstream riffle to pool transition**
B9	0.8	2	Fat	1.3	Asymmetric, with higher flow at the inner half	Extensive; non-circular pool	present	gradual
B2	0.78	4.6	Angu-lar	3.5	Asymmetric, with higher flow at the outer half	Eroded; circular pool	absent	steep

[2] According to Blanckaert (2015, fig1) IBFS can occur as closed/open zone often characterised by a presence/absence of an inner core of horizontal recirculating flow.

Following this, two bends (B2 and B9) with the largest IBFS extent(Table 5), but which belong to different bend types: B9 a fat bend form and B2 shows an angular bend form (Table 6) were selected from the studied set of bends. For these bends, descriptive analyses of near-surface, near-bed flow (see methods for the description of these zones) and of the macro-scale bed topography was performed in order to elaborate the vertical characteristics of the flow separation zone, as in flume experiments it has been observed that the IBFS has a distorted vertical profile (Blanckaert, 2015), whereby, the zone extends farther near the surface and diminishes towards the bed.

3.4.5 Common features between the two bends

In both bends, B2 and B9, near-surface (U_{surf}) and near-bed (U_{bed}) velocity at the inflow (upstream of the bend apex) was fairly asymmetrical (fig 22A and B; fig 24A and B). In bend 9, at the inflow cross-section (see, fig 23 cross-section 133) highest velocity (U_{bed} and U_{surf}) occurs at the inner-half of the bend (i.e. closer to inner bank) whereas in bend 2 at the corresponding section (fig 25, cross-section 200) it is shifted on the outer half of the cross section.

As usually found in rivers, in the upstream arms of both bends, U_{surf} was higher than U_{bed}, particularly before the bend apex, as U_{bed} is reduced by bed roughness. In the curving region of both bends, the filament of highest velocity flow (reflected by U_{surf} and U_{bed}) is then directed over onto the deeper parts of the bend, i.e. towards outer banks (fig 22 and 24). Velocity magnitude of the horizontal recirculation zone occurring within the IBFS is higher near the surface than near the bed in both bends (see table 5) i.e. a stronger flow reversal occurs near the surface compared to near-bed, which is probably again influenced by bed roughness.

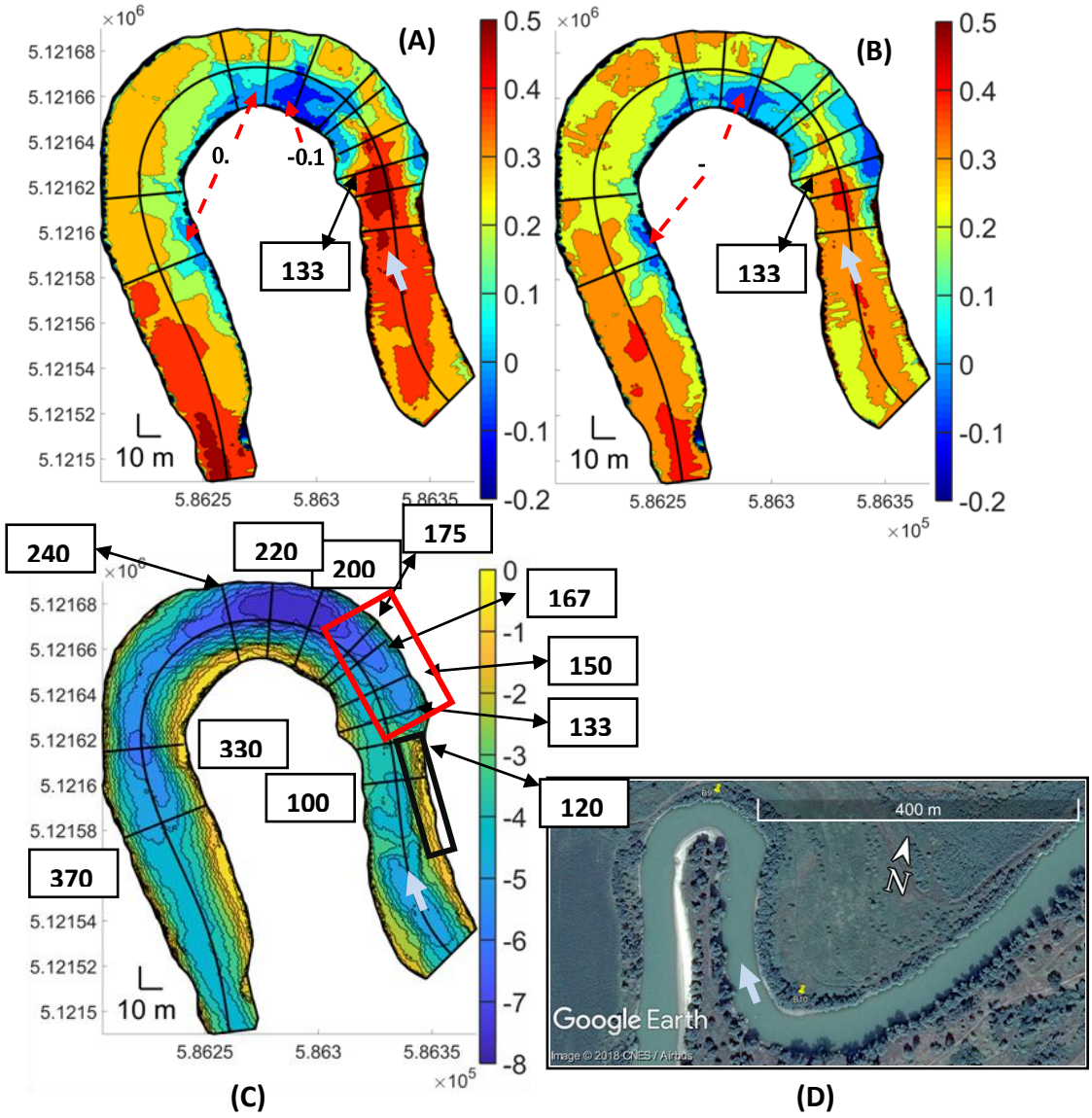

Fig 22. Planform view, flow velocities and bathymetry of **bend B9** featuring a **fat geometry** and the largest IBFS size within the studied set of bends. (A) U_{surf} (derived from near-surface cells, on average starting from c. 0.1- and ending c. 0.3 m depth, mean U_{surf} zone depth= 0.2 m, SD= 0.1) with numbers in black highlighting the zero and reversed flow contours (marked with red arrows) (B) U_{bed} (derived from near-bed cells, on average starting from c. 2.3- and ending c. 2.5 m, mean U_{bed} zone depth= 0.2, SD= 0.1) with numbers in black highlighting the zero and reversed flow contours (marked with red arrows) (C) Depth contours [3] with the **red box** marking the riffle to pool transition, the **black box** marking the location of concave upstream bank bench and **black lines** with labels of the respective cross-sections marking

[3]Contours interpolated on a 0.5*0.5 m grid, at contour interval level of 50 for velocities and 20 for depth contours, for best clarity and visual interpretation (using Matlab, filled contour command function).

cross sections such as the area of maximum flow separation (200-220); inflow cross-section into the bend (133); highest curvature change (167). D) Google Earth image of B9 at lower discharge level (dated: 2017), also showing upstream planform and the point bar.

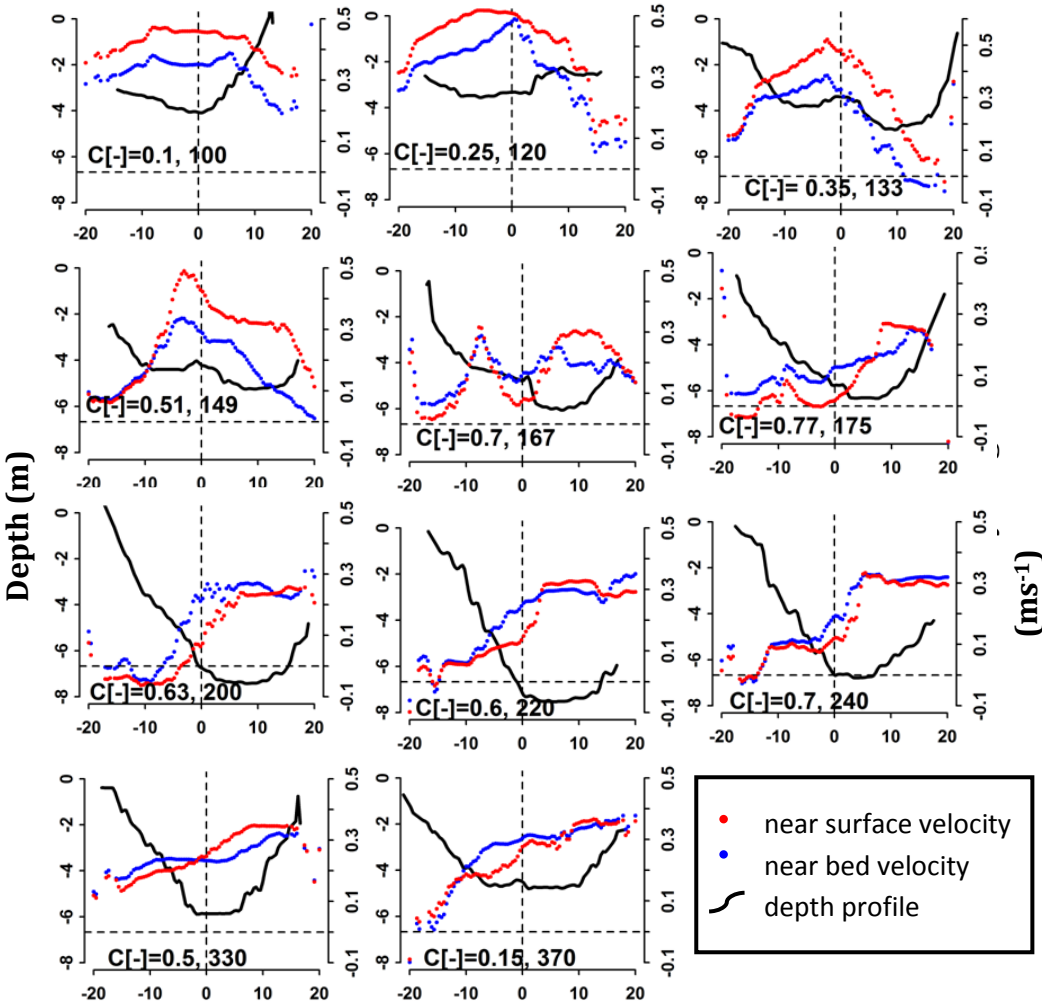

Fig 23. Selected cross-sectional profiles of bend B9 with depth, surface and near-bed flow velocities. With additional information on local curvature as C [-] and cross section number. Note: horizontal dashed black lines in cross-sectional profiles represent zero flow velocity.

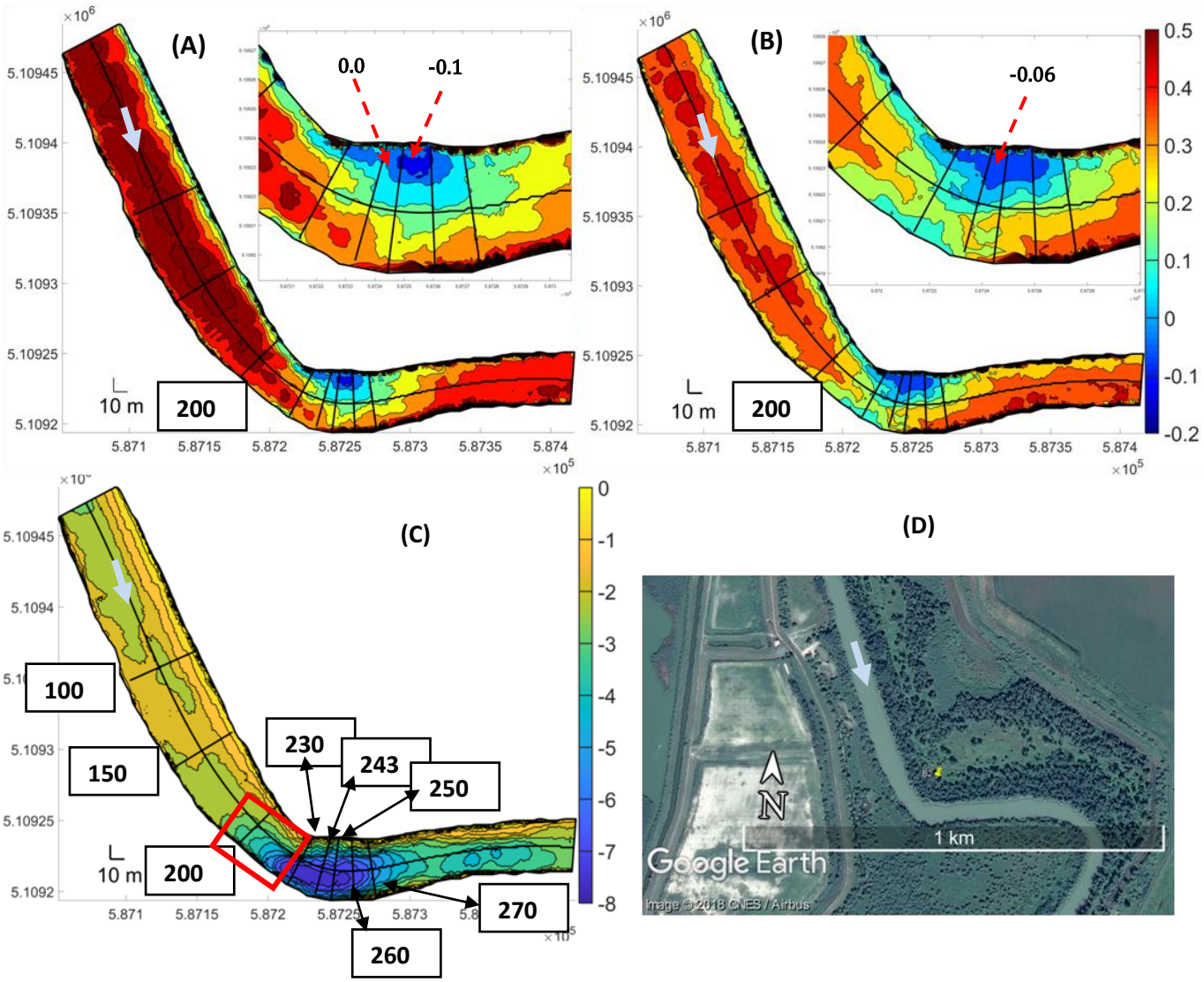

Fig 24. Planform view, flow velocities and bathymetry of **bend B2** featuring an **angular shape** and the second-largest IBFS size within the studied set of bends (A) U_{surf} (derived from near-surface cells, on average starting from c. 0.1 and ending c. 0.2 m) with numbers in black highlighting the zero and reversed flow contours (marked with red arrows). (B) U_{bed}(derived from near-bed cells, on average starting from c. 1.7 and ending c. 2 m) with numbers in black highlighting the zero and reversed flow contours (marked with red arrows). (C) Depth contours[4] with the **red box** marking the riffle to pool transition, **black lines** mark key cross sections such as- area of max flow separation (cs 243-260); inflow cross section into bend (cs200); highest curvature change (cs243) (D) Google Earth image at lower discharge level (dated: 2017), showing straighter upstream arm and narrow point bar.

[4]Contours interpolated on a 0.5*0.5 m grid, at contour interval level of 50 for velocities and 20 for depth contours, for best clarity and visual interpretation (using Matlab, filled contour command function).

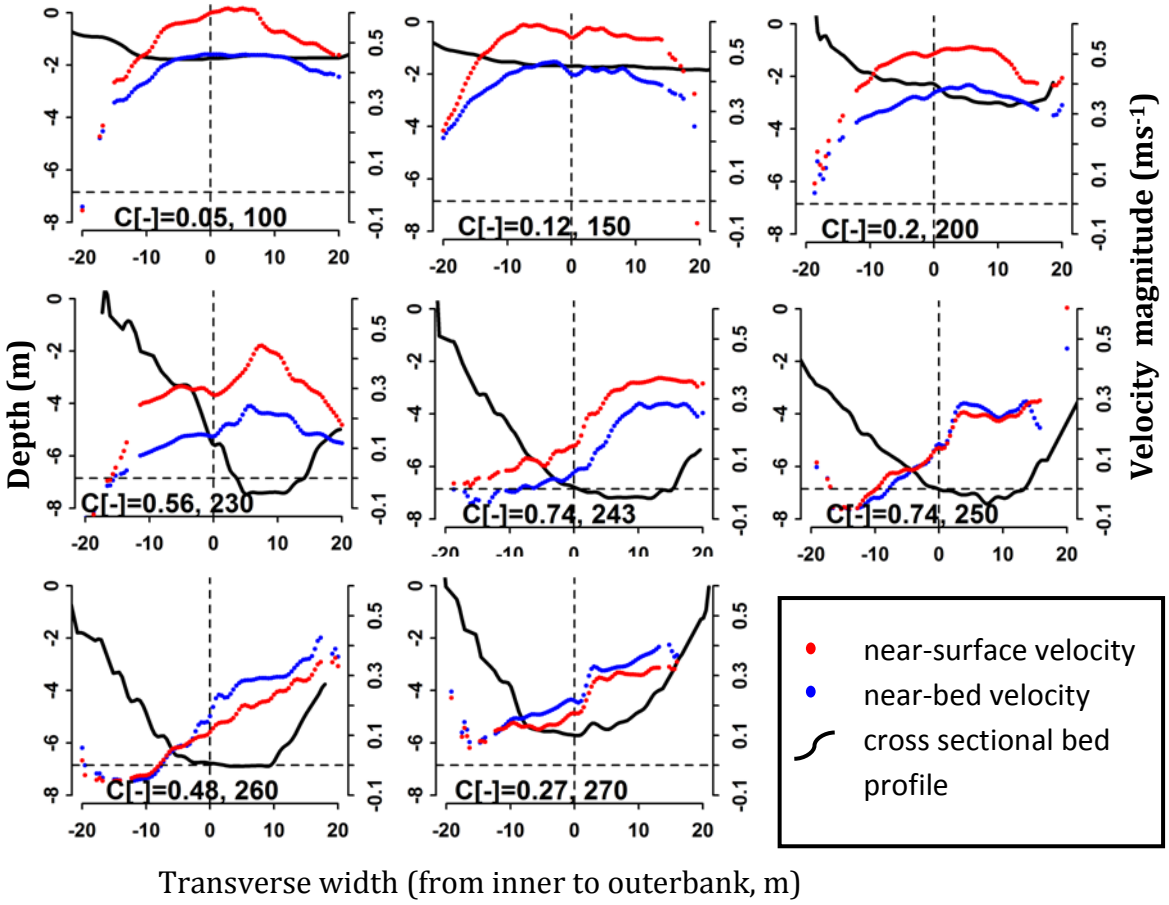

Fig 25. Selected cross-sectional profiles of bend B2 with depth, surface and near-bed flow velocities.With additional information on local curvature as C [-] and cross section number. Note: dashed horizontal black lines in cross-sectional profiles represents the zero flow velocity.

3.4.6 Contrasting features between the two bend forms

Flow differences occurring at the inflow and apex of the fat (as bend B9) and angular (as bend B2) bend forms may be also linked to the clear bed topographic differences between the two bends. Four qualitative macro-scale bed features were found to differ between the two bends (Table 6). First, a well developed concave bank bench (Fig S5 in appendix B)was present at the upstream arm of bend B9 (Fig 22 marked by a black box), while, it was clearly absent at a comparable location on the upstream arm of bend B2. Second, presence of an extensive (exposed and submerged) point bar on the inner bank starting at the apex of bend B9, while an absence at the corresponding location in bend B2 (Fig 22D, 24D). This point bar in B9 also extends below the water surface (see, cross sections 200-220 in Fig 23C) whereas

B2 even displays a localised eroded zone in the corresponding part of the convex bank (between cross-sections 243-250 in (Fig 25C). Third, the absent point bar in bend B2 gives the adjacent pool a circular appearance (Fig 24C) compared to pool at bend B9 where a point bar exists (Fig 22C). Fourth, the riffle in bend B9 slopes gradually into the deepest pool (Fig 22C, marked by red rectangle) as the riffle is deeper, while for bend B2 this slope is very acute where riffle is relatively shallower (Fig 24C, marked by red rectangle) this was evident from the closely placed riffle to pool depth contours of bend B2 in contrast to the relatively widely spaced ones of bend B9.

In addition, these bed-topography and flow differences between bend B2 (angular) and bend B9 (fat) obviously also contribute to the phenomenon of double IBFS zones present in bend B9 in contrast to the single one in bend B2. This is evidenced by near-surface and near-bed dead flow and or horizontal recirculation (marked red arrows in Fig 22 and Fig 24, panels A and B). In bend B9, the first IBFS occurs in the first half of the apex (cross section 200), whereby it constitutes of a horizontal recirculation core that of considerable width (1/2 of channel width) and a near-surface velocity of about -0.1 ms^{-1} and near-bed velocity of c. -0.05 ms^{-1} (table 5). The second IBFS in bend B9 occurs near the bend exit (between cross-sections 330 and 370, Fig 23) but which lacks a horizontal core and instead constitutes of dead flow. In bend B2, the IBFS occurs at the apex tip and is of similar lateral extent as that of bend B9 (Table 5), while the horizontal recirculation core is much narrower (1/5 of channel width) with near-surface and near-bed velocities of about -0.1 ms^{-1} and -0.06 ms^{-1}, respectively (Table 5).

3.5. Discussion

3.5.1 Inter-relationships among geometric and hydraulic parameters relevant to IBFS zones

Morphometric and hydraulic geometry variables were re-sampled for each bend by use of the PyRIS code (Monegaglia et al., 2018) which also enabled the placement of field data points onto cross sections aligned normal to the channel centerline. Taking advantage of the high number of data points (see table S2 in appendix B) measured during the field campaign and the resultant high number cross sections (no. of cross sections = 300-600)placed at a mean spacing of c. 1 m (standard deviation= 0.02-0.06 m) (Table S3 in appendix B). This enabled us to capture detailed changes in morphometry (curvature and width) and hydraulic geometry (depth), occurring at finer spatial resolution (1 m). So that detailed level of the spatial resolution of flow and bathymetry on a mid-sized river represents

a key methodological novelty of this study as, none of the previous studies has acquired field data with a similar or finer spatial resolution (for example, Parsons, 2002; Ferguson et al., 2003). Although, in a few previous studies (Parsons, 2002; Vermeulen et al., 2014), field data have been recorded from several bends in the field most were not used for the purpose of an in-depth study on the governing factors of the IBFS phenomenon.

Previous studies have reported meander planform geometry to be related to pool depth (Markham & Thorne, 1992; Parsons, 2002). The studied set of bends were also characterized by an increase in the pool depth (H_p) with increasing bend curvature ($C_{max}B$) whereby, a leveling-off of the pool depth occurs as bend curvature exceeds c. 0.5. While, the increasing pool depth in relation to with higher curvature has been observed to be a non-linear trend, as observed by (Thorne, 1989) on the Red River (300 m in width), whereby, for very high curvature bends ($C_{max}B > 0.8$), the pool depth started to reduce after a leveling-off had occurred around $C_{max}B$ c. 0.5. However, Parsons, (2002) reported a rather linear increase in pool depth to the increasing curvature values from a small gravel-bed river (3-5 m wide), River Dean, demonstrating, that no leveling off occurs and certainly no reduction of pool depth concurs with very high bend curvatures. For high curvature, Prut meander bends the stabilization or leveling off is, therefore, a manifestation of negative feedback that limits the scouring process so that it prevents over deepening of the pools. Stabilization of pool depth is known to be effected by the outer-bank height (Osman & Thorne, 1988). Whereby, with increasing scouring at the pool the outer bank destabilizes and collapses, leaving the sediments at the bank toe, this, in turn, leads to outer bank advancement (Thorne, 1991). Hence, leveling of pool depth (H_p) in the studied set of bends confirms the existence of negative feedback among the flow - sediment - bend planform causal loop that affects the hydraulic geometry by stabilizing the pools at bend apices of high curvature bends and that also prevents over deepening therein. In general, trend of higher pool depth in relation to higher bend curvatures has been observed both in flume (Blanckaert, 2010) and field studies (Parsons, 2002) along with its particular relevance to flow separation at inner and or outer banks among the sharper bends (Alford et al., 1982; Andrle, 1994; Nanson, 2010; Vermeulen, 2015).

Furthermore, the depth ratio (H_{ratio}) parameter used in this study physically defines the deepening pool relative to the upstream riffle which can affect flow processes from riffle into the pools, for instance, a plunge or downwelling of high vertical velocities from riffle to pools has been noted to occur (Vermeulen, 2015). In accordance, an abrupt change in the bed

topography from riffle to the pool in the angular bends can, therefore, promote the sudden downwelling of flow therein, for example, a quick riffle to pool bed transition in bend B2, an angular bend (indicated by a red box in Fig 25C) could further explain the anomalous deepening of the pool in angular with regard to the shallower upstream riffle in the bend. Overall, the significantly high depth ratio (H_{ratio}) in angular bends (Cr > 3) as compared to fat bends (Cr < 3), not only establishes a novel linkage between hydraulic geometry and bend planform shape but in turn also implicates a possible role of this linkage towards modifying the autogenic processes including flow-bed interactions occurring at the apex of such bends.

Thereby, besides just bend curvature the differences of fat and angular bends in terms of their planform shape can also be identified as key influential factors to hydraulic geometry of bends, particularly, for varying bed topography. Interestingly, the planform shapes of the bends studied by Alford et al (1982) in the Houston River, Andrle (1994) in the Mansfield Creek, Jurmu and Andrle (1997) in the Roaring Brook and closely resemble the typical angular bend shapes in this study (also see. Fig 3A and Bin chapter 2, for examples of angular shapes as opposed to the fatter bend geometries). Some characteristics of angular bends revealed in this study (see results) have been reported elsewhere before. For instance, Carey (1969) termed an angular bend as "abruptly turning bend" on the lower Mississippi River which featured an obviously absent point bar, similar to bend B2 reported herein (Fig 24D). Other features such as the presence of a circular pool at the bend apex which gives it a typical bulbous appearance is due to an eroded point bar at the inner bank (Andrle 1994, Vermeulen et al., 2014) which was only observed in typical angular bends such as bend B2 and bend B15 (see bend B2 in Fig 24D and bend B15 in Fig S6C and D in appendix B) and not all high curvature bends where even point bar was observed to be present (for example, bend B9, Fig 22C). On the other hand, an increased cross-sectional width at the apex (denoted as Bp in this study) showed no relationship with higher bed curvatures ($C_{max}B$) or angularity (Cr), which is commonly observed to occur in bends of high curvature (Page and Nanson 1982, Nanson 2010). This demonstrates the variability amongst features of hydraulic geometry features such as the bar-pool morphology within the high curvature bend shapes which underpins the unconventional or anomalous nature of angular bend planforms.

To summarize, bend planform induces intricacies among flow-bed processes that produce the observed variability in the hydraulic geometry. Thereby, differences between angular and fat bends can, therefore, affect the flow structure specifically at the bend apex. This is particularly true for features of the IBFS that are explicitly known to be driven by the

flow-bed interactions occurring in meander bends (Dietrich and Smith 1983; Vermeulen 2015; Blanckaert 2010).

3.5.2 Factors influencing the lateral extent of IBFS

In order to discern the lateral extent or the size of IBFS, a sensitivity analysis was developed which was based on a global (pooled data from 14 bends), quantile based (Q_{90}) threshold using the rolling standard deviation of cross sectional V/U (transverse/downstream velocity magnitude, see methods for details). Thus, resulting IBFS delineation is seen to be robust (Fig 17), comparable and reproducible. Subsequently, the selection of boundary points of IBFS zone was delineated by point density-dependent concave-hull function in a GIS environment. It is due to the above-mentioned rationale in fact that even the mild bends on the Prut with a curvature as low as 0.3 (R/B = 3.3) show some degree of IBFS. This contradicts the general view that only high curvature bends (B/R > 0.5) display any IBFS and that only high curvature leads to IBFS (Hickin 1977, Blanckaert 2010). The presence of IBFS in low curvature bends has previously been observed in a few field studies, for instance, Leeder & Bridges (1975) reported bends of curvature as low as 0.12 to display IBFS. Also, Parsons (2002), in his doctoral thesis, reported lower curvature bend to display IBFS despite selecting only bends with flow separation zones wider than one-eighth of the channel width. Moreover, the lateral extent of IBFS zone observed in this studied set of bends is similar to the range of values reported elsewhere (Leeder & Bridges, 1975; Ferguson et al., 2003). This means that increasing bend sharpness leads to an enhancement of the IBFS size (lateral extent) but bend curvature does not directly determine the presence or absence of the IBFS itself. And that also corroborates with suggestions of Ferguson et al (2003), which is bends of higher curvature tend to develop the greater extent of flow separation; however, they only compared two bends studied under comparable hydrologic conditions on Dean River. Parsons (2002) also demonstrated the bend curvature to be weakly related to IBFS area in a set of 22 bends from a wadeable river. However, he parameterized bend curvature as the mean curvature of the bend instead of the maximum curvature used in the current analyses and that could explain the weakness of the relationship, as the maximum change in curvature scales better with the size of of the IBFS zone. Along with the bend curvature ($C_{max}B$) increasing pool depth (H_p) also weakly affects the lateral extent of IBFS at the Prut bends. A mechanistic explanation of this could be the local increase in the cross section due to the pools facilitates the generation of an adverse pressure gradient thereby, promoting horizontal low recirculation (Vermeulen 2015), a core component of the flow separation zone.

Furthermore, the simple knowledge of $C_{max}B$ (a proxy of bend sharpness) could only moderately explain the variance in the lateral extent of IBFS zones in the studied set of bends (Fig 21A). Indeed other factors such as inflow conditions (Parsons 2002, Ferguson 2003), abrupt bank line breaks (Parsons 2002), and flow inertia (Leeder and Bridges 1975) have also been known to contribute to the size of separation at inner banks in natural rivers.

The bend angularity (Cr) displayed no discernible relationship with the lateral extent of IBFS and the fact that comparable lateral extent of IBFS occurs among bends of fat and angular geometries was rather unexpected (for instance see bend B9 and B2 in Fig 21A), as these bends display contrasting hydraulic features, such as the depth ratio (H_{ratio}) and aspect ratio (B/H) (Table 4). Such features might then be expected to modify flow-bed interactions in high curvature bends that are commonly known to display extensive IBFS zones. For example, the presence and absence of bed features (bar-pool morphology) can lead to fundamentally different hydrodynamic characteristics in sharp bends (Blanckaert 2011). This highlights the variability among the IBFS features such as the horizontal recirculation core that can be indirectly linked to factors other than just planform shape parameters (bend curvature or angularity), contrary to my observation on lateral extent of this zone that is more directly affected by the bend curvature. Therefore, factors such as presence, size and location of the point bars and or the pool can modify the IBFS features variously in different planform shapes and are discussed in the next sections.

3.5.3 Flow and bed-topography interactions in angular v/s fat bends

Next, in order to understand how the perilously discussed variability affects the IBFS features in typical angular and fat geometries, the contrasting macro-scale bed topographic features and their possible mechanistic linkages with flow processes in the two typically occurring bend shapes on Prut River: fat (bend B9) and angular (bend B2) was discussed in detail. Although the concave bank bench causes higher velocity to shift towards the inner half of the upstream arm in bend B9 (Fig 23 cross section 120), this did not seem affect the flow field around the apex, as the high velocity flow was deflected near the outer bank (Fig 23 cross section 175). Hence, contrary to the previous views on flow in high curvature bends featuring concave bank benches (Page and Nanson 1982; Andrle 1994; Nanson 2010), bend B9 did not erode the point bar but instead features an extensive point bar. A probable reason for an absence of concave bench in bend B2 could be a lower cross-sectional area in upstream

arm of the bend, due to a shallower riffle, as channel expansion is known to favor flow reversal that causes accretion (Woodyer 1975).

On the other hand, an absence or a locally eroded point bar at the apex has been generally observed in naturally occurring high curvature bends, (Page and Nanson 1982; Nanson 2010). This upholds particularly true for meander bends with planform attributes similar to that of angular bends studied here (for example, bend B2 and bend B15, Fig 14). An account from the Lower Mississippi of an 'abruptly curving bend' (angular bend), was found to feature a locally eroded point bar (Carey, 1969). While, in a typical 'hairpin bend' (at the bend) on the Barwon River studied by Woodyer, (1975) a point bar was observed to develop. Notwithstanding, both these cases displayed concave bank accretions according to Woodyer et al., (1979), irrespective of their distinct planform geometries. Physically, the local erosion of point bar occurs as a result of the inverted-erosion deposition pattern around the apex of sharp bends, whereby, over tightening of a bend, leads to an extensive flow separation at outer bank which shifts high velocity core towards the inner bank, leading to higher shear stress there (Hickin, 1978; Reid, 1984). Other morphological factors that promote erosion at the inner banks (point bar) or that are indicative of the prevalence of inversion of the classical erosion- deposition processes were noted as, shifting of the thalweg towards inner bank (Jurmu and Andrle, 1997) and the widening of channel at the apex (Page & Nanson, 1982; Nanson, 2010; Vermeulen, 2015). A commonality between the bends studied by these authors (Vermeulen et al., 2014; Nanson, 2010; Alford et al, 1982; Andrle, 1994 and Jurmu and Andrle, 1997) is the widened channel at the apex of these bends.

Notwithstanding, in the angular bend (bend B2), no sign of horizontal flow recirculation is visible near the surface or bed flow at the outer bank, (see Fig 24A and B), nor does the thalweg appear to be shifted more towards the inner bank. Also, no significant widening of the channel width occurs at the apex and any signs of concave bank deposition were also absent (Fig 24C). Despite such inconsistencies in bend B2, presence of a locally eroded point bar in the bend suggests an inversion of erosion-deposition processes even though presence flow separation in bends is known to inhibit erosion due to overall lower shear stresses therein (Nanson, 2010). This suggests a likely tendency for inward migration at the convex bank (Andrle, 1994) or halted bend migration (Hickin, 1978) implying bends stabilization over longer time periods. Again, a general absence and or erosion of a point bar in studies mentioned above indicates a similarity in the underlying causal flow-sediment-bend geometry feedback occurring in these streams and or river bends, irrespective of the

differences in the size and physical-geographical settings. However, these rivers do share common features like presence of cohesive floodplain deposit material; vertical outer banks and a low stream gradient, which parallels the settings of Prut river (see study area description).

Contrastingly, presence of a submerged point bar in the fat bend B9 creates two distinct regions i.e. a shallower depth region over the bar and deeper region in adjacent pools. Similar, bar-pool morphology has been simulated in flume environment (Blanckaert, 2011) and reported from field studies (Ferguson et al 2003) of high curvature bend forms, along with its implications on the flow processes around the apex. For instance, a known effect of point bar is the shoaling of flow at inner bank and topographic steering of flow towards the outer bank (Dietrich & Smith, 1983) that pushes the bulk of the flow towards the channel center. Overall, this could help in generalizing a complete lack or locally eroded point as a characteristic typical to angular bend planforms rather than those of fat bend forms.

The deepening of the pool in bend B2 occurred within a very short distance from its upstream riffle (Fig 24C), implying an abrupt variation in bed topography that spatially corresponds with the abrupt increase of curvature in the bend. Nanson, (2010) reported a similar feature that she termed as 'steep-bar riffle forms' that were followed by deeper pools which developed in highly sharp bends studied therein. It was suggested to form by higher shear at bend apex. Such behavior is again highly unconventional when compared to slowly varying bed topography of classical meander bends that are longer in lengths (Pittaluga et al., 2009). Again this suggests a hydraulic geometry feature what could be typical to only angular geometries, owing to their planform shape attributes i.e. a straighter upstream arm preceding a quickly turning apex. Interestingly, Vermeulen, (2015) reported the three-dimensional flow structure through a modeled longitudinal slice made at the apex of a sharp bend. He found that flow impinges onto the bed of the scour-hole with relatively higher magnitudes of vertical velocity typically hitting the exit end of the scour. Notably, the bend studied by Vermeulen (2015) also displayed typical angular planform (*see fig 1 in* Vermeulen, 2015) i.e. quickly turning apex with straighter arms and the longitudinal slice displayed a steeper transition from inflow riffle to the pool.

One can, therefore, infer a strong plunging of flow from the inflow riffle to the pool in bend B2 characterized by higher vertical velocities compared to that in bend B9. Such impingement, in turn, could have implication in the scouring process at pool particularly in its

formation and maintenance at angular bends. While, this factor could also promote IBFS by means of a sudden increase in the channel's capacity to vertically accommodate more flow causing reduced mean velocities and momentum therein (Ferguson et al., 2003), this also supported by the relationship between pool depth (H_p) and lateral extent of IBFS of bends as discussed in the previous section. Overall, this further explains the comparable lateral extent of IBFS between bend B2 and B9 despite of their contrasting depth ratio (H_{ratio}) which seems to be a consequence of a sudden and pronounced increase in channel depth at the pool in bend B2 (angular) which is governed by strong plunging driven by quicker transition from shallow riffle into a very deep pool.

3.5.4 Contrasting features of IBFS in angular and fat bends

The occurrence of a second IBFS zone has been previously observed in a field study at an asymmetric compound bend (Frothingham and Rhoads, 2003) and also in sharply curving flumes (193-degree curving) (Blanckaert, 2011, Constantinescu et al., 2011). However, in this study, this phenomenon has been reported for the first time from a natural fat river bend (hairpin geometry), particularly as a contrasting flow feature between fat and angular bend types (Fig 22A and 24A).

Blanckaert (2011) observed a second IBFS zone to only develop when bar-pool morphology was present and was missing with a lack of a bed-topography under similar hydraulic treatments in his hairpin-shaped flume (analogous to fat bend B9). According to the author the occurrence of this zone was due to the pronounced reduction of curvature, which causes the water surface gradient to vanish and a subsequent reversal of pressure gradient so that higher/lower flow occurs at outer/inner banks. On the contrary, a locally eroded point bar at the apex and a subsequent lack of a second IBFS zone near bend exit in bend B2, despite its abruptly changing curvature, points towards a greater role of developed bar-pool morphology in bends for the production of a second IBFS zone. This also suggests that a mere abrupt change in spatial curvature from high/low at apex/bend-exit is not an exclusive condition in inducing a second IBFS zone near bend exit.

Moreover, the concurrence of the second IBFS location in bend B9 with a break in the lee of the point bar near the bend exit (Fig 22C) represents a strikingly similarity to the secondIBFS zone produced in the lee zone of point bar formed at the downstream part of a compound meander bend studied by Frotingham and Rhoads (2003). In fact, compound

meander bends feature more than a single peak their planform much similar to that in of fatter bends forms, albeit the curvature peaks are not as strongly defined in fat forms than in compound bends (Güneralp & Marston, 2012). One can thus expect an underlying similarity in the mechanism and conditioning involved in the generation of a second IBFS zone in fat and compound bends. Whereby, the second IBFS is induced and maintained by a cumulative effect of upstream high curvature that pushes the fast flow towards the outer half of the channel and presence of lee zone in the apex point bar. Apart, from this, the second IBFS zone can be expected to promote the development of sediment accretion at the inner bank of the downstream arm of fat bend owing to the lower flow velocity associated with the zone. Similarly, lack of the second IBFS was also confirmed from a comparable angular bend B15 (Cr > 4) from the studied set of bends, that also features an eroded point bar (see, Fig S6C and D in appendix B).

Although a horizontal flow recirculation core occurs in both bends, the maximum horizontal recirculation of flow near the surface (Fig 22A and 24A) covered a larger fraction of the cross-sectional width at the apex of bend B9 (c. half channel width) compared to bend B2 (c. a fifth of the channel width) (Table 5). This extent of recirculation core has been observed to be affected by several factors in both field and flume meander bends. Mainly, higher bend curvature (angle of the turn) displayed a greater lateral extent of flow reversal between two sharp bends of a small River Dean (Ferguson et al 2003). Markedly, both bends B2 and B9 display similar bend curvature values (Table 6). Again, fully developed bed topography was observed was not only govern the closed or open structure of IBFS but also the lateral extent of recirculation core formed therein (see, Blanckaert 2011). In Blanckaert's (2011) experiments, the without bed configuration had a non-detectable recirculation core at the apex of the flume compared to that of a fully developed bed treatment i.e. with a point bar. Similarly, in a flume study by Blanckaert et al., (2013) whereby, in two consecutively placed 90-degree bends the presence of mobile bed led to the development of a point bar and consequent recirculation of flow just above it.

On the contrary, under similar hydraulic treatment but without sediments (no bed topography), no recirculation was observed. In addition to this, a lack of strong flow reversal at the inner bank was postulated to be an effect of the lacking bed topography, that was observed when comparing flow in different curving flumes i.e. 90 and 193 degrees with flat a bed (Kashyap et al., 2013). This suggests that in case of bend B9 (fat) the presence of a point bar enhances the recirculation zone extent, whereas, a lack of a point bar in bend B2 (angular)

will result in a smaller extent of the recirculation zone. On the other hand, the lateral extent of the recirculation zones could also possibly contribute to the extensive point bar growth in bend B9, as the recirculation zones at inner banks are known to effectively trap sediments (Leeder and Bridges, 1975), and therefore, in bend B9 (fat) it might be able to trap sediments farther away from the inner bank (towards the centerline) compared to the case of bend B2.

3.5.5 Implications for meander bend morphodynamics

The above-mentioned interactions between flow-bed topography and their effect on the features of IBFS suggest a clear morphodynamic influence, mainly for the contrasting developmental trajectories for fat compared to angular river bends. The presence of a second IBFS zone in the fat bend (bend B9) suggests that these bends might be prone to multilobing over longer time-scales. As, the processes involved in the generation of the second IBFS could also promote the outer bank erosion at the corresponding location leading to multilobing in such bends (Blanckaert, 2011). In addition to this an apparent similarity between the physical location of the second IBFS in the studied fat bend to that of a compound bend studied elsewhere (Frothingham & Rhoads, 2003) further strengthens the view that fat bends might indicate to an early stage of a compound meander bends. Whereas absence of the second IBFS and a locally eroded point bar in bend B2 indicates an inverted erosion-deposition occurring in this bend that could lead to an initial bend stabilization and an eventual inward (towards the inner bank) migration. These postulations are in line with the historical bank-line migration of the two bend forms occurring on a relatively shorter time scale (25 years) (Fig 26). Whereby, bend B9 (fat) displayed no lateral migration (Fig 26A), a characteristic typical to bends of curvature higher than c. 0.5 (Hickin & Nanson, 1984). Bend B9 however, displayed down-valley migration of its upstream arm, a typical way of bend tightening (Hickin, 1978; Andrle, 1994).

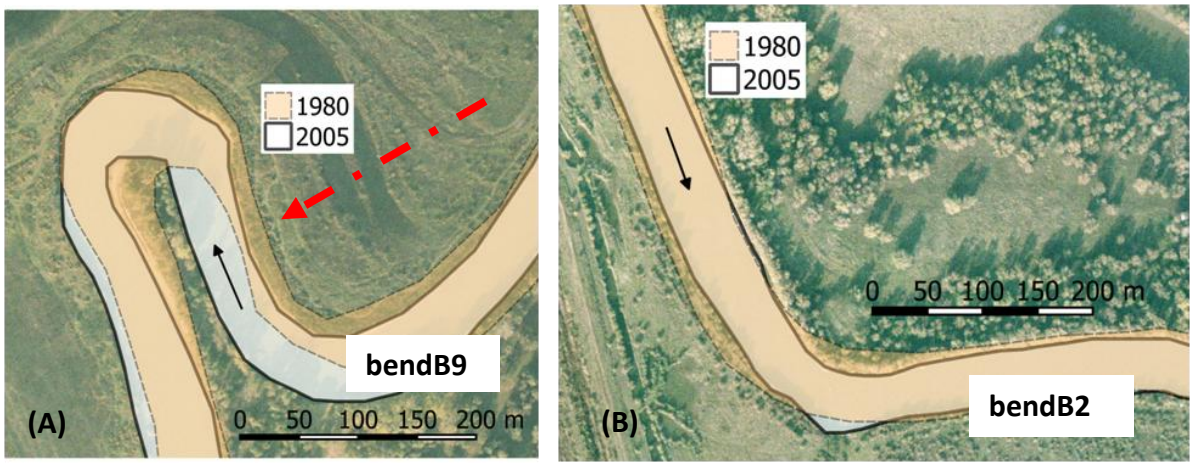

Fig 26. A 25-year period bank-line migration for the two bends. (A) bend B9 (fat bend) and (B) bend B2 (angular bend) (GIS workflow was as per the methods elaborated in chapter 1). Note: the red line in panel (A) presents a transect through the old bend scroll formed by the downvalley movement of the upstream arm of bend B (prior to 1980 and such scrolls are visibly missing in panel (B).

Moreover, the visible bend scroll traces on this bend (fig 13 A, red arrow) indicative of long-term movement of the upstream arm which extends the above mentioned a probable effect of the action of flow deflected due to presence of a second IBFS. On the other hand, bend B2 (angular) displayed no discernible movement for the same period (Fig 26B), hinting towards typical stabilization behavior of this type of bend form. The overall discussed differences in planform shapes of angular and fat bends that affect the hydraulic geometry features and the interactions between flow and bed-topography can thereby create varying morphodynamic responses between these bends (Fig 27).

It is, however, necessary to point out here that the counter-rotating cell formed at the outer banks (Bathurst et al., 1977) was not analyzed for the current study and presents a limitation on inferences or interpretations on outer bank morphodynamics. Furthermore, the fate of the second IBFS in different discharge levels also imposes limitations on the realization of its role in the erosion at the outer bank and in inducing multilobing. Since, varying effects of the upstream and downstream bends have been discerned on individual bend cases (Hooke, 1995; Howard, 1996), each of the considered bends (B9 and B2) are not isolated systems and any inferences on their morphodynamic development should consider the conditions in upstream or downstream bends.

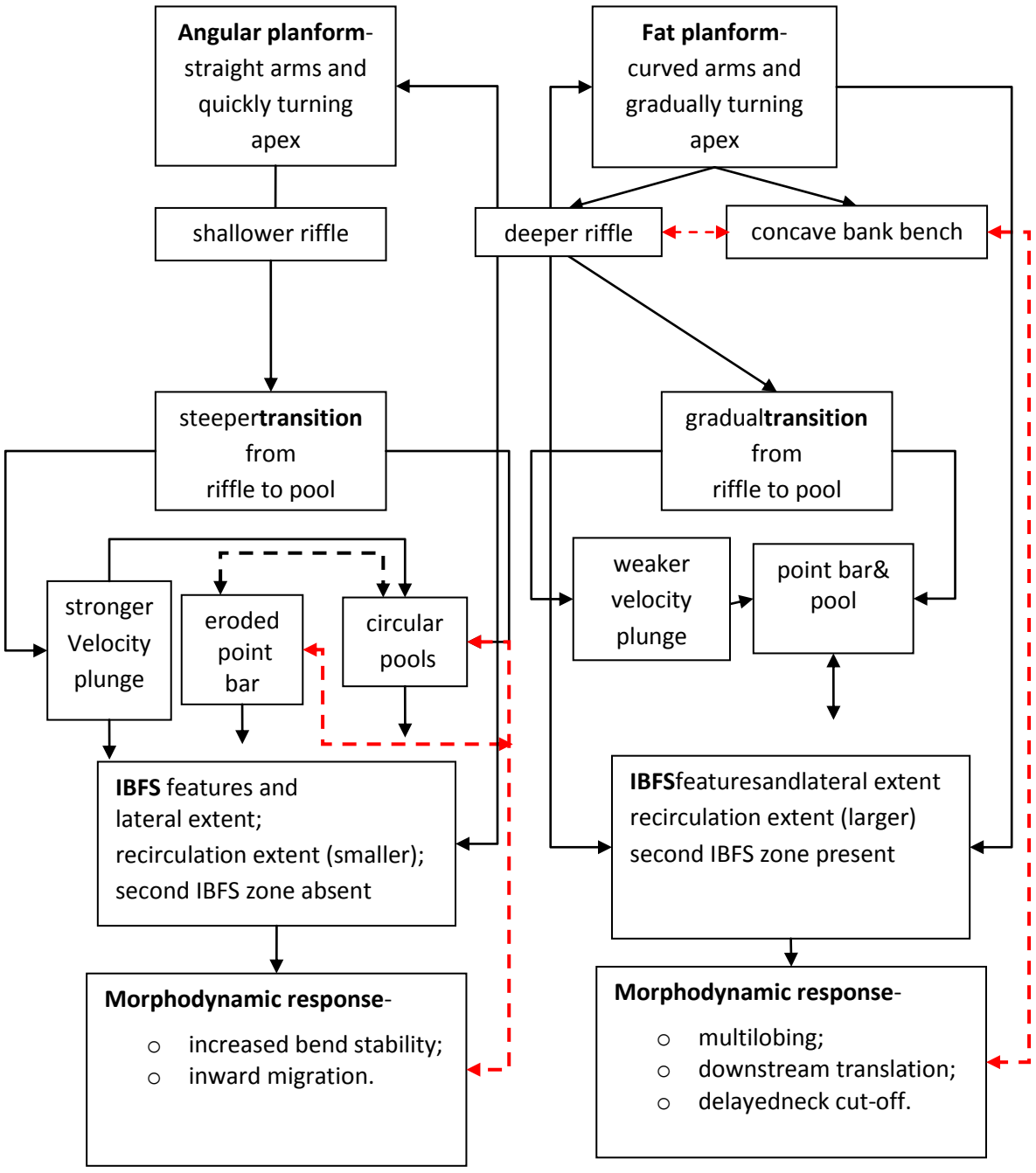

Fig 27. A conceptual mechanistic model of hydromorphological processes in angular versus fat bends on the Prut River, with possible cause and effect linkages. Black arrows indicate a directional effect; Red arrows indicate negative feedback; Black dashed arrows indicate a bi-directional cause and effect.

6. Conclusion

Autogenic (in-channel) flow-bed features in meander bends are found to vary with bend planform shape and play an important role in modifying flow and sediment processes and eventually the morphodynamics. In this chapter, I analyze the variation in IBFS and its features along with planform shapes and hydraulic geometry parameters influencing it in meander bends of the Prut River (Romania/Moldova).

The enhancement of the lateral extent of IBFS at the bend apex was essentially related to an increased bend curvature. The results also confirm that in real rivers IBFS zones can occur within bends of very low curvature, that is those dubbed as mild curving and are rather conventionally occurring bends in river planforms, implicating that, bend curvature is not an explicit factor involved in determining the presence or absence of IBFS. Other factors like an increased pool depth seemed to facilitate the enhancement of IBFS among the sharper bends, though not invariably. Hydraulic geometry features were discerned to be significantly affected by the planform shape of the bends. And that negative feedback is suggested to exist between bend planform, flow and sedimentation that affect the hydraulic geometry in that it leads to a stabilization of pool depths in bends of increasing curvature. A novel hydraulic geometry feature of angular bends was the greater pool depth compared to their upstream riffle.

Apart from the quantitative differences, several qualitative differences were discerned between angular and fat bends. Angular bend (B2) features a locally eroded point bar at the apex in comparison to that in the fat bend (B9), which was attributed to the extensive horizontal recirculation at the apex of the fat bend that is able to trap sediments farther away from the inner bank. The bar-pool morphology further seemed to play a crucial role in the generation of a second IBFS zone in the fat bend as opposed to the occurrence of a single zone in the angular bend. Moreover, a second IBFS zone in fat bend has morphodynamic implications for the developmental trajectory of these bends that might become more prone to multilobing than their angular counterparts where complete stabilization or an inward migration might be expected.

4. General discussion

4.1. Methodological approaches in studying river meanders

Studies on meander planform and dynamics are based on early work on real rivers(Jefferson, 1902; Fisk, 1944; Leopold & Wolman, 1957) and from experiments (Friedkin, 1945)mostly on topics dealing with river channel morphometry and migration dynamics. The similarity in the planimetric view of rivers soon motivated studies on the generality of the forms and underlying processes driving them (Leopold and Wolman 1960). This was followed by a plethora of research aimed at deepening the understanding of meander planform morphometry (Langbein and Leopold 1966; Brice 1973; Feguson1975), associated morphodynamics (Hickin 1977, 1978; Hooke 1977, 1987; Hooke and Harvey 1983) and hydraulic processes (Bagnold 1960; Hooke 1975; Leeder & Bridges 1975; Dietrich et al., 1979,).Research on river meandering has thereby broadly moved forward by two main approaches, namely empirical research and modeling (Hooke 2013), and often also with an amalgamation of both (Ferguson et al 2003). The empirical approach includes fieldwork on real rivers (Lawler et al., 1997; Ferguson et al., 2003; Nanson, 2010; Engel & Rhoads, 2012; Schnauder & Sukhodolov, 2012; Vermeulen et al., 2014) or laboratory studies (Whiting & Dietrich, 1993a, 1993b; Blanckaert, 2002; Abad & García, 2005; Zeng et al., 2008; Kashyap et al., 2010; Termini & Piraino, 2011),while the modeling approach is based on theoretical and numerical models (Ikeda et al., 1981; Parker & Andrews, 1986; Johannesson & Parker, 1989; Zolezzi & Seminara, 2001a; Camporeale et al., 2005, 2007). Over the last few decades, empirical data have driven research aimed at studying meander planform morphometry and dynamics has been carried out at varying spatio-temporal scales and thereby applied an array of methodological approaches (see, Hooke 1984; and Hooke 2013 for review on approaches). These scales range from cross-sectional or channel width to reach scale in space and from a single event to geological scale in time (Güneralp et al, 2012). For instance, the analysis of historical-geographical sources like maps and imagery has been frequently used in back-tracing channel change over longer temporal scales (> 100 years) (Hickin, 1974; Hooke, 1977b; Glover, 1986; Hooke, 2003). On the contrary, for shorter temporal scales channel changes approaches such as the use of erosion pins on the field have been used(Thorne and Lewin, 1979; Lawler, 1993 for a review on field-based techniques). Thereby, the availability of long-term data has greatly advanced the understanding of meander morphodynamics associated with longer temporal and spatial,

scales such as river planform evolution(Gervasoni, 1989; Hooke, 1995; Gilvear et al., 2000; Güneralp, 2007; Gautier et al., 2010).

Compared to planform morphometry and evolution, studies focusing on hydraulic flow, sediment and geometry interactions associated with meanders have been empirically elaborated mostly at smaller spatial scales, and rarely with data from multiple bends. For example, such studies have been conducted for processes at the scale of cross sections (Blanckaert & de Vriend, 2003) or in lab flumes for single bends (Termini, 2009; Kashyap et al., 2010; Blanckaert, 2011)or in configurations involving a small number of bends (Abad & Garcia, 2009; Kashyap et al., 2013). Though such approaches offer an in-depth understanding of precise form-process linkages by virtue of controlled manipulation of factors, the fact that they have been carried in artificial environments (eg. flumes) presents a clear risk of an oversimplification of the study system. For instance, a constant radius of curvature (Zeng et al., 2008), smooth vertical inner and outer banks (Blanckaert, 2009; Constantinescu et al., 2011), no upstream bends in cases of individual bend flumes (Kashyap et al., 2010), sediment gradation or missing macro-scale bed features like riffles, bar and pools morphology(Balen et al., 2010; Koken et al., 2013)and non-erodible banks (Whiting and Dietrich, 1993a; Whiting and Dietrich, 1993b; Termini, 2009) display some of the features where flume experiment differ from field studies.

On the other hand, data collections from real rivers are scarce and presented mostly with coarsely placed surveys resulting in a low number of actual field data points in individual bends (de Vriend& Geldof, 1983; Ferguson et al., 2003; Frothingham & Rhoads, 2003; Sukhodolov, 2012). Only a handful studies have been published that used extensive field surveys to elaborate meander bend planform, flow and bed conditions and the linkages therein (Vermeulen et al., 2014; Vermeulen, 2015). Moreover, studies that also included unconventional bend types have been even scarcer compared to studies on the classical meandering bends. Even fewer are those studies that surveyed a large set of simple bend geometries for flow and bathymetry(Parsons, 2002; Nanson, 2010). Notably, none exists from continental Europe, as Parson’s work has been conducted in small streams of England.

4.2. The methodological approach adopted for this work

I selected a 400-km long segment of Prut river flowing between Romania and Moldova, a lowland river in its quasi-freely meandering form, so that, it still retains much its original meandering form and dynamics and for which historical maps and images were made available covering almost a century (1915-2005).

In chapter 2, I used the PyRIS (Monegaglia et al 2018) algorithm, a newly developed state-of-the-art, fully automated software to elaborate channel morphometry and migration data from the historical cartography sources. A rather common approach is to extract the channel centerline through curve fitting or splines applied on skeletonized bankline points spaced at regular intervals(see, Güneralp, 2007; Legleiter & Kyriakidis, 2007). For the current study, the calculated centerline points were spaced at half a river width and therefore were sensitive to smaller changes in the bankline direction in contrast to circle fitting methods through meander bends (Hooke, 1984). Next, individual bends were delineated following the automatic detection of inflexion points, so that a meander bend was defined between two consecutive inflexion points on the centerline, which represents a key novelty of the PyRIS algorithm (Monegegalia et al., 2018). A bend-scale approach was incorporated in the design of the analysis, as it has been known to be a natural scale for analyzing meander form and process linkages in rivers (Schwenk et al., 2015).

Next, bend-wise morphometry information was derived from the extracted spatial centerline series, such as curvature, channel width and bend length while morphodynamic data such as bend averaged migration magnitudes were also obtained. This allowed the calculation of bend morphometric parameters such as dimensionless bend curvature ($C_{max}B$) as maximum curvature in bend-centerline spatial series normalized by bend averaged width, intrinsic wavenumbers (λ) and bend sinuosity (S). These represent important parameters often used throughout meandering literature to describe characteristics of meandering (Leopold and Wolman 1960). Even though PyRIS takes into account the initial and final location of the bends and easily deals with situations like cut-off events, and numbers the bends accordingly in the following time point. However, several smaller low curving (almost straight) sections were sometimes included as bends and had to be manually screened out. Besides, intrinsic wavenumber (λ)was calculated, a dimensionless value representing bend length(Zolezzi & Güneralp, 2016). Its dimensionless nature allows for comparison across modelling and real river examples. These are well-established metrics for studying meander form and dynamics

(Hooke, 1984), mainly as they scale with variables that control meandering (Leopold and Wolman 1960). Similar to this, curvature ratio (ratio of C_{max} to C_{mean}, denoted by Cr) was calculated which has been previously used as a descriptor of bend (and bend cut-off) shape and size (Howard and Hemberger 1991; Schwenk et al., 2015) but never for objectively differentiating between fat and angular cases. With this information, I designed an analysis to characterize simple meander bend shapes, focusing on the high curvature bend types: angular and fat bends, hence on distinct physically meaningful parameter categories.

I also undertook an analysis of the channel adjustment trajectory of the river through the 90 year period, by interpreting the temporal trends for the indicators of channel adjustments such as channel width (B), migration rates (Z), bend sinuosity (S). Taking advantage of the high number of bends studied (> 118) whose development could be tracked over the 90–year period (and that were not cut off during that period), I formulated a bend shape-transition analyses, whereby, "a change or no change" in bend shape was recorded as a transition (for example: sharp to round or vice versa, see results Fig 12 in chapter 2) between any two consecutive time periods analyzed (1915-1960, 1960-1980 and 1980-2005). The need of longer time scale data between time points (> 20 years) also limits the research investigating into individual bend-shape transformations or metamorphosis into numerically dubbed bend shape types, even though models of change that elaborate several modes of meander bend movement in simple bends are well documented(Daniel, 1971; Brice, 1974; Hooke, 1977).

In chapter 3, I elaborated a research perspective building upon that of(Vermeulen, 2014), who studied the hydrodynamics and bed features in sharp meander bends that are mapped for higher point density of 3-D velocity components from a large tropical meandering river (Mahakam River, Indonesia), and on that of Parsons, (2002) by highlighting the need to incorporating numerous river bends.

Based on the work of Vermeulen's and Parsons's, I designed my study approach by combining the features of 1) studying numerous bends from larger (non-wadeable) meandering river system 2) through recording detailed three-dimensional velocity, bathymetry data including GPS information for precise description of bend morphology, in order to contribute to describe the inter-relationships occurring among bend planform shapes, point bar formation, meander migration, and the characteristics of flow separation zones formed at the inner-bank. Compared to the Mahakam River studied by Vermeulen (2015),

Prut river is a temperate mid-sized river that features unconventional bends giving some reaches a typical zigzagging appearance, with vertical banks but that generally lack a widening at the apex, which is also contrary to that noted in similar zigzagging, smaller, temperate streams studied by Andrle, (1994). Parsons, (2002) analyzed numerous bends (n > 20) but used the coarser placement of cross sections for studying the phenomenon of flow separation in a relatively smaller river, DeanRiver (3-5 m) compared to this study.

An Acoustic Doppler Current Profiler (ADCP) mounted on a moving vessel was deployed to survey the selected meander bends on the Prut River. ADCPs are particularly apt for capturing flow and bathymetry information from mid-sized to larger systems (non-wadeable) river and have been therefore been used in rivers falling in a range of river sizes, some examples are- the Parana River, Argentina(Szupiany et al., 2007), the Po River, Italy,(Guerrero & Lamberti, 2011) and the Lower-Mekong River (Bravard et al., 2014). Furthermore, the use of ADCP has become increasingly popular in measuring river discharge(Yorke & Oberg, 2002) and studying a wide range of flow and bed morphology features in meander bends (Dinehart & Burau, 2005; Engel & Rhoads, 2015; Flener et al., 2015; Petrie, Diplas, Gutierrez, & Nam, 2013; Szupiany et al., 2007; Bart Vermeulen, 2015). For this study, a vessel mounted ADCP enabled recording data over larger areal extents of meander bends of the Prut River within a smaller time-frame and in a rather continuous manner through a network of the mesh created by zigzag and longitudinal runs(Fig 16). This produced a combined dataset of flow and bathymetry recorded at 14 meander bends, under stable discharge rates (see Fig S7 in appendix B), which has not been available to any earlier study. Due to its continuous data collection feature, ADCP provided a higher spatial resolution of velocity data, compared to the point measurements that have been used in the past for similar studies objectives (Parsons, 2002; Ferguson et al 2003; Nanson, 2010), and the differential-GPS feature provided higher grade of spatial resolution that was used to define banklines and spatial centreline series through the PyRIS software (Monegaglia et al., 2018). However, a major limitation was the manner of use of Acoustic Doppler Current Profiler (ADCP) in this study, i.e. the moving vessel surveys, which provided low-resolution temporal picture of flow dynamics, this also represents a practical limitation of the instrument and a trade-off has to be made between collecting either a time-integrated or spatially intensive dataset(Muste et al., 2004a, 2004b)However, for the aims of chapter 3 i.e. in dealing with the macro-scale features of flow and bed topography and the delineation of IBFS extent necessitated higher density of data points, particularly at the bend apex.

Following, the above mentioned partially innovative methodological approaches, the present thesis aimed to provide new empirical data-based insights on the long-term channel adjustments, bend-scale planform morphometry, hydraulic conditions, and morphodynamics, particularly, among different bend shape types. In particular, the thesis aimed to fill the following gaps in the current understanding of the meander bend form and dynamics:

- Planform and bend geometry characterization from a large set of simple bends along with channel adjustments that had occurred over a 90-year period on Prut River
- Morphometric quantification of occurring unconventional bend shape types based on bend curvature, wavenumbers and curvature ratio
- Quantification and comparison of bend-scale morphodynamics between sharp and round and angular and fat bends.
- Quantification of relationships among planform and hydraulic geometry variables of selected meander bends on Prut River
- Quantification of the lateral extent of IBFS
- Establishing relationships of IBFS formation with bend planform shapes and hydraulic geometry
- A qualitative understanding of differences among IBFS features of angular opposed to fat bends in light of flow and bed features.

4.3 Key research findings

Lowland meandering rivers around the globe have especially been heavily regulated; so that only very few 'free-flowing' rivers remain across Europe (Tockner et al., 2009). In chapter 2, I presented the analysis on long term channel adjustments, bend morphometry and morphodynamics of one the last nearly-freely meandering rivers in Europe, the Prut (Romania/Moldova), derived from historical cartographic sources spread over a century. There, both conventional and unconventional river bends occur and could be studied comparatively, as they were formed under the same hydrological and geomorphic conditions. Round and fat bends are conventionally occurring bends characterized by low curvature ratios ($Cr < 3$) and longer bend lengths ($\lambda<0.1$), and provide in the planform a rounder and fuller appearance. In contrast, sharp and angular bends can be collectively termed as unconventionally occurring bends displaying high curvature ratios ($Cr>3$), whereby, sharp

bends are mostly short however angular bends display more variable bend lengths, these bends give rivers a typical zigzagging planimetric appearance.

Indicators of channel adjustments display signs of increasing incision and reduced dynamics of Prut over the last century which coincides with a reduction(Fig 12) in number and types of shape transitions between bends, especially, among conventional (round and fat) to unconventional (sharp and angular) bends and vice versa. The morphometric and migration characteristics of the unconventional bends were indicative of their formative conditions, which appear to be autogenically driven on Prut River i.e. occurring within the flow-bed-bank-sediment-geometry causal loop, rather than previously discerned solely allogenic forcing, mainly in the form of cohesive and or erosion-resistant outcrops. However, some allogenic factors such as fallen trees into the channel might have an additional role to play and would require further investigation.

Autogenic flow (in-channel) and bed processes responsible for prevalent hydro-morphodynamics of meander bends such as the lateral extent (size) of separating flow at the inner bank and their interactions therein have been scarcely explored so far from real river bend examples. In chapter 3, I presented field-data based evidence collected from 14 bends on the Prut River in order to comprehend the inter-relationships among hydraulic geometry and planform shapes and their effect on the characteristics of inner-bank flow separation zone (IBFS). The lateral extent of IBFS was significantly higher (IBFS= 6.1+ 45.8 $C_{max}B$ + 8.2; R^2= 0.55; $p < 0.001$; N=14) in bend curvatures ($C_{max}B > 0.5$), and the flow tends to separate among a wide range of bend shapes, including round bends (hydraulically mild). Hydraulic geometry parameters like pool depth also weakly affect the IBFS size (IBFS = -14+ 10.3 H_p + 10.2; R^2= 0.30; $p<0.02$; N=14), as it shows a typical stabilizing relationship with bend curvature, whereby, for bend curvature higher than c. 0.5 pool depth ceases to increase, thus suggesting the existence of negative autogenic feedback within the bend planform-flow-sediment loop.

Besides, their obvious planform shape differences, the fat and angular bends also displayed several qualitative differences amongst their macro-scale bed features. Also, the quantitative hydraulic geometry responses concur with their planform differences, for instance, an increased depth ratio (H_{ratio}) with a higher angularity of bends (H_{ratio} = 0.83 + 0.41 Cr;R^2 = 0.44; $p < 0.005$; N=14). Collectively, these contrasting features tend to affect the characteristics of the IBFS zone, namely the extent of the horizontal recirculation and

frequency of occurrence of the IBFS itself within the contrasting bend shape types encountered on the Prut River. These results have implications on bend developmental trajectories of the two contrasting bend types, as the fat bend showed signs of multilobing and delayed cut-off, whereas the angular bend might stabilize and or migrate inwards.

4.4. Implications of the research findings

Studies on the planform morphology and dynamics of unconventional meander bend (i.e. sharp and angular bends) are rare, even though information on form-process linkages occurring within such meanders is most important to morphodynamic modeling and management of meandering rivers. The results presented in chapter 2 on meander planform morphometry and temporal dynamics from the example of Prut, a meandering, quasi-free flowing river in Europe therefore, has several implications ranging from river channel restoration, long-term planform evolution, morphodynamic models of planforms featuring unconventional bend forms and on the hydrodynamics and morphodynamic character of individual bends.

Meandering Rivers around the world face a magnitude of human-induced pressures, such as channelization(Talbot & Lapointe, 2002; Surian & Rinaldi, 2003), alteration of flow and sediment regimes (Ward and Stanford 1995; Dai et al 2016) which are aggravated by climate-induced effects (Ashmore and Church 2001; Goudie, 2006). Thus, field-based information on long-term channel adjustments from a typical meandering river presents valuable baseline data for future research work on such rivers, particularly due to a paucity of long-term datasets such as historical imagery i.e. extending over a period of c. 100 years.

Another key gap in studying meandering rivers has been the classification and nomenclature of unconventional bend shape types such as those occurring in the higher curvature categories. Results on the morphometric characterization of bend shapes implicated clear numerical planform differences between the conventional- round and fat forms compared to the unconventional- sharp and angular forms, respectively. Such a detailed characterization of meander morphometry is vital to river channel restoration, particularly those aimed at re-meandering of channels(Garcia et al., 1994; Abad & Garcia, 2006; Kondolf, 2006).

At the bend-scale, shape parameters are known to govern flow and bed processes in meandering rivers (Dietrich et al 1979, Camporeale et al., 2005) and in turn modifying the

hydrodynamic (Blanckaert 2011, Leeder and Bridges, 1975) and morphodynamic regimes (Vermeulen et al., 2014; Andrle 1994). For instance, the adaptive phase lag linked to the curvature and the slowly varying bed topography (Pittluga et al., 2009). Therefore, results on ranges of parameters reported herein such as wavenumbers (λ, Fig 10 in chapter 2) associated with contrasting geometries could hold important implications on meander morphodynamic regimes, typically as these values scale well with factors controlling meandering features (Leopold and Wolman 1960).

A complete understanding of the formative conditions of unconventional bend types in nature is still lacking. Contrasting views exist on the maintenance of typical zigzagging planforms of such river planforms, from being autogenic in nature (Vermeulen et al., 2014) to an overriding effect of allogenic factors such as bank vegetation(Pizzuto & Meckelnburg, 1989; Güneralp& Marston, 2012). The observed non-linear migration and curvature and bend shape transitions on the Prut River indicate a role of autogenic feedback in the generation and maintenance of sharp and angular geometries.

Moreover, process-based mathematical models aimed at simulating meander planforms (Ikeda et al., 1981; Pittaluga & Seminara, 2011) that take into account form-process linkages, morphodynamic influences and process-based evolution of meandering planforms
(Güneralp& Marston, 2012), still cannot reproduce angular and sharper forms. Therefore, deeper insights on bend-shape transitions under the observed historical channel adjustment trajectory may provide a more realistic view of the morphodynamics of the unconventional bend forms.

Multi-bend scale data from field-based investigations of meander flow and bathymetry have so far been rarely published. In chapter 3, I use a novel dataset compiled from fieldwork on 14 meander bends of the Prut River (Romania/Moldova) in order to understand the dynamics of meandering channel that display several unconventional bend forms- sharps and angulars. Insights gained into flow and bed processes such as the IBFS zones has implications for bend hydraulics (flow and sediment distribution), morphodynamics (erosion, deposition, migration) and bend evolution trajectories (stabilization, cut-offs and multilobing) occurring at meander bend scale.

The results on the variation in macro-scale features of bed i.e. bar-pool morphology have implications on the gross flow processes occurring at the bend apex including the lateral extent of IBFS. Also, a missing point bar can enhance flow separation at the outer bank(Hodskinson & Ferguson, 1998).

Horizontal recirculation occurring within IBFS is known to trap sediments at the inner banks (Leeder & Bridges, 1975). Fat bend forms were found to feature an extensive zone of recirculation therein compared to the angular bends that display a much smaller size of recirculation zones. This has implication on point bar formation in these bends and also for the topographic steering phenomenon caused by point bars(Dietrich & Smith, 1983). Additionally, the formation of a second IBFS also has an effect of deflecting flow towards the outer banks that could lead to differing evolution of bends, whereby fat bends indicate a trajectory suggesting their proneness to multilobing, while angular bends being prone to complete stabilization or inward migration over time(Fig 26 in chapter 3).

Bend planform and hydraulic geometry are highly interlinked(Leopold & Wolman, 1960) which impact flow structure around meander bends(Bagnold, 1960; Camporeale et al., 2005). The observation on pool-depth stabilization in high curvature bends not only corroborates previous findings from rivers of varying size and physio-geographical settings (Thorne, 1989; Vermeulen, 2015) but also extends the idea of the existence of a negative feedback loop between flow-sediment-bend shape (chapter 3) and might suggest an indirect role of dampened morphodynamics on sharper bend shapes. Such feedbacks also have implications for restorative works aimed at re-meandering or meso-habitat restoration in meandering rivers.

Statistically confirmed contrast in depth ratios (H_{ratio}) for angular bends compared to fat bends seem to implicate differing intermediate time-scale hydrodynamic regimes in these bends. Moreover, the reported velocity plunge at the bend apex enhanced by a sudden riffle to pool transition in angular bends might be able to add to the existing knowledge on the formation of anomalous bed topographical features, such as the eroded point bars in unconventional bends (angular), which in contrast are maintained in more conventionally occurring (fat) bends.

4.5 Suggestions for future research work

There is a need for river modeling able to display zigzagging characteristics in their planform. A similarity in the planform shapes of rivers across broad geo-climatic settings revealed some similarity in the processes involved. Both allogenic (ex-channel) and autogenic (in-channel) seem to be creating such planform patterns. Therefore, clear cause and effect links are still largely unknown and remain open for further research. Numerical modeling on the recorded dataset could further help in elaborating mechanistic understanding of the cause-effect linkages among the geometric and hydraulic variables, which could contribute to the understanding of formative conditions of unconventional bends and their morphodynamic characteristics. Analyzing the role of 3-D flow and outer bank dynamics coupled with information on bank line migration from Prut meander dataset could provide new insights into bank erosion sub-models that are a key component of meander morphodynamic models. Feedbacks occurring between flow separation- sedimentation-scouring-bend geometry still present a current knowledge gap (Vermeulen et al., 2014).

References

Abad, J. D., & M. H. Garcia, 2006. RVR Meander : A toolbox for re-meandering of channelized streams. Computers & Geosciences, Elsevier 32: 92–101.

Abad, J. D., & M. H. Garcia, 2009. Experiments in a high-amplitude Kinoshita meandering channel : 1. Implications of bend orientation on mean and turbulent flow structure. Water Resources Research, Wiley Online Library 45: 1–19, http://dx.doi.org/10.1029/2008WR007016.

Abad, J. D., & M. H. García, 2005. Hydrodynamics in Kinoshita-generated meandering bends : importance for river-planform evolution. 4th IAHR Symposium on River, Coastal and Estuarine Morphodynamics, RCEM 2005. : 761–771.

Ackers, P., & F. G. Charlton, 1975. Theories and relationships of river channel patterns- A discussion. Journal of Hydrology Elsevier 26: 359–362.

Alford, J. J., R. H. Baumann, & A. J. Lewis, 1982. Circular meander pools. Earth Surface Processes and Landforms 7: 183–188.

Andrle, R., 1994. Flow structure and development of circular meander pools. Geomorphology 9: 261–270.

Ashmore, P., & M. Church, 2001. The impact of climate change on rivers and river processes in Canada. , ir.lib.uwo.ca.

Bagnold, R. A., 1960. Some Aspects of the Shape of River Meanders Some Aspects of the Shape of River Meanders. US Government Printing Office.

Balen, W. Van, W. S. J. Uijttewaal, K. Blanckaert, W. Van Balen, W. S. J. Uijttewaal, & K. Blanckaert, 2010. Large-eddy simulation of a curved open-channel flow over topography Large-eddy simulation of a curved open-channel flow over topography. physics of fluids 22: 075108.

Batalla, R. J., 2003. Sediment deficit in rivers caused by dams and instream gravel mining. Are view with examples from NE Spain. Cuaternario y Geomorfología, Asociación Española para el Estudio del Cuaternario y la Sociedad Española … 17: 79–91.

Batalla, R. J., & C. M. Go, 2004. Reservoir-induced hydrological changes in the Ebro River basin (NE Spain). Journal of hydrology 290: 117–136.

Bathurst, J. C., C. R. Thorne, & R. D. Hey, 1977. Direct measurements of secondary currents in river bends. Nature Publishing Group 269: 504–506.

Best, J. L., & A. C. Brayshaw, 1985. Flow separation—a physical process for the concentration of heavy minerals within alluvial channels. Journal of the Geological Society Geological Society of London 142: 747–755.

Blanckaert, K., 2002. Flow around bends in rivers. In 2th international conference, new trends in water and environmental engineering for safety and life: eco-compatible solutions for aquatic environments,. Capri (Italy).

Blanckaert, K., 2009. Saturation of curvature-induced secondary flow, energy losses, and turbulence in sharp open-channel bends: Laboratory experiments, analysis, and modeling. Journal of Geophysical Research 114: F03015, http://doi.wiley.com/10.1029/2008JF001137.

Blanckaert, K., 2010. Topographic steering, flow recirculation, velocity redistribution, and bed topography in sharp meander bends. Water Resources Research 46: 1–23.

Blanckaert, K., 2011. Hydrodynamic processes in sharp meander bends and their morphological implications. Journal of Geophysical Research: Earth Surface 116: n/a-n/a, http://doi.wiley.com/10.1029/2010JF001806.

Blanckaert, K., 2015. Flow separation at convex banks in open channels. Journal of Fluid Mechanics 432–467.

Blanckaert, K., & H. J. De Vriend, 2003. Nonlinear modeling of mean flow redistribution in curved open channels. Water Resources Research 39: 1–14.

Blanckaert, K., & H. J. De Vriend, 2004. Secondary flow in sharp open-channel bends. Journal of Fluid Mechanics 498: 353–380.

Blanckaert, K., M. G. Kleinhans, S. J. Mclelland, W. S. J. Uijttewaal, B. J. Murphy, A. Van De Kruijs, D. R. Parsons, & Q. Chen, 2013. Flow separation at the inner (convex) and outer (concave) banks of constant-width and widening open-channel bends. Earth Surface Processes and Landforms 716: 696–716.

Blondeaux, P., & G. Seminara, 1985. A Unified Bar-Bend Theory of River Meanders. Journal of Fluid Mechanics 157: 449–470.

Bravard, J.-P., M. Goichot, & H. Tronchère, 2014. An assessment of sediment-transport processes in the Lower Mekong River based on deposit grain sizes, the CM technique and flow-energy data. Geomorphology Elsevier 207: 174–189.

Bravard, J.-P., N. Landon, J.-L. Peiry, & H. Piégay, 1999. Principles of engineering geomorphology for managing channel erosion and bedload transport, examples from French rivers. Geomorphology Elsevier 31: 291–311.

Brice, J. C., 1973. Meandering pattern of the White River in Indiana—an analysis Fluvial geomorphology. State University of New York at Binghamton Paris: 178–200.

Brice, J. C., 1974. Evolution of Meander Loops. Geological Society of America Bulletin 85: 581–586, http://gsabulletin.gsapubs.org/content/85/4/581.abstract.

Burckhardt, J. C., & B. L. Todd, 1998. Riparian forest effect on lateral stream channel migration in the glacial till plains. JAWRA Journal of the American Water Resources

Association Wiley Online Library 34: 179–184.

Burge and Smith, 1999. Confined meandering river eddy accretions: sedimentology, channel geometry and depositional processes. Fluvial sedimentology VI: 113–130.

Callander, R. A., 1978. River Meandering. Annual Review of Fluid Mechanics 10: 129–158, https://ui.adsabs.harvard.edu/abs/1978AnRFM..10..129C.

Camporeale, C., P. Perona, A. Porporato, & L. Ridolfi, 2005. On the long-term behavior of meandering rivers. Water Resources Research 41: 1–13.

Camporeale, C., P. Perona, A. Porporato, & L. Ridolfi, 2007. Hierarchy of models for meandering rivers and related morphodynamic processes. Reviews of Geophysics 45:.

Carey, W. C., 1963. The Mechanisms of Turns in Alluvial Streams. The Military Engineer .

Carey, W. C., 1969. Formation of flood plain lands. .

Carson, M. A., & M. F. Lapointe, 1983. The inherent asymmetry of river meander planform. The Journal of Geology University of Chicago Press 91: 41–55.

Chen, Z., Z. Wang, B. Finlayson, J. Chen, & D. Yin, 2010. Implications of flow control by the Three Gorges Dam on sediment and channel dynamics of the middle Yangtze (Changjiang) River, China. Geology Geological Society of America 38: 1043–1046.

Comiti, F., M. Da Canal, N. Surian, L. Mao, L. Picco, & M. A. Lenzi, 2011. Geomorphology Channel adjustments and vegetation cover dynamics in a large gravel bed river over the last 200 years. Geomorphology Elsevier B.V. 125: 147–159, http://dx.doi.org/10.1016/j.geomorph.2010.09.011.

Constantine, C. R., T. Dunne, & G. J. Hanson, 2009. Geomorphology Examining the physical meaning of the bank erosion coefficient used in meander migration modeling. Geomorphology Elsevier B.V. 106: 242–252, http://dx.doi.org/10.1016/j.geomorph.2008.11.002.

Constantine, J. A., T. Dunne, J. Ahmed, C. Legleiter, & E. D. Lazarus, 2014. Sediment supply as a driver of river meandering and floodplain evolution in the Amazon Basin, Nat. Geosci., 7, 899–903. .

Constantinescu, G., M. Koken, & J. Zeng, 2011. The structure of turbulent flow in an open channel bend of strong curvature with deformed bed : Insight provided by detached eddy simulation. Water Resources Research 47: 1–17.

Crosato, A., 2009. Physical explanations of variations in river meander migration rates from model comparison. Earth Surface Processes and Landforms 34: 2078–2086, http://www3.interscience.wiley.com/journal/121517813/abstract.

Dai, Z., S. Fagherazzi, X. Mei, & J. Gao, 2016. Decline in suspended sediment concentration delivered by the Changjiang (Yangtze) River into the East China Sea between 1956 and

2013. Geomorphology Elsevier 268: 123–132.

Daniel, J. F., 1971. Channel movement of meandering Indiana streams U.S. Geological Survey Professional Paper. : 732.

Davies, T. R. H., & C. C. Tinker, 1984. Fundamental characteristics of stream meanders. Geological Society of America Bulletin Geological Society of America 95: 505–512.

Davis, D. H., 1908. A study of river meanders on the middle rouge. The Journal of Geology University of Chicago Press 16: 755–764.

Davy, B. W., & T. R. H. Davies, 1979. Entropy concepts in fluvial geomorphology: a reevaluation. Water Resources Research Wiley Online Library 15: 103–106.

De Vriend, H. J., 1981. Velocity redistribution in curved recangular channels. Journal of Fluid Mechanics 107: 423–439.

De Vriend, H. J., & J. Geldof, 1983. Main flow velocity in short river bends. Journal of hydraulic engineering 109: 991–1011.

Dietrich, W. E., 1987. Mechanics of flow and sediment transport in river bends River channels: Environment and process. Blackwell Oxford: 179–227.

Dietrich, W. E., G. Day, & G. Parker, 1999. The Fly River, Papua New Guinea: Inferences about river dynamics, floodplain sedimentation and fate of sediment. Varieties of fluvial form John Wiley and Sons, New York 345–376.

Dietrich, W. E., & J. D. Smith, 1983. Influence of the point bar on flow through curved channels. Water Resources Research 19: 1173–1192.

Dietrich, W. E., & J. D. Smith, 1984. Bed load transport in a river meander. Water Resources Research Wiley Online Library 20: 1355–1380.

Dietrich, W. E., J. D. Smith, & T. Dunne, 1979. Flow and sediment Transport in a sand bedded meander. The Journal of Geology 87: 305–315.

Dinehart, R. L., & J. R. Burau, 2005. Averaged indicators of secondary flow in repeated acoustic Doppler current profiler crossings of bends. Water Resources Research 41: 1–18.

Doltu, C., & M. Dumitran, 2011. Considerations on the sediments transport in river beds. Lucrările Seminarului Geografic" Dimitrie Cantemir" 41–50.

Dynesius, M., & C. Nilsson, 1994. Fragmentation and flow regulation of river systems in the northern third of the world. Science American Association for the Advancement of Science 266: 753–762.

Einstein, A., 1926. The Cause of the Formation of Meanders in the Courses of Rivers and of the So-Called Baer ' s Law. Die Naturwissenschaften 14: 223–224.

Einstein, H. A., & H. W. Shen, 1964. A study on meandering in straight alluvial channels.

Journal of Geophysical Research (1896-1977) John Wiley & Sons, Ltd 69: 5239–5247, https://doi.org/10.1029/JZ069i024p05239.

Engel, F. L., & B. L. Rhoads, 2012. Interaction among mean flow, turbulence, bed morphology, bank failures and channel planform in an evolving compound meander loop. Geomorphology Elsevier B.V. 163–164: 70–83, http://dx.doi.org/10.1016/j.geomorph.2011.05.026.

Engel, F. L., & B. L. Rhoads, 2015. Three-dimensional flow structure and patterns of bed shear stress in an evolving compound meander bend. Earth Surface Processes and Landforms 1226: 1211–1226.

Engelund, F., 1974. Flow and bed topography in channel bends. Journal of the Hydraulics Division 100.

Ettmer, B., & C. A. Alvarado-Ancieta, 2010. Morphological development of the Ucayali River, Peru without human impacts. Waldökologie, Landschaftsforschung und Naturschutz 10: 77–84.

Federici, B., & G. Seminara, 2003. On the convective nature of bar instability. Journal of Fluid Mechanics Cambridge University Press 487: 125–145.

Ferguson, R. I., 1973. Regular meander path models. Water Resources Research Wiley Online Library 9: 1079–1086.

Ferguson, R. I., 1975. Meander irregularity and wavelength estimation. Journal of Hydrology 26: 315–333.

Ferguson, R. I., 1976. Disturbed periodic model for river meanders. Earth Surface Processes Wiley Online Library 1: 337–347.

Ferguson, R. I., 1979. River meanders: regular or random. Statistical applications in the spatial sciences. Pion, London 228–241.

Ferguson, R. I., D. R. Parsons, S. N. Lane, & R. J. Hardy, 2003. Flow in meander bends with recirculation at the inner bank. Water resources research, 39. http://dx.doi.org/10.1029/2003WR001965.

Fisk, H. N., 1944. Geological investigation of the alluvial valley of the lower Mississippi River: US Army Corps of Engineers. Mississippi River Commission .

Flener, C., Y. Wang, L. Laamanen, E. Kasvi, J. Vesakoski, & P. Alho, 2015. Empirical Modeling of Spatial 3D Flow Characteristics Using a Remote-Controlled ADCP System: Monitoring a Spring Flood. Water 7: 217–247.

Frascati, A., & S. Lanzoni, 2009. Morphodynamic regime and long-term evolution of meandering rivers. Journal of Geophysical Research: Earth Surface Wiley Online Library 114.

Friedkin, J. F., 1945. Laboratory study of the meandering of alluvial rivers United States Waterways Experiment Station. United States Waterways experiment station.

Frothingham, K. M., & B. L. Rhoads, 2003. Three-dimensional flow structure and channel change in an asymmetrical compound meander loop, Embarras River, Illinois. Earth Surface Processes and Landforms 644: 625–644.

Furbish, D. J., 1988. River-bend curvature and migration: how are they related?. Geology 16: 752–755.

Furbish, D. J., 1991. Spatial autoregressive structure in meander evolution. Geological Society of America Bulletin Geological Society of America 103: 1576–1589.

Garcia, M. H., L. D. Bittner, & Y. Nino, 1994. Mathematical modeling of meandering streams in Illinois: a tool for stream management and engineering (HES 43).

Garcia, X.-F., I. Schnauder, & M. T. Pusch, 2011. Complex hydromorphology of meanders can support benthic invertebrate diversity in rivers. Hydrobiologia 685: 49–68, http://link.springer.com/10.1007/s10750-011-0905-z.

Gautier, E., D. Brunstein, P. Vauchel, J. Jouanneau, M. Roulet, C. Garcia, J. Guyot, & M. Castro, 2010. Channel and floodplain sediment dynamics in a reach of the tropical meandering Rio Beni (Bolivian Amazonia). Earth Surface Processes and Landforms 1853: 1838–1853.

Gervasoni, G. B., 1989. Evolution of the Po River: an Example of the Application of Historic Maps In Petts, G. E. (ed), Historical Change of Large Alluvial rivers : Western Europe. John Wiley & Sons.

Gilvear, D., S. Winterbottom, & H. Sichingabula, 2000. Character of channel planform change and meander development: Luangwa River, Zambia. Earth Surface Processes and Landforms 436: 421–436.

GloverJ. E, Martin E.H., and Shen H.W.,1986. Classification and Behavior of Meander Migration. Hydrologist, U.S: Geological Survey 7–9.

Gorycki, M. A., 1973. Hydraulic drag: a meander-initiating mechanism. Geological Society of America Bulletin Geological Society of America 84: 175–186.

Goudie, A. S., 2006. Global warming and fluvial geomorphology. Geomorphology 79: 384-394.

Graf, N., 2008. 50 years of channel change on a reach of the Big Blue River, Northeast Kansas. Kansas State University.

Greco, S. E., & R. E. Plant, 2003. Temporal mapping of riparian landscape change on the Sacramento River, miles 196–218, California, USA. Landscape Research Taylor & Francis 28: 405–426.

Guerrero, M., & A. Lamberti, 2011. Flow Field and Morphology Mapping Using ADCP and Multibeam Techniques : Survey in the Po River. Journal of Hydraulic Engineering 137: 1576–1587.

Güneralp et al, 2012. Advances and challenges in meandering channels research. Geomorphology 163–164: 1–9.

Guneralp, I., 2007. Curvature-migration relations and planform dynamics of meandering rivers. University of Illinois at Urbana-Champaign.

Guneralp, I., & R. a. Marston, 2012. Process-form linkages in meander morphodynamics: Bridging theoretical modeling and real world complexity. Progress in Physical Geography .

Güneralp, I., & B. L. Rhoads, 2008. Continuous characterization of the planform geometry and curvature of meandering rivers. Geographical Analysis 40: 1–25.

Güneralp, I., & B. L. Rhoads, 2009. Empirical analysis of the planform curvature-migration relation of meandering rivers. Water Resources Research 45: 1–15.

Güneralp, İ., & B. L. Rhoads, 2011. Influence of floodplain erosional heterogeneity on planform complexity of meandering rivers. Geophysical Research Letters 38: n/a-n/a, http://doi.wiley.com/10.1029/2011GL048134.

Gurnell, A., & G. Petts, 2006. Trees as riparian engineers: the Tagliamento River, Italy. Earth Surface Processes and Landforms: The Journal of the British Geomorphological Research Group Wiley Online Library 31: 1558–1574.

Hasegawa, K., 1989. Universal bank erosion coefficient for meandering rivers. Journal of Hydraulic Engineering American Society of Civil Engineers 115: 744–765.

He, F., V. Bremerich, C. Zarfl, J. Geldmann, J. N. W. David, W. Darwall, S. D. Langhans, K. Tockner, & S. C. Jähnig, 2018. Freshwater megafauna diversity : Patterns , status and threats. 1395–1404.

Hickin, E. J., 1974. The development of meanders in natural river-channels. American Journal of Science. , 414–442.

Hickin, E. J., 1977. Hydraulic factors controlling channel migration. Research in Fluvial Geomorphology: Proceedings of the 5th Guelph Geomorphology Symposium. Geobooks Norwich, UK: 59–66.

Hickin, E. J., 1978. Mean flow structure in meanders of the Squamish River, British Columbia. Canadian Journal of Earth Sciences NRC Research Press 15: 1833–1849, http://dx.doi.org/10.1139/e78-191.

Hickin, E. J., & G. C. Nanson, 1975. The Character of Channel Migration on the Beatton River, Northeast British Columbia, Canada. Geological Society of America Bulletin 86: 487–494, http://gsabulletin.gsapubs.org/content/86/4/487.abstract.

Hickin, E. J., & G. C. Nanson, 1984. Lateral Migration Rates of River Bends. Journal of Hydraulic Engineering 110: 1557–1567.

Hodskinson, a., & R. I. Ferguson, 1998. Numerical modelling of separated flow in river bends: model testing and experimental investigation of geometric controls on the extent of flow separation at the concave bank. Hydrological Processes 12: 1323–1338.

Hooke, J., 1977a. An Analysis of Changes in River Channel Patterns: The Example of Streams in Devon. University of Exeter, 96.

Hooke, J., 1984a. Changes in river meanders : a review of techniques and results of analyses. Progress in Physical Geography 8: 473–508.

Hooke, J., 2003. River meander behaviour and instability: A framework for analysis. Transactions of the Institute of British Geographers 28: 238–253.

Hooke, J. M., 1977b. The distribution and nature of changes in river channel patterns: The example of Devon. River Channel Changes, K. J. Gregory (Ed.), Wiley, 265–280.

Hooke, J. M., 1987. Changes in Meander Morphology. In Gardiner, V. (ed), Proceedings of the First International Conference on Geomorphology. : 591–609.

Hooke, J. M., 1995. River channel adjustment to meander cutoffs on the River Bollin and River Dane, northwest England. Geomorphology Elsevier 14: 235–253.

Hooke, J. M., 1997. Styles of channel change. In C.R. Thorne, R. D. H. and M. D. N. (ed), Applied fluvial geomorphology for river engineering and management. John Wiley & Sons: 237–268.

Hooke, J. M., 2004. Cutoffs galore!: Occurrence and causes of multiple cutoffs on a meandering river. Geomorphology 61: 225–238.

Hooke, J. M., 2007. Spatial variability, mechanisms and propagation of change in an active meandering river. Geomorphology 84: 277–296, http://linkinghub.elsevier.com/retrieve/pii/S0169555X06002339.

Hooke, J. M., 2013a. Treatise on Geomorphology. Treatise on Geomorphology. Elsevier, http://www.sciencedirect.com/science/article/pii/B9780123747396002414.

Hooke, J. M., & A. M. Harvey, 1983. Meander changes in relation to bend morphology and secondary flows. Spec. Public int. Ass. Sediment. John Wiley & Sons 121–132.

Hooke, J. M., & L. Yorke, 2010. Rates, distributions and mechanisms of change in meander morphology over decadal timescales, River Dane, UK. Earth Surface Processes and Landforms 35: 1601–1614.

Hooke, R. L. B., 1975. Distribution of Sediment Transport and shear stress in a Meander Bend. The Journal of Geology 83: 543–565.

Horton, A. J., J. A. Constantine, T. C. Hales, B. Goossens, M. W. Bruford, & E. D. Lazarus, 2017. Modification of river meandering by tropical deforestation. Geology 511–514.

Howard, a D., 1996. Modelling Channel Evolution and Floodplain Morphology. Floodplain Processes. , 15–62.

Howard, A.. ., 1992. Modelling channel migration and floodplain sedimentation in meandering streams. Lowland Floodplain Rivers: Geomorphological Perspectives. Edited by P. A. Carling and G. E. Petts. , 1–41.

Howard, A. D., & A. T. Hemberger, 1991. Multivariate characterization of meandering. Geomorphology. , 161–186.

Howard, A. D., & T. R. Knutson, 1984. Sufficient conditions for river meandering: A simulation approach. Water Resources Research 20: 1659–1667, http://dx.doi.org/10.1029/WR020i011p01659.

Hudson, P. F., & R. H. Kesel, 2000. Channel migration and meander-bend curvature in the lower Mississippi River prior to major human modification. Geology 28: 531–534.

Ikeda, S., G. Parker, & K. Sawai, 1981. Bend theory of river meanders. Part 1. Linear development. Journal of Fluid Mechanics Cambridge University Press 112: 363–377.

Ikeda, S., M. Yamasaka, & J. F. Kennedy, 1990. Three-dimensional fully developed shallow-water flow in mildly curved bends. Fluid dynamics research IOP Publishing 6: 155.

Imran, J., G. Parker, & C. Pirmez, 1999. A nonlinear model of flow in meandering submarine and subaerial channels. Journal of Fluid Mechanics Cambridge University Press 400: 295–331.

Jefferson, M., 1902. Limiting width of meander belts. National Geographic Society.

Johannesson, H., & G. Parker, 1989. Velocity redistribution in meandering rivers. Journal of Hydraulic Engineering 115: 1019–1039.

Jurmu, M. C., & R. Andrle, 1997. Morphology of a wetland stream. Environmental Management 21: 921–941.

Kashyap, S., AM. Asce, G. Constantinescu, M. Asce, C. D. Rennie, G. Post, & R. Townsend, 2013. Influence of bend angle on flow, secondary circulation, and bed shear stress in a high curvature channel bend. Journal of Geophysical Research: Earth Surface 118: 480–496.

Kashyap, S., C. D. Rennie, & R. Townsend, 2010. Flow Around Submerged Groynes in a Sharp Bend Using a 3D LES Model. River Flow 2010. : 643-650.

Kinoshita, R., 1961. Investigation of channel deformation in Ishikari River. Report of Bureau of Resources Department of Science and Technology 174.

Kiss, T., & V. Blanka, 2012. River channel response to climate- and human-induced hydrological changes: Case study on the meandering Hernád River, Hungary. Geomorphology Elsevier B.V. 175–176: 115–125, http://dx.doi.org/10.1016/j.geomorph.2012.07.003.

Kiss, T., K. Fiala, & G. Sipos, 2008. Alterations of channel parameters in response to river regulation works since 1840 on the Lower Tisza River (Hungary). Geomorphology 98: 96–110.

Kleinhans, M. G., F. Schuurman, W. Bakx, & H. Markies, 2009. Meandering channel dynamics in highly cohesive sediment on an intertidal mud flat in the Westerschelde estuary, the Netherlands. Geomorphology Elsevier B.V. 105: 261–276, http://dx.doi.org/10.1016/j.geomorph.2008.10.005.

Koken, M., G. Constantinescu, & K. Blanckaert, 2013. Hydrodynamic processes, sediment erosion mechanisms, and Reynolds-number-induced scale effects in an open channel bend of strong curvature with flat bathymetry. Journal of Geophysical Research: Earth Surface 118: 2308–2324.

Kondolf, G. M., 1997. Hungry Water : Effects of Dams and Gravel Mining on River Channels. Environmental management 21: 533–551.

Kondolf, G. M., 2006. River Restoration and Meanders. Ecology and Society 11.

Kondolf, G. M., & M. L. Swanson, 1993. Channel adjustments to reservoir construction and gravel extraction along Stony Creek, California. Environmental Geology 21: 256–269.

Lagasse, P. F., L. W. Zevenbergen, W. J. Spitz, C. R. Thorne, A. Associates, & F. Collins, 2004. Methodology for Predicting Channel Migration.

Langbein, W. B., & L. B. Leopold, 1966. River meanders - Theory of minimum variance. Physiographic and hydraulic studies of rivers. Geological Survey Professional Paper 422-H 1–15.

Latrubesse, E. M., J. C. Stevaux, & R. Sinha, 2005. Tropical rivers. 70: 187–206.

Lauer, J. W., & G. Parker, 2008. Net local removal of floodplain sediment by river meander migration. Geomorphology Elsevier 96: 123–149.

Lawler, D., 1993. The measurement of riverbank erosion and lateral channel change: a review. Earth Surface Processes and Landforms. , http://onlinelibrary.wiley.com/doi/10.1002/esp.3290180905/abstract.

Lawler, D. M., J. Couperthwaite, L. J. Bull, & N. M. Harris, 1997. Bank erosion events and processes in the Upper Severn basin. , hal.archives-ouvertes.fr.

Leeder, M. R., & P. H. Bridges, 1975. Flow separation in meander bends. Nature 253: 338–339.

Legleiter, C. J., & P. C. Kyriakidis, 2007. Forward and Inverse Transformations between Cartesian and Channel-fitted Coordinate Systems for Meandering Rivers 1. Mathematical Geology 38: 927–958.

Leopold, B. L., & M. G. Wolman, 1957. River Channel Patterns: Braided, Meandering and Straight. US Government Printing Office.

Leopold, L. B., & M. G. Wolman, 1960. River meanders. Geological Society of America Bulletin Geological Society of America 71: 769–793.

Lorenz, A. W., S. C. Jähnig, & D. Hering, 2009. Re-meandering German lowland streams: qualitative and quantitative effects of restoration measures on hydromorphology and macroinvertebrates. Environmental management Springer 44: 745–754.

Magdaleno, F., & J. a. Fernández-Yuste, 2011. Meander dynamics in a changing river corridor. Geomorphology Elsevier B.V. 130: 197–207, http://dx.doi.org/10.1016/j.geomorph.2011.03.016.

Malin, M. C., & K. S. Edgett, 2003. Evidence for Persistent Flow and Aqueous Sedimentation on Early Mars. Science 302: 1931–1934.

Marani, M., S. Lanzoni, D. Zandolin, G. Seminara, & A. Rinaldo, 2002. Tidal meanders. 38:.

Markham, A. J., & C. R. Thorne, 1992. Geomorphology of gravel-bed river bends. Dynamics of gravel-bed rivers John Wiley and Sons Chichester 433–450.

Monegaglia, F., G. Zolezzi, I. Güneralp, A. J. Henshaw, & M. Tubino, 2018. Environmental Modelling & Software Automated extraction of meandering river morphodynamics from multitemporal remotely sensed data. Environmental Modelling and Software Elsevier Ltd 105: 171–186, https://doi.org/10.1016/j.envsoft.2018.03.028.

Moreira, A., & M. Y. Santos, 2007. Concave hull : A k-nearest neighbours approach for the computation of the region occupied by a set of points. , repositorium.sdum.uminho.pt.

Motta, D., J. D. Abad, E. J. Langendoen, & M. H. García, 2012. The effects of floodplain soil heterogeneity on meander planform shape. Water Resources Research 48: n/a-n/a, http://doi.wiley.com/10.1029/2011WR011601.

Murgatroyd, A. L., & J. L. Ternan, 1983. The impact of afforestation on stream bank erosion and channel form. Earth Surface Processes and Landforms Wiley Online Library 8: 357–369.

Muste, M., K. Yu, & M. Spasojevic, 2004a. Practical aspects of ADCP data use for quantification of mean river flow characteristics ; Part I : moving-vessel measurements. Flow measurement and instrumentation 15: 1–16.

Muste, M., K. Yu, & M. Spasojevic, 2004b. Practical aspects of ADCP data use for quantification of mean river flow characteristics; Part I: moving-vessel measurements. Flow measurement and instrumentation Elsevier 15: 1–16.

Nagabhushanaiah, H. S., 1967. Meandering of rivers. Hydrological Sciences Journal Taylor & Francis 12: 28–43.

Nakano, D., & F. Nakamura, 2008. The significance of meandering channel morphology on the diversity and abundance of macroinvertebrates in a lowland river in Japan. Aquatic Conservation: Marine and Freshwater Ecosystems 18: 780–798.

Nanson, G.. C., & E.. J. Hickin, 1983. Channel migration and incision on the Beatton River. Journal of Hydraulic Engineering 109: 327–337.

Nanson, G. C., 1980. A regional trend to meander migration. The Journal of Geology University of Chicago Press 88: 100–108.

Nanson, G. C., & E. J. Hickin, 1986. A statistical analysis of bank erosion and channel migration in western Canada. Geological Society of America Bulletin Geological Society of America 97: 497–504.

Nanson, R. a., 2010. Flow fields in tightly curving meander bends of low width-depth ratio. Earth Surface Processes and Landforms 35: 119–135.

Nelson, J. M., & J. D. Smith, 1989. Flow In Meandering Channels With Natural Topography. River meandering 12: 69–102.

O'Neill, M. P., & A. D. Abrahams, 1986. Objective identification of meanders and bends. Journal of Hydrology 83: 337–353.

Odgaard, A. J., 1986. Meander flow model. I: Development. Journal of Hydraulic engineering American Society of Civil Engineers 112: 1117–1135.

Osman, A. M., & C. R. Thorne, 1988. Riverbank stability analysis. I: Theory. Journal of Hydraulic Engineering American Society of Civil Engineers 114: 134–150.

Ottevanger, W., 2013. Modelling and parameterizing the hydro- and morphodynamics of curved open channels. TU Delft, repository.tudelft.nl.

Ottevanger, W., K. Blanckaert, & W. S. J. Uijttewaal, 2012. Processes governing the flow redistribution in sharp river bends. Geomorphology Elsevier B.V. 163–164: 45–55, http://dx.doi.org/10.1016/j.geomorph.2011.04.049.

Page, K., & G. Nanson, 1982. Concave-bank benches and associated floodplain formation. Earth Surface Processes and Landforms Wiley Online Library 7: 529–543.

Parker, G., & E. D. Andrews, 1986. On the time development of meander bends. Journal of Fluid Mechanics 162: 139–156.

Parker, G., P. Diplas, & J. Akiyama, 1983. Meander bends of high amplitude. Journal of Hydraulic Engineering American Society of Civil Engineers 109: 1323–1337.

Parker, G., K. Sawai, & S. Ikeda, 1982. Bend theory of river meanders. Part2: Nonlinear

deformation of finite-amplitude bends. Journal of Fluid Mechanics 115: 303–314.

Parsons, D. R., 2002. Flow Separation in Meander Bends. The University of Sheffield.

Petrie, J., P. Diplas, M. Gutierrez, & S. Nam, 2013. Combining fixed- and moving-vessel acoustic Doppler current profiler measurements for improved characterization of the mean flow in a natural river. Water Resources Research 49: 5600–5614.

Petts, G. E., & A. M. Gurnell, 2005. Dams and geomorphology: research progress and future directions. Geomorphology Elsevier 71: 27–47.

Phillips, J. D., M. C. Slattery, & Z. A. Musselman, 2005. Channel adjustments of the lower Trinity River, Texas, downstream of Livingston Dam. Earth Surface Processes and Landforms: The Journal of the British Geomorphological Research Group Wiley Online Library 30: 1419–1439.

Pittaluga, M. B., G. Nobile, & G. Seminara, 2009. A nonlinear model for river meandering. Water Resources Research 45: 1–22.

Pittaluga, M. B., & G. Seminara, 2011. Nonlinearity and unsteadiness in river meandering : a review of progress in theory and modelling. Earth Surface Processes and Landforms 36: 20–38.

Pizzuto, J. E., & T. S. Meckelnburg, 1989. Evaluation of a linear bank erosion equation. Water Resources Research 25: 1005.

Provansal, M., S. Dufour, F. Sabatier, E. J. Anthony, G. Raccasi, & S. Robresco, 2014. Geomorphology The geomorphic evolution and sediment balance of the lower Rhône River (southern France) over the last 130 years : Hydropower dams versus other control factors. Geomorphology Elsevier B.V. 219: 27–41, http://dx.doi.org/10.1016/j.geomorph.2014.04.033.

R Core Team (2017). R: A language and environment for statistical computing. R Foundation for Statistical Computing, Vienna, Austria. URL https://www.R-project.org/.

Radoane, M., I. Persoiu, F. Chiriloaei, I. Cristea, & D. Robu, 2017. Styles of Channel Adjustments in the Last 150 Years Channel bed level. Landform Dynamics and Evolution in Romania 489–518.

Rădoane, M., N. Rădoane, I. Cristea, & D. Gancevici-oprea, 2007. Evaluarea modificărilor contemporane ale albiei râului Prut pe graniţa românească. Revista de Geomorfologie 10: 57-71.

Rădoane, N., 2002. Geomorfologia bazinelor hidrografice mici. Editura Universităţii din Suceava.

Reid, J. ., 1984. Artificially Induced Concave Bank Deposition as a Means of Floodplain Erosion Control.

Rhoads, B. L., & K. D. Massey, 2010. Flow structure and channel change in a sinuous grass-lined stream within an agricultural drainage ditch: Implications for ditch stability and aquatic habitat. River Research and Applications 52: 39–52.

Rhoads, B. L., & M. R. Welford, 1991. Initiation of river meandering. Progress in Physical Geography 15: 127–156.

Richards, K., 1987. Fluvial geomorphology. Progress in physical geography Sage Publications Sage CA: Thousand Oaks, CA 11: 432–457.

Rinaldi, M., N. Surian, F. Comiti, & M. Bussettini, 2015. A methodological framework for hydromorphological assessment, analysis and monitoring (IDRAIM) aimed at promoting integrated river management. Geomorphology Elsevier 251: 122–136.

Rodriguez, J. F., F. A. Bombardelli, M. H. Garcia, K. M. Frothingham, B. L. Rhoads, & J. D. Abad, 2004. High-resolution Numerical Simulation of Flow Through a Highly Sinuous River Reach. water resources management 177–199.

Romanescu, G., C. Stoleriu, & A.-M. Romanescu, 2011. Water reservoirs and the risk of accidental flood occurrence. Case study: Stanca-Costesti reservoir and the historical floods of the Prut river in the period July-August 2008, Romania. Hydrological Processes 25: 2056–2070, http://doi.wiley.com/10.1002/hyp.7957.

Roscoe G. Jackson II, 1975. Velocity bed-form texture patterns of meander bends in the lower Wabash River of Illinois and Indiana. Geological Society of America Bulletin 86: 1511–1522.

Roscoe G. Jackson II, 1981. Sedimentology of mudy fine- grained channel deposits in meandering streams of the American middle west. Journal of sedimentary Petrology 51: 1169–1192.

Rosgen, D. L., & H. L. Silvey, 1996. Applied river morphology. Wildland Hydrology Pagosa Springs, Colorado.

Rossell, R. P., & F. C. K. Ting, 2013. Hydraulic and contraction scour analysis of a meandering channel: James River Bridges near Mitchell, South Dakota. Journal of Hydraulic Engineering American Society of Civil Engineers 139: 1286–1296.

Rozovskiĭ, I. L., 1957. Flow of water in bends of open channels. Academy of Sciences of the Ukrainian SSR.

Salit, F., G. Arnaud-Fassetta, L. Zaharia, M. Madelin, & G. Beltrando, 2015. The influence of river training on channel changes during the 20th century in the Lower Siret River (Romania). Géomorphologie: relief, processus, environnement Groupe français de géomorphologie 21: 175–188.

Schnauder, I., & a. N. Sukhodolov, 2012. Flow in a tightly curving meander bend: Effects of seasonal changes in aquatic macrophyte cover. Earth Surface Processes and Landforms 37:

1142–1157.

Schumm, S. A., 1963. Sinuosity of Alluvial Rivers on the Great Plains. Geological Society of America Bulletin 74: 1089–1100.

Schumm, S. A., 1968. River adjustment to altered hydrologic regimen, Murrumbidgee River and paleochannels, Australia. US Government Printing Office.

Schwendel, A. C., A. P. Nicholas, R. E. Aalto, G. H. Sambrook Smith, & S. Buckley, 2015. Interaction between meander dynamics and floodplain heterogeneity in a large tropical sand-bed river: the Rio Beni, Bolivian Amazon. Earth Surface Processes and Landforms, http://doi.wiley.com/10.1002/esp.3777.

Schwenk, J., & E. Foufoula-Georgiou, 2017. Are process nonlinearities encoded in meandering river planform morphology?. American Geophysical Union.

Schwenk, J., S. Lanzoni, & E. Foufoula-georgiou, 2015. The life of a meander bend : Connecting shape and dynamics via analysis of a numerical model. Journal of Geophysical Research : Earth Surface 690–710.

Seminara, G., 2006. Meanders. Journal of Fluid Mechanics 554: 271, http://www.journals.cambridge.org/abstract_S0022112006008925.

Seminara, G., & M. Tubino, 1989. On the process of meander formation; Sur le processus de formation des méandres. International symposium on river sedimentation. 4 (1989-06-05). China Ocean, Beijing, 873–880.

Shields FD, J., S. S. Knight, & J. M. Stofleth, 2005. Alternatives for riverine backwater restoration by manipulation of severed meander bend Impacts of Global Climate Change. : 1–12.

Shields Jr, F. D., A. Simon, & L. J. Steffen, 2000. Reservoir effects on downstream river channel migration. Environmental Conservation 27: 54–66.

Sukhodolov, A. N., 2012. Structure of turbulent flow in a meander bend of a lowland river. Water Resources Research 48: 1–21.

Sun, T., P. Meakin, & T. Jøssang, 2001. A computer model for meandering rivers with multiple bedload sediment sizes: 2. Computer simulations. Water Resources Research Wiley Online Library 37: 2243–2258.

Sun, T., P. Meakin, T. Jøssang, & K. Schwarz, 1996. A simulation model for meandering rivers. Water resources research Wiley Online Library 32: 2937–2954.

Surian, N., & M. Rinaldi, 2003. Morphological response to river engineering and management in alluvial channels in Italy. Geomorphology 50: 307–326.

Szupiany, R. N., M. L. Amsler, J. L. Best, & D. R. Parsons, 2007. Comparison of fixed-and moving-vessel flow measurements with an aDp in a large river. Journal of Hydraulic

Engineering 133, no. 12 (2007): 1299-1309 133: 1299–1309.

Talbot, T., & M. Lapointe, 2002. Modes of response of a gravel bed river to meander straightening : The case of the Sainte-Marguerite River, Saguenay Region. Water resources research 38: 1–7.

Tanner, W. F., 1960. Helicoidal flow, a possible cause of meandering. Journal of Geophysical Research Wiley Online Library 65: 993–995.

Termini, D., 2009. Experimental observations of flow and bed processes in a large-amplitude meandering flume. Journal of Hydraulic Engineering American Society of Civil Engineers 135: 575–587.

Termini, D., & M. Piraino, 2011. Experimental analysis of cross-sectional flow motion in a large amplitude meandering bend. Earth Surface Processes and Landforms 36: 244–256, http://doi.wiley.com/10.1002/esp.2095.

Thomson, J., 1876. On the origin of windings of rivers in alluvial plains, with remarks on the flow of water round bends in pipes. Proc. Roy. Soc. London Ser. A 26: 5–8.

Thorne and Lewin, 1979. Bank processes, bed material movement and planform development in Meandering river. Adjustments of the Fluvial System 117–167.

Thorne, C. E., & M. R. Welford, 1994. The Equilibrium Concept in Geomorphology. Annals of AAG 84: 666.

Thorne, C. R., 1989. Bank processes on the Red River between Index, Arkansas and the Shreveport, Louisiana.

Thorne, C. R., 1991. Bank Erosion and Meander Migration of the Red and Mississippi Rivers, USA. Hydrology for the Water Management of Large River Basins 301–313.

Thorne, C. R., 1992. Bend Scour and Bank Erosion on the Meandering Red River, Louisiana Lowland Floodplain Rivers: Geomorphological Perspectives. Edited by P. A. Carling and G. E. Petts. : 95–115.

Thorne, S. D., & D. J. Furbish, 1995. Influences of coarse bank roughness on flow within a sharply curved river bend. Geomorphology 12: 241–257.

Tockner, K., U. Uehlinger, & C. T. Robinson, 2009. Rivers of Europe. Academic Press.

Urban, M. A., & B. L. Rhoads, 2003. Catastrophic human-induced change in stream-channel planform and geometry in an agricultural watershed, Illinois, USA. Annals of the Association of American Geographers Taylor & Francis 93: 783–796.

Van Alphen, J. S. L. J., P. M. Bloks, & P. Hoekstra, 1984. Flow and grain size pattern in a sharply curved river bend. Earth Surface Processes and Landforms 9: 513–522, http://doi.wiley.com/10.1002/esp.3290090605.

Vermeulen, B., 2014. Complex flow and Morphology in the Markham River, Indonesia. , http://ieeexplore.ieee.org/lpdocs/epic03/wrapper.htm?arnumber=6929983.

Vermeulen, B., 2015. Flow structure caused by a local cross-sectional area increase and curvature in a sharp river bend. Journal of Geophysical Research: Earth Surface 120: 1771–1783.

Vermeulen, B., A. J. F. Hoitink, S. W. Van Berkum, & H. Hidayat, 2014a. Sharp bends associated with deep scours in a tropical river : The river Mahakam (East Kalimantan, Indonesia). Journal of Geophysical Research : Earth Surface 119: 1441–1454.

Vermeulen, B., A. J. F. Hoitink, G. Zolezzi, J. D. Abad, & R. Aalto, 2016. Multiscale structure of meanders. Geophysical Research Letters.

Ward, J. V, & J. A. Stanford, 1995a. The serial discontinuity concept: extending the model to floodplain rivers. Regulated Rivers: Research & Management Wiley Online Library 10: 159–168.

Ward, J. V, & J. A. Stanford, 1995b. Ecological connectivity in alluvial river ecosystems and its disruption by flow regulation. Regulated rivers: research & management Wiley Online Library 11: 105–119.

Welcomme, R. L., 1985. River fisheries. FAO.

Whiting, P. J., & W. E. Dietrich, 1993a. Experimental studies of bed topography and flow patterns in large-amplitude meanders: 1. Observations. Water Resources Research Wiley Online Library 29: 3605–3614.

Whiting, P. J., & W. E. Dietrich, 1993b. Experimental studies of bed topography and flow patterns in large-amplitude meanders: 2. Mechanisms. Water Resources Research Wiley Online Library 29: 3615–3622.

Williams, G. P., 1984. Paleohydrological methods and some examples from Swedish fluvial environments II—river meanders. Geografiska Annaler: Series A, Physical Geography Taylor & Francis 66: 89–102.

Williams, G. P., 1986. River Meanders and Channel size. Journal of hydrology 88: 147–164.

Woodyer, K. D., 1975. Concave-bank benches on Barwon River, N.S.W. Australian Geographer 13: 36–40.

Xu, D., Y. Bai, J. Ma, & Y. Tan, 2011. Geomorphology Numerical investigation of long-term planform dynamics and stability of river meandering on fluvial fl floodplains. Geomorphology Elsevier B.V. 132: 195–207, http://dx.doi.org/10.1016/j.geomorph.2011.05.009.

Yorke, T. H., & K. A. Oberg, 2002. Measuring river velocity and discharge with acoustic Doppler profilers. Flow Measurement and Instrumentation Elsevier 13: 191–195.

Zaharia, L., F. Grecu, G. Ioana-Toroimac, & G. Neculau, 2011. Sediment transport and river channel dynamics in Romania–variability and control factors Sediment transport in aquatic environments. InTech.

Zeng, J., G. Constantinescu, K. Blanckaert, & L. Weber, 2008. Flow and bathymetry in sharp open-channel bends Experiments and predictions. Water Resources Research 44.

Zinger, J. A., B. L. Rhoads, & J. L. Best, 2011. Extreme sediment pulses generated by bend cutoffs along a large meandering river. Nature Geoscience Nature Publishing Group 4: 1–4, http://dx.doi.org/10.1038/ngeo1260.

Zolezzi, G., & I. Güneralp, 2016. Geomorphology Continuous wavelet characterization of the wavelengths and regularity of meandering rivers. Geomorphology Elsevier B.V. 252: 98–111, http://dx.doi.org/10.1016/j.geomorph.2015.07.029.

Zolezzi, G., & G. Seminara, 2001a. Downstream and upstream influence in river meandering. Part 1. General theory and application to overdeepening. Journal of Fluid Mechanics 438: 183–211.

Zolezzi, G., & G. Seminara, 2001b. Downstream and upstream influence in river meandering. Part 2. Planimetric development. Journal of Fluid Mechanics 438: 213–230.

Appendix A: Supplementary material for Chapter 2

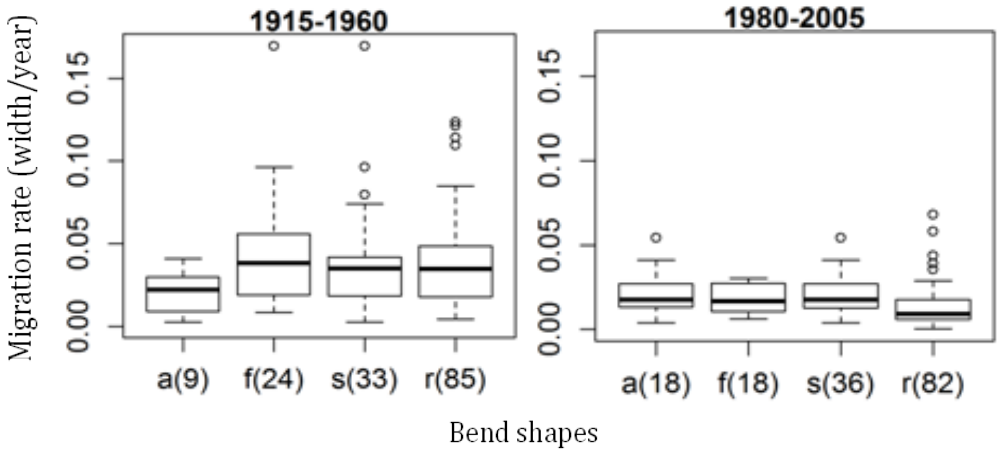

Fig S 1.Migration rates of bends of differing shape types during two analyzed periods (a-angular, f-fat, r-round and s-sharp, in the brackets, is the number of each bend types)

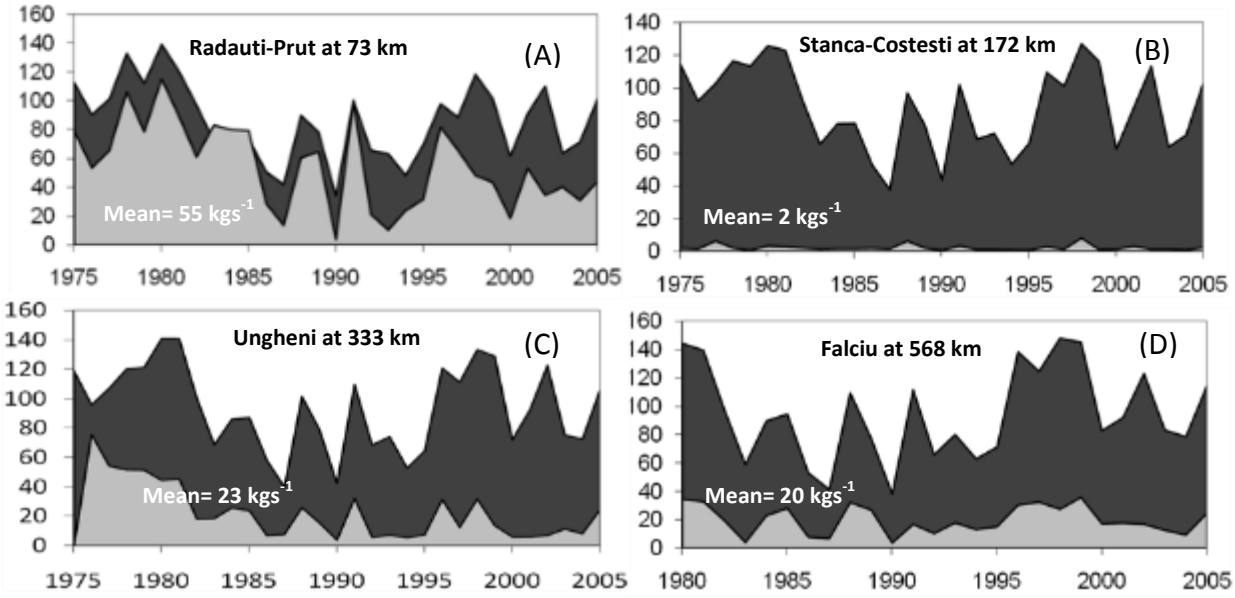

Fig S 2.Yearly (1975-2005) water and sediment discharge data from gauging stations located along the length of Prut River, dark grey colored area is water (m^3s^{-1}) and light grey is sediment discharge (kgs^{-1}). (A) Radauti-Prut, (B) Stanca-Costesti (C) Falciu Ungheni gauge station (Modified from Rădoane et al., 2007).

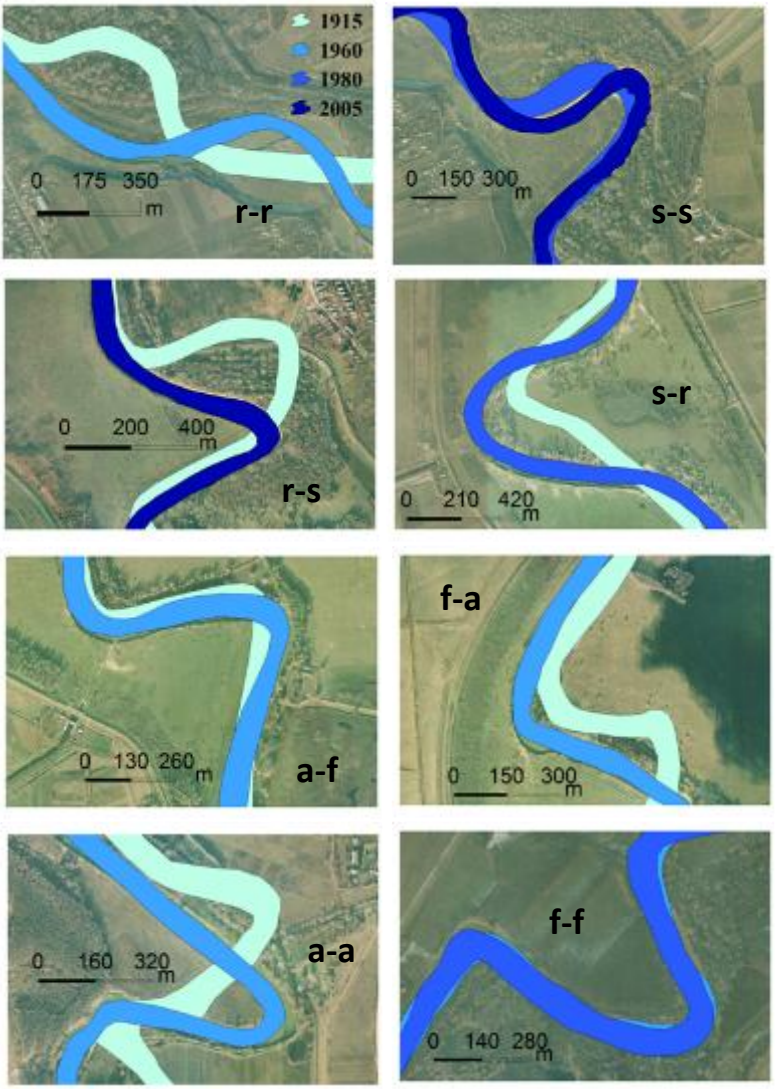

Fig S 3.Bend-shape transitions between sharp and round types and angular and fat types occurring in different time periods on the Prut. Legend description- a-a= angular to angular; f-f= fat to fat; r-r= round to round; s-s= sharp to sharp; a-f= angular to fat; f-a= fat to angular; s-r= sharp to round; r-s= round to sharp. Flow direction is from top to bottom.

Table S 1. Details to shape transitions result in round (r) and sharp (s).

Mode of transition	**1915-1960 (Mean Z in m/yr, Number of transition)**	**1960-1980 (Mean Z in m/yr, Number of transition)**	**1980-2005 (Mean Z in m/yr, Number of transition)**
r-r	2.6, 5	1.5, 7	1.3, 8
s-s	2.5, 24	1.4, 30	1.4, 28
r-s	2, 9	1.3, 6	0.9, 3
s-r	4, 9	1.9, 4	1.1, 8

Table S 2. Details to shape transitions results fat (f) and angular bends (a). The number of transition imply the total number of transition occurring between particular shape types during a given period.

Mode of transition	**1915-1960 (widths/yr, Number of transition)**	**1960-1980 (widths/yr, Number of transition)**	**1980-2005 (widths/yr, Number of transition)**
f-f	3.7, 9	1.5, 11	0.9, 6
a-f	1.5, 4	1.2, 4	1.6, 3
f-a	2.1, 15	1.2, 2	1.2, 9
a-a	1.9, 4	1.5, 15	1.1,14

Appendix B: Supplementary material for Chapter 3

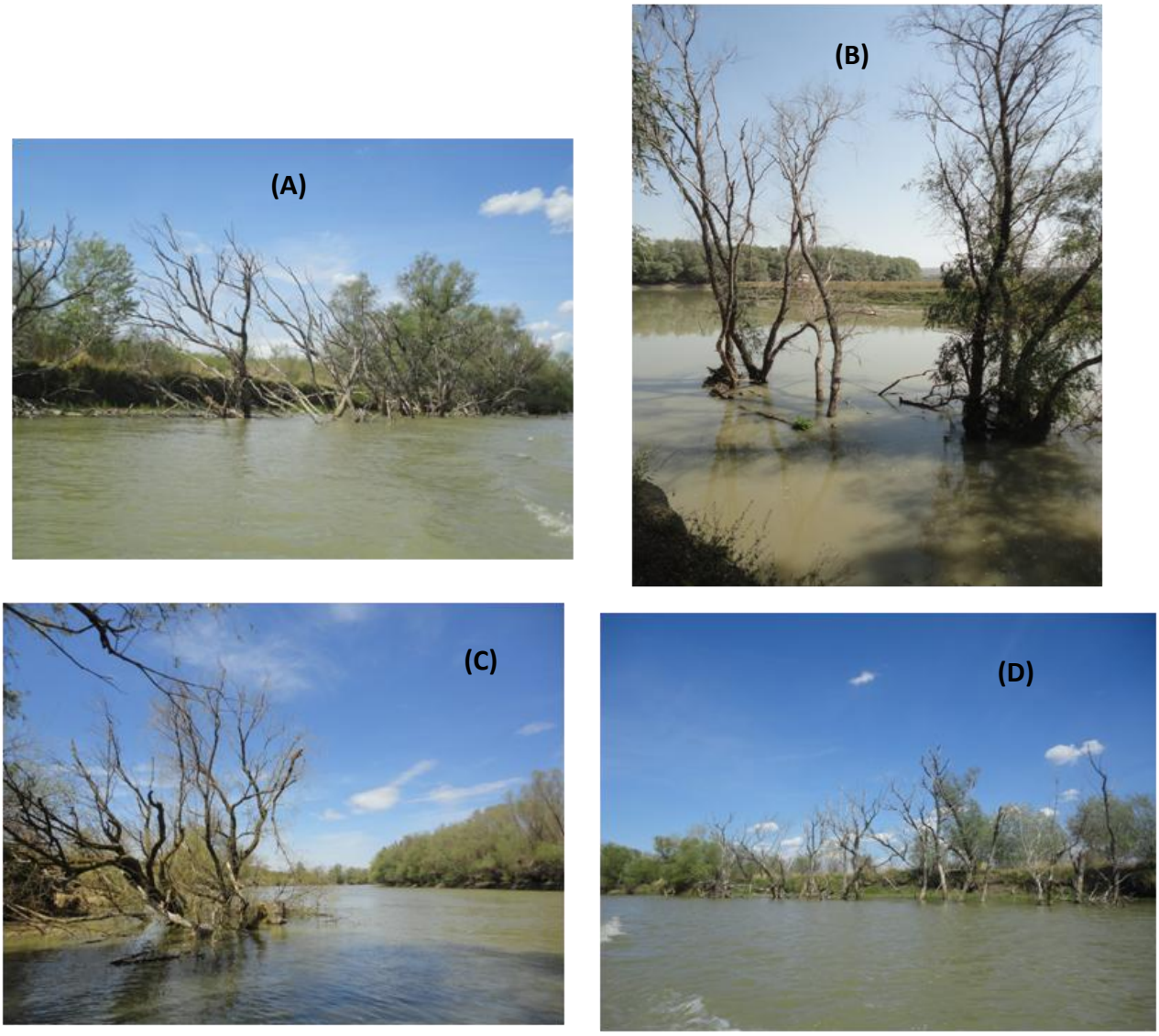

Fig S 4.Fallen trees in the Prut channel.

Fig S 5 Concave bank bench formed on the upstream arm of bend B9 (marked by red arrow). Flow direction is marked by black arrow.

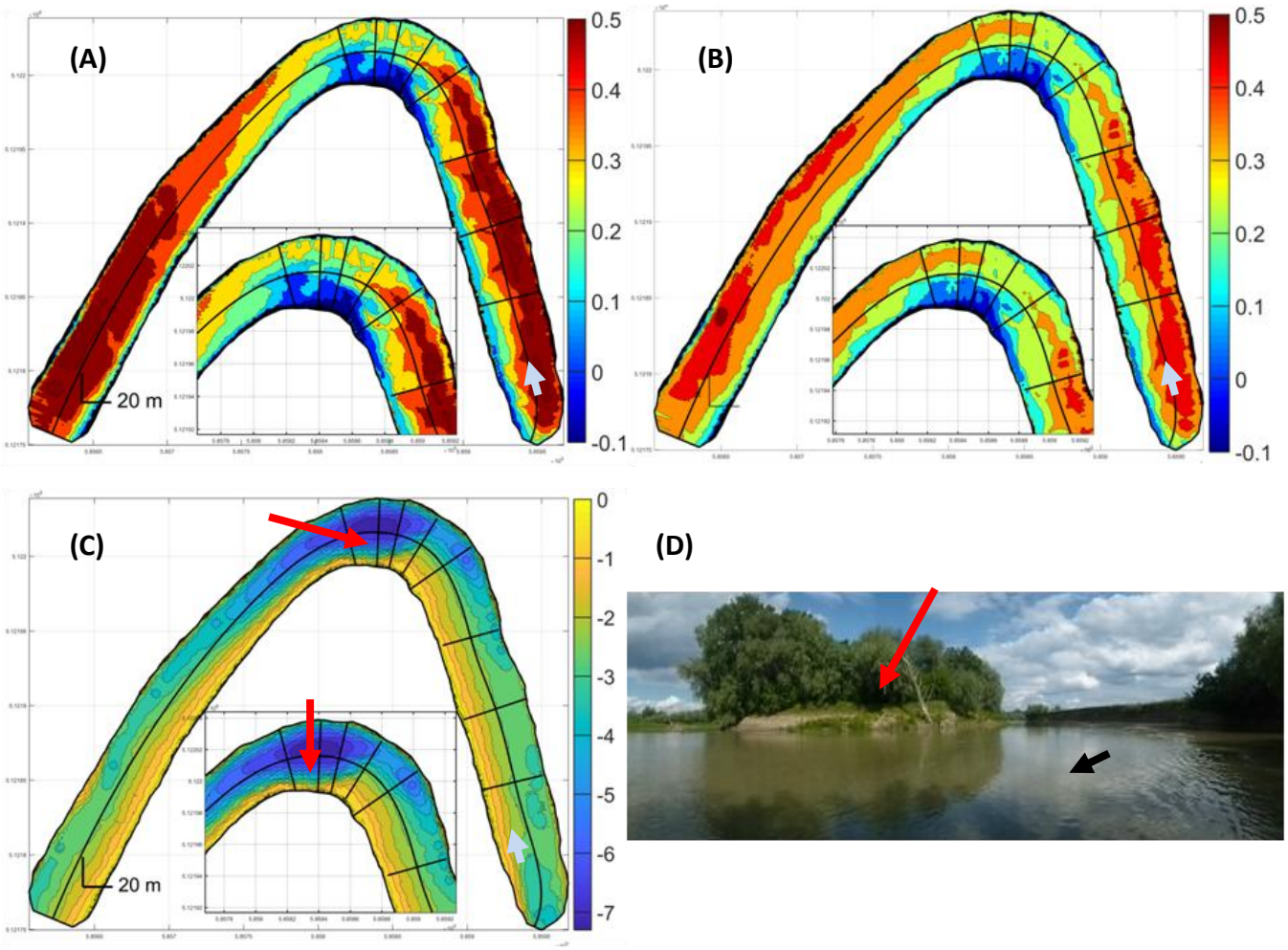

Fig S 6.Example of an angular bend (Cr > 4), bend B15. A) U_{surf} velocity B) U_{bed} velocity C) Bathymetry with missing point bar (marked by red arrow) D) photo of missing point bar at the apex (marked by red arrow, flow direction is marked by black).
Note: insets in panel A, B and C show zoomed portions of apex for better visual.

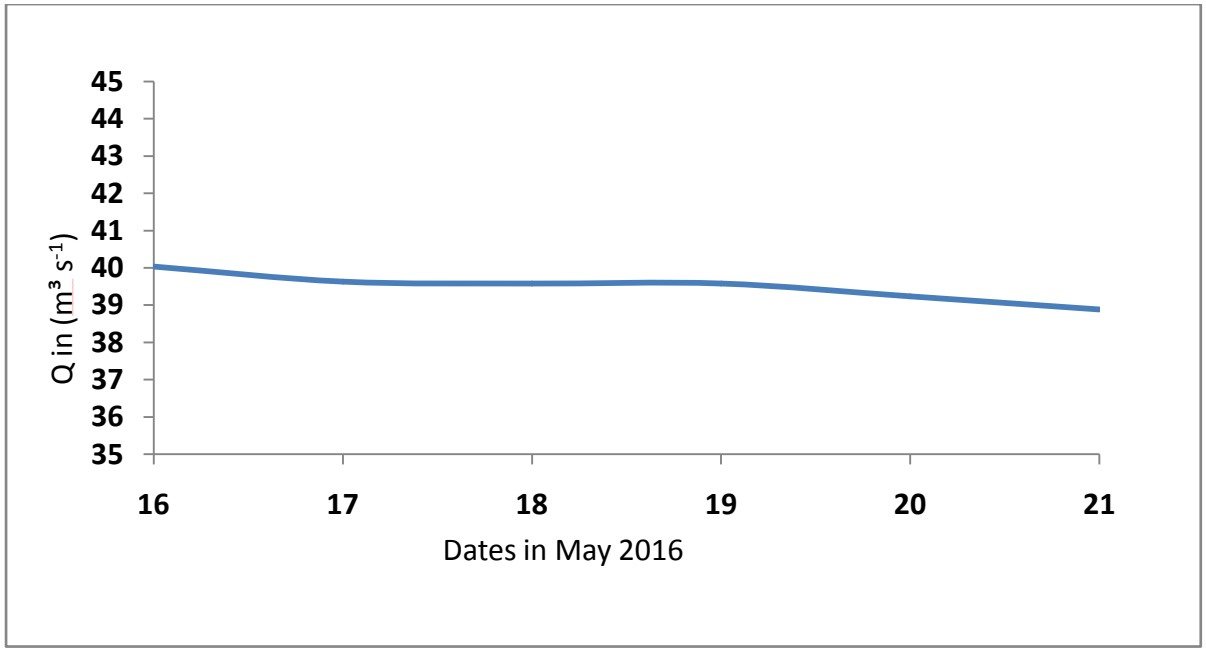

Fig S 7. Mean daily discharge for the field survey period.

Table S 3. The number of data points measured using ADCP surveys on Prut, River.

Bend name	Raw data points (no. of sounding points) i.e. each point is a beam record, there were 4 beams.	Hydrosurveyor datapoints	Pyris datapoints
B1	52306	4690	33612
B2	40350	7710	30567
B3	38383	2687	25098
B4	30849	3061	28324
B5	28000	2679	34802
B6	29275	2190	42531
B7	28782	2958	24411
B9	27139	3892	42696
B10	27551	5757	25013
B11	24898	4227	37441
B12	22274	2492	27930
B13	28577	3876	35978
B14	30747	3047	33040
B15	39190	8524	55225
B16	37218	6851	43235

Table S 4.Additional hydraulic information for studied bends. Note: velocity U is averaged over bend; cell start and end zones are measured from the surface towards the bed in meters and presented as the minimum (nearer to surface) – maximum (nearer to bed).

Bend ID	Q (m^3/s)	U (m/s)	U (SD)	surface cell start	Surface cell end	middle cell start	middle cell end	Bottom cell start	bottom cell end
B10	39.6	0.38	0.11	0.05-0.1	0.02-0.44	0.07-2	0.08-2.5	0.14-4	0.15-4.45
B2	39.2	0.39	0.15	0.05-0.1	0.02-0.68	0.07-3.07	0.08-3.76	0.13-6.15	0.15-6.6
B9	39.6	0.28	0.12	0.05-0.1	0.02-0.7	0.07-3.1	0.08-3.7	0.14-6.1	0.15-6.6
B15	39.6	0.35	0.17	0.05-0.1	0.02-0.7	0.07-3	0.08-3.6	0.14-5.9	0.15-6.6
B1	40.0	0.34	0.1	0.05-0.1	0.02-0.6	0.07-2.7	0.09-3.5	0.14-5.33	0.15-5.60
B7	39.2	0.33	0.13	0.05-0.1	0.02-0.7	0.07-0.3	0.08-3.6	0.14-5.8	0.15-6.1
B12	39.2	0.44	0.11	0.05-0.1	0.02-0.4	0.07-1.9	0.08-2.3	0.13-3.8	0.15-4.1
B13	38.9	0.35	0.14	0.05-0.1	0.02-0.6	0.07-2.61	0.08-3.1	0.14-5.2	0.15-5.6
B16	39.6	0.23	0.12	0.05-0.1	0.02-0.7	0.08-3.07	0.1-3.7	0.2-6.1	0.2-6.6
B4	39.2	0.36	0.13	0.05-0.1	0.02-0.59	0.07-2.6	0.08-3.2	0.14-5.3	0.15-5.6
B8	39.6	0.31	0.13	0.05-0.1	0.02-0.64	0.07-3.0	0.08-3.6	0.14-5.8	0.15-6.1
B3	40.0	0.3	0.1	0.05-0.1	0.03-0.59	0.15-2.63	0.18-3.2	0.3-5.3	0.3-5.6
B11	39.6	0.3	0.11	0.05-0.1	0.03-0.7	0.12-3.1	0.14-3.8	0.2-6.27	0.3-6.6
B6	39.6	0.31	0.09	0.05-0.1	0.06-0.62	0.12-2.8	0.15-3.4	0.3-5.6	0.3-6.1

Q= mean daily discharge; U = mean depth-averaged velocity; SD= standard deviation; surface cel = range of depth below the water surface where ADCP data were collected; middle cell = range of depth in the water column where ADCP was collected; bottom cell = range of depth from water column to bed where ADCP data were collected.

Table S 5. Bend-wise mean cross sectional spacing after PyRIS was applied

Bend name	Cross-sectional spacing	SD (m)	No. of cross sections
B1	1.5	0.06	454
B2	1.3	0.04	374
B3	1.5	0.06	325
B4	1.3	0.06	358
B5	0.9	0.03	403
B6	1	0.02	540
B7	1.4	0.05	305
B9	0.8	0.02	488
B10	1.2	0.06	317
B11	0.9	0.03	435
B12	1.3	0.03	356
B13	0.9	0.04	413
B14	1.2	0.04	422
B15	1	0.03	640
B16	0.6	0.02	484

Acknowledgement

Firstly, I would like to express my deepest gratitude to my academic advisors PD Dr Martin T. Pusch and Associate Prof. Guido Zolezzi for their continuous support during my Ph D study and related research, for their patience, motivation, and immense knowledge. Dr Pusch's guidance helped me in all the time of my research and writing of this thesis. He justified the German title of "*doctor vater*" (meaning, doctor father) as he motivated me to develop a scientific temperament and also nurtured my scientific interests at the same time. Dr Zolezzi, greatly enhanced my knowledge on "geomorphology of meandering rivers", our numerous discussions helped shape my outlook towards this discipline of river science. He also encouraged me towards interdisciplinary collaboration within the SMART framework, which added immensely to my learning curve.

I would like to specifically thank the following people: Mr Stefan Gramada, whose painstaking efforts in retrieving the historical maps from archives of Military unit in Romania fueled the work elaborated in chapter 2 and who also provided significant input in later processing of GIS maps and imagery. Prof Maria Radoane, who supported in acquiring the maps and imagery for the Prut River. Dr Federico Monegaglia, for tailor fitting the PyRIS code to my data. Dr Milad Niroumand Jadidi for helping with Arc GIS tools. Mr Federico Castro Monzon for introducing me to R software. Dr Gabriela Costea, who along with Dr Pusch greatly facilitated and established most of my academic network in Romania and without whom much of my fieldwork there would not have been possible. Dr Marian Paraschiv, who worked with me relentlessly on the Prut and also educated me on the flora and fauna found on the banks of the river. Dr Koen Blanckaert for scientific advice on chapter 3. Dr Mauro Carolli for scientific advice, revisions and his help with Matlab. Dr Robert Ladwig for helping me with coding in Matlab. Alexis Guislain who helped in

improving the quality of the text. And Anna Jaeger in helping create an initial German translation of the thesis summary.

From my host institution, IGB, Berlin, I would like to thank PD Dr Thomas Mehner, whose course on scientific writing greatly boosted my scientific writing skills, Dr Kirsten Pohlmann who was very supportive during the PhD. Dr Ina Severin who took care of the SMART program administrative work, Ms Katrin Lehmann for facilitating my stay at IGB. From the SMART PhD program, I would like to express my gratitude to Dr Marina Rogato who relentlessly supported me with administrative matters, and especially without whom my secondment at the University of Trento would not be possible. For the initial administrative support, I would like to thank Nejwa Bettaz from the Dahlem Research School at Freie Universität Berlin.

Last but definitely not the least; I would like to thank my family, mentors and friends. Especially, my mother and father Mrs Neelam Bisht and Mr Parvinder Singh Bisht who have been a constant pillar of support and love throughout my life and my sister Sneha Bisht whose loving presence has always encouraged me. My uncle, Mr Narender Rawat who early on sowed the seed of scientific temper in me and who's nurturing presence has hugely impacted my personal life and career. I am also deeply indebted of Prof Prakash Nautiyal at HNBGU, Srinagar, who inducted me in the world of Freshwater Ecology during my masters and who believed and cultivated my dream of becoming a river scientist.

This journey would not have been possible without my loving friends that complete my international family. I would like to thank all the SMARTies who encouraged and motivated me through their kind support. Specifically, Dr Oleksandra Shumilova, on whom I could always count upon for help. Dr India Mansour with whom I could share my deeper thoughts with conversations that lasted hours. Dr Gregorio Lopez Moreira for supporting me in my initial days in Trento. Dr Jaime Gaona and Dr Fenghzi He for their kind support

towards the end. Neha Khandekar for her spiritual advice. Many thanks to Karin Bauske for the selfless support and for being there as an emotional anchor during my ups and downs. Dr Karin Meinikmann for her friendship and the caring ways. Thanks to Clara, Anna and Marta for taking me to dancehall classes. To Garabet and Giovanni for fun times we shared and the football sessions. Thanks to, Tamanna Relhan for the special encouragement during my final days of writing. I can't thank enough my '*brothers*' Jason Galloway and Alexis Guislain, who have constantly been by my side since all of this started.

This meandering endeavour has not only been of a scientific nature but also about personal awakening and much more… it has been a transformation.

"The end is the beginning" – Jason Galloway (2019)

Statement of academic integrity

I hereby certify that the submitted thesis “The form, flow and dynamic character of meanders in a lowland river” is my own work and that all published or other sources of material consulted in its preparation have been indicated. I have clearly pointed out any collaboration that has taken place with other researchers and stated my own personal share in the investigations in the Thesis Outline. I confirm that this work has not been submitted to any other university or examining body for a comparable academic award.

Berlin, 25.02.2020

Tarun Bisht